General Disclaimer

One or more of the Following Statements may affect this Document

- This document has been reproduced from the best copy furnished by the organizational source. It is being released in the interest of making available as much information as possible.

- This document may contain data, which exceeds the sheet parameters. It was furnished in this condition by the organizational source and is the best copy available.

- This document may contain tone-on-tone or color graphs, charts and/or pictures, which have been reproduced in black and white.

- This document is paginated as submitted by the original source.

- Portions of this document are not fully legible due to the historical nature of some of the material. However, it is the best reproduction available from the original submission.

$S_{2}fr$

X-693-76-268

NASA TM X- 71239

FINE STRUCTURE IN 3C 120 AND 3C 84

L. K. HUTTON

DEC 1976
RECEIVED
NASA STI FACILITY
INPUT BRANCH

DEC 1976
RECEIVED
NASA STI FACILITY
INPUT BRANCH
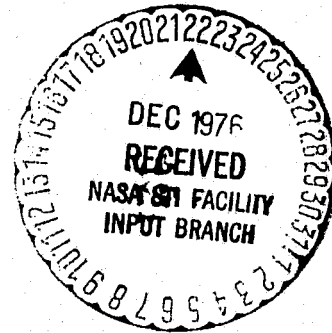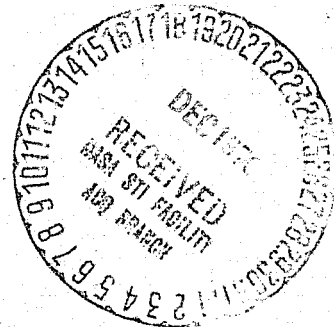
DECEMBER 1976

ASTRONOMY PROGRAM
UNIVERSITY OF MARYLAND
COLLEGE PARK, MARYLAND

GODDARD SPACE FLIGHT CENTER
GREENBELT, MARYLAND

APPROVAL SHEET

Title of Thesis: Fine Structure in 3C 120 and 3C 84

Name of Candidate: Laura Katherine Hutton
Doctor of Philosophy, 1976

Thesis and Abstract Approved: *[signature]*

William C. Erickson
Professor
Department of Physics & Astronomy

Date Approved: 24 August 1976

VITA

Name: Laura Katherine Hutton

Permanent Address: 8577 Brae Brooke Drive
                     Lanham, Maryland 20801

Degree and date to be conferred: Ph. D.   December, 1976

Date of birth: ███████ ██

Place of birth: ████████ ██████

Secondary education: Radnor Senior High School, Radnor, Pennsylvania

Collegiate institutions
    Pennsylvania State Universtiy   1968-71   B. S.   June, 1971
    University of Maryland   1971-73   M. S.   December, 1973
    University of Maryland   1974-76   Ph. D.   December, 1976

Major: Astronomy

Minor: Physics

Publications: see next pages

Positions held:
    Undergraduate assistant - Pennsylvania State University,
                              summers 1970, 1971.
    Teaching assistant - University of Maryland, 1971-72.
    Research assistant - University of Maryland (working at Goddard
                         Space Flight Center), 1973-76.

Professional society memberships:
    Sigma Pi Sigma
    American Astronomical Scoiety .

PUBLICATIONS

H. F. Hinteregger, C. W. Catuna, C. C. Counselman, R. A. Ergas, R. W. King, C. A Knight, D. S. Robertson, A. E. E. Rogers, I. I. Shapiro, A. R. Whitney, T. A. Clark, L. K. Hutton. G. E. Marandino, R. A. Perley, G. M. Resch, N. R. Vandenberg. Nature Phys. Sci. 240, 159, 1972. "Cygnus X-3 Radio Source: Lower Limit on Size and Upper Limit on Distance"

L. K. Hutton, T. A. Clark, W. M. Cronyn. B. A. A. S. 5, 35, 1973. "High Resolution Observations of Cas A at 26.3 MHz"

L. K. Hutton, T. A. Clark, W. C. Erickson, G. M. Resch, N. R. Vandenberg, S. H. Knowles, A. B. Youmans. A. J. 79, 1248, 1974. "Meter-Wavelength VLBI. I. Cassiopeia A"

A. E. E. Rogers, H. F. Hinteregger, A. R. Whitney, C. C. Counselman, I. I. Shapiro, J. J. Wittels, W. K. Klemperer, W. W. Warnock, T. A. Clark, L. K. Hutton, G. E. Marandino, B. O. Ronnang, O. E. H. Rydbeck, A. E. Niell. Ap. J. 193, 293, 1974. "The Structure of Radio Sources 3C 273B and 3C 84 Deduced from the Closure Phase and Visibility Amplitudes Observed with Three-Element Interferometers"

J. J. Wittels, C. A. Knight, I. I. Shapiro, H. F. Hinteregger, A. E. E. Rogers, A. R. Whitney, T. A. Clark, L. K. Hutton, G. E. Marandino, A. E. Niell, B. O. Ronnang, O. E. H. Rydbeck, W. K. Klemperer, W. W. Warnock. Ap. J. 196, 13, 1975. "Fine Structure of 25 Extragalactic Radio Sources"

D. M. Gibson, M. Viner, S. Peterson, T. Clark, L. Hutton, C. Ma, W. Webster, H. Hinteregger, A. Rogers, I. Shapiro, A. Whitney, J. Wittels, A. Niell, G. Resch. B. A. A. S. 7, 498, 1975. "An Extraordinary Radio Outburst in Algol: Flux and Structure Observations"

L. K. Hutton, T. A. Clark, I. I. Shapiro, J. J. Wittels, H. F. Hinteregger, C. A. Knight, A. E. E. Rogers, A. R. Whitney, A. E. Niell, B. O. Ronnang, O. E. H. Rydbeck. B. A. A. S. 7, 413, 1975. "Results of Closure Phase Analysis of VLBI Data"

T. A. Clark, W. C. Erickson, L. K. Hutton, G. M. Resch, N. R. Vandenberg, J. J. Broderick, S. H. Knowles, A. B. Youmans. A. J. 80, 923, 1975. "Meter-Wavelength VLBI. II. The Observations"

T. A. Clark, L. K. Hutton, C. Ma, I. I. Shapiro, J. J. Wittels, D. S. Robertson, H. F. Hinteregger, C. A. Knight, A. E. E. Rogers, A. R. Whitney, A. E. Niell, G. M. Resch, W. J. Webster. Ap. J. 206, L107, 1976. "An Unusually Strong Radio Outburst in Algol: VLBI Observations"

J. J. Wittels, W. D. Cotton, C. C. Counselman, I. I. Shapiro, H. F. Hinteregger, C. A. Knight, A. E. E. Rogers, A. R. Whitney, T. A. Clark, L. K. Hutton, B. O. Ronnang, O. E. H. Rydbeck, A. E. Niell, Ap. J. 206, L75, 1976. "Apparent Superrelativistic Expansion of the Extragalactic Radio Source 3C 345"

W. D. Cotton, R. B. Geller, I. I. Shapiro, J. J. Wittels, T. A. Clark, L. K. Hutton, H. F. Hinteregger, C. A. Knight, A. E. E. Rogers, A. R. Whitney. B. A. A. S. 8, 366, 1976. "Evolution of the Radio Fine Structure of 3C 273B and 3C 279"

J. J. Wittels, W. D. Cotton, C. C. Counselman, I. I. Shapiro, H. F. Hinteregger, C. A. Knight, A. E. E. Rogers, A. R. Whitney, T. A. Clark, L. K. Hutton, B. O. Ronnang, O. E. H. Rydbeck. B. A. A. S. 8, 366, 1976. "Apparent Superrelativistic Expansion of the Extragalactic Radio Source 3C 345"

I. I. Shapiro, J. J. Wittels, C. C. Counselman, A. R. Whitney, H. F. Hinteregger, C. A. Knight, A. E. E. Rogers, T. A. Clark, L. K. Hutton, D. S. Robertson, B. O. Ronnang, O. E. H. Rydbeck, A. E. Niell. B. A. A. S. 8, 366, 1976. "Proper-Motion Evidence Against a Galactic Origin for Quasars"

Clark, L. K. Hutton, G. E. Marandino, C. C. Counselman, D. S.

FINE STRUCTURE IN 3C 120 AND 3C 84

by

Laura Katherine Hutton

Dissertation submitted to the Faculty of the Graduate School
of the University of Maryland in partial fulfillment
of the requirements for the degree of
Doctor of Philosophy
1976

ABSTRACT

Title of thesis: Fine Structure in 3C 120 and 3C 84

Laura Katherine Hutton, Doctor of Philosophy, 1976

Thesis directed by: Professor William C. Erickson

Seven epochs of very-long-baseline radio interferometric
observations of the Seyfert galaxies 3C 120 and 3C 84, at 3.8-cm
wavelength using stations at Westford, Massachusetts, Goldstone,
California, Green Bank, West Virginia, and Onsala, Sweden, have been
analyzed for source structure.   An algorithm for reconstructing the
brightness distribution of a spatially confined source from fringe
amplitude and so-called "closure phase" data has been developed and
successfully applied to artificially generated test data and to data on
the above-mentioned sources.

Over the two year time period of observation, 3C 120 was observed
to consist of a double source showing apparent super-relativistic
expansion and separation velocities.   The total flux changes comprising
one outburst can be attributed to one of these components.   3C 84 showed
much slower changes, evidently involving flux density changes in
individual stationary components rather than relative motion.

Some previously proposed explanations for the behavior of compact
radio sources are briefly re-examined in the light of the present maps.
The possibility that the apparently divergent behavior of the two sources
studied is in fact due to variations of a similar mechanism is also
discussed.

ACKNOWLEDGEMENTS

TABLE OF CONTENTS

LIST OF FIGURES

LIST OF TABLES

Chapter I

INTRODUCTION

"The history of radio interferometry is one of steadily increasing baselines to obtain ever higher resolution" (Bare et al. 1967). And 1967 was a good year in the history of radio interferometry. Early in that year, the first interferometers with totally unconnected elements were tested, nearly simultaneously in Canada (Broten et al. 1967a) and in the United States (Bare et al. 1967), and baseline lengths leapt from the order of 100 km to virtually the diameter of the Earth. The first fringes on a transcontinental baseline (Algonquin Park, Ontario to Penticton, British Columbia) were obtained on May 21, 1967 (Cohen 1969), and, by July of the same year, angular size measurements on a large number of sources were in progress (e. g. Broten et al. 1967b; Broten et al. 1967c; Clark, Cohen, and Jauncey 1967; Clark et al. 1968a; Clark et al. 1968b; Kellermann et al. 1968; Gubbay et al. 1969a; Gubbay et al. 1969b). As the supposed synchrotron self-absorption cutoffs in the radio spectra and the rapid time variations had suggested, structure was apparent in many compact sources on scales from 1 to 10 milliseconds of arc at centimeter wavelengths.

The early experiments, intended to search for interesting objects, provided only very scanty sampling of the fringe visibility function. Only general statements could be made about the approximate angular size of the brightness distributions. The theoretically expected relationships (see e. g. Kellermann and Pauliny-Toth 1968) between source size and radio spectrum were, however, confirmed.

The first systematic sampling of a source's visibility function came as a by-product of an attempt in October 1970 to measure gravitational light bending by the sun (Robertson et al. 1971). The two quasars 3C 273B and 3C 279 were tracked for the entire period of mutual visibility for several days, as the latter was occulted by the sun. Tell-tale variations in the fringe amplitude as a function of time of day revealed that both sources had observable structure (Knight et al. 1971). The simplest interpretation was that of a double source in both cases. In February 1971, the experiment was repeated (without the sun), revealing changes in the structure of both sources (Whitney et al. 1971).

-1-

Under the same simplest assumptions, both sources showed apparent velocities of expansion well above the velocity of light.

These startling results provided impetus for the establishment of a source structure monitoring program on the so-called "Goldstack" (or Goldstone/Haystack) interferometer, which began in April 1971 under the guise of the "Quasar Patrol". By May 1973, array elements were added in West Virginia and Sweden, increasing greatly the regions of the (u,v) plane which could be sampled. The present study will concern itself with data from these observing sessions.

In particular, the objects chosen for study are the closest of the strong ones, the radio galaxies 3C 84 (NGC 1275) and 3C 120. In angular size, they are among the largest sources that we observed, perhaps for that reason, so that a given interferometer provides the best relative resolution and also the best absolute (as measured in parsecs) resolution that it was capable of producing. Furthermore, the distances of the radio galaxies are more widely accepted than those of the quasars, a point which must be considered when computing apparent velocities of expansion.

Chapter II constitutes a description of the experiments themselves and the data reduction procedures used. More general mapping techniques than the traditional Gaussian-component modeling methods proved necessary to handle the apparently complex structure of 3C 84, especially, and to make full use of the "closure" method (Rogers et al. 1974) of extracting phase information from VLBI data. An algorithm for reconstructing a general confined source from the data was developed for this study, and is discussed in Chapter III. Chapters IV and V present the results of application of these algorithms to the data on 3C 120 and 3C 84. And finally, in Chapter VI, conclusions are drawn about both the mapping algorithm and the sources.

Chapter II

THE QUASAR PATROL

The experiments that will be considered were conducted between
April 1972 and October 1975 at a frequency of 7.85 GHz (wavelength 3.8
cm) using left circular polarization, with some subset of the following
stations: the 120-ft (36.6-m) antenna at Haystack Observatory ("H") near
Westford, Massachusetts; the 210-ft (64-m) "Mars" antenna at the
Goldstone Tracking Station ("G") near Barstow, California; the 140-ft
(43-m) telescope at the National Radio Astronomy Observatory ("N") at
Green Bank, West Virginia; and the 85-ft (25.6 m) antenna at the Onsala
Space Observatory in Sweden ("S"). An 85-ft (26-m) dish at Fairbanks,
Alaska ("F") was also running on some of the early sessions, but the
amplitudes are virtually uncalibrated and are not of much use for the
analysis of source structure. All data was recorded on the NRAO Mark I
VLBI system. The sessions ranged from 12-hour Goldstack runs to 5-day,
4-station marathons that recorded upwards of 3 tons of magnetic tape.

This chapter endeavors to describe the observing sessions
themselves, from planning and scheduling, through set-up and running of
the stations, and the initial stages of data reduction and calibration,
from the point of view of the astronomer interested in source structure.
For analysis of some of the same data from the points of view of
astrometry and geodesy the reader is referred to Wittels 1975 and
Robertson 1975.

A.   THE GEOMETRY OF VERY LONG BASELINES

The geometry of the interferometer is of interest to the astronomer
for purposes of fringe processing, of course, and because it determines
the sampling of the visibility function. A summary of the subject is
therefore in order.

The baseline itself is expressed as a vector which points from
"station 1" to "station 2", represented as the difference in geocentric
Cartesian coordinates of the two stations expressed in
light-microseconds. The fringe spacing at any given moment is determined

by the apparent length of the baseline as seen from the source (Figure II.1), or, in other words, projected onto a plane perpendicular to a unit vector pointing toward it. The two-dimensional coordinate system (u,v) is defined in this plane, with u increasing to the east and v increasing to the north. The delay, between the arrival of the same wavefront at the two stations, is just the projection of the baseline onto the source unit vector. When all these quantities are measured in wavelengths, u and v represent the two-dimensional spatial frequency that the interferometer samples and the delay is the total fringe phase.

As the earth-fixed coordinate system rotates under the sky, the projected baseline traces out an ellipse in the (u,v) plane. Thus a number of different spatial frequencies may be sampled with the same pair of stations. The eccentricity of the ellipse depends on the declination of the source, forming a circle for a source at the North Pole and a straight line for one on the equator. As a result, the coverage of the (u,v) plane is generally poorer for the more southerly sources. Also radio telescopes generally have limit stops, the ultimate limit stop being the Earth itself, so that the entire ellipse is seldom sampled. With multiple baselines the coverage is much improved, but often still is far from ideal. This sorry situation marks the greatest single obstacle to mapping of compact radio sources through VLBI.

To maximize the coverage, it is desirable to have the various baselines in an array as different in length as possible, for minimum redundancy. "Crossing points", or places in the (u,v) plane sampled by more than one baseline, can be useful, however. If calibration of each baseline is not possible, crossing points may be used to tie together at least the relative scale factors between different baselines.

Before leaving the topic of geometry, consider a triplet of stations. The baseline vectors sum to zero, of course, and so do the delays and hence the phases, for a point source. If, however, the radio source is resolved to a different degree on the different baselines, its apparent location may differ, and then the phases will not "close". This deviation from zero provides another clue to the structure of the source.

B. BANDWIDTH SYNTHESIS FOR THE ASTRONOMER

Both geodesy and astrometry depend upon accurate measurements of
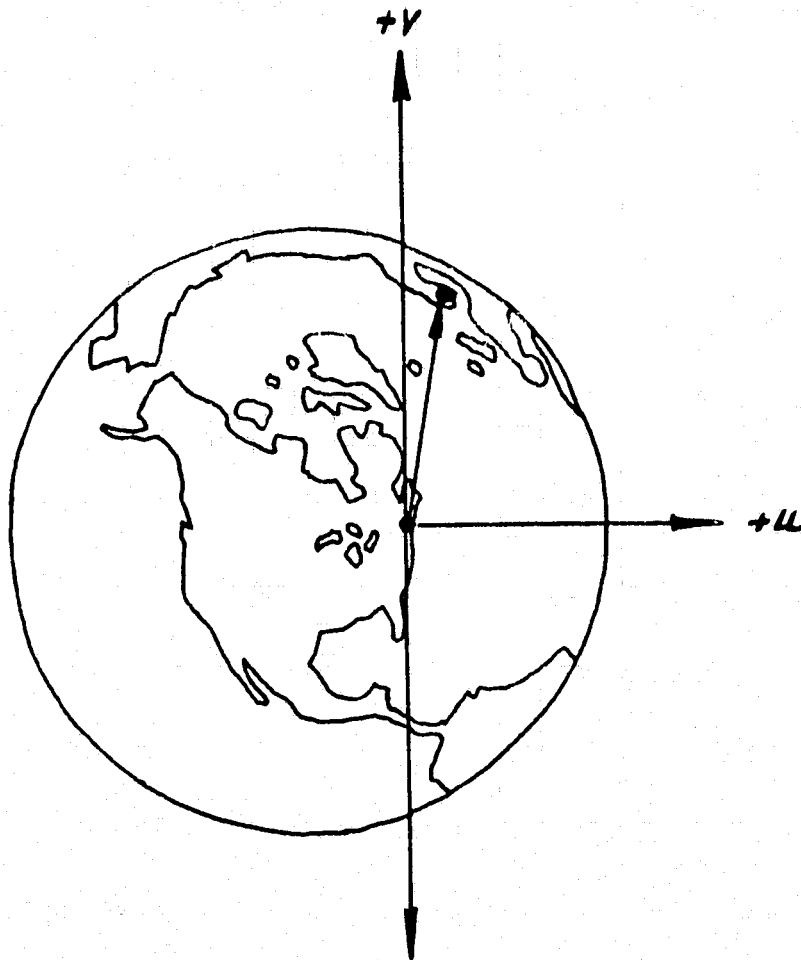
Figure II.1. The projected Haystack/Onsala baseline as seen from a northerly radio source. As the Earth rotates, the projected baseline will trace out an ellipse in the (u,v)-plane. v is positive to the north and u is positive to the east, in the direction of increasing right ascension.

the geometric delay. Here, however, VLBI is severely hampered by its
bandwidth restrictions, which come about because of the limited data
capacity of the tape recorders. The sky is full of fringes, so to speak,
and they all look alike. It is impossible to isolate a source in any one
of them. Fortunately, the necessary wide bandwidth does not have to be
contiguous; it may be synthesized from an array of narrow passbands in
the same way that an aperture may be synthesized from an array of
antennas.

In fact, it is instructive from the astronomical point of view to
consider the bandwidth synthesis system in the (u,v) plane. At each of
several different frequencies, a single interferometer has a different
resolution; it becomes, in effect, several interferometers. The beam
pattern of the resulting array no longer consists of identical fringes.
The "white-light fringe" has been isolated to an extent which depends on
the maximum frequency spacing, and with an ambiguity which depends on the
minimum spacing. The geodesist usually prefers to think of the beam
pattern in the delay domain and call it a "delay resolution function".
He measures the geometric delay as the rate of change of fringe phase
with frequency, rather than with resolution. Mathematically, however, he
does precisely what an astronomer does to locate a point source with a
synthesis array. (For the gory details of theory and practice see Rogers
1970, Hinteregger 1972 and Whitney 1974.)

Thus the typical Quasar Patrol experiment is spent switching in
rapid succession (0.2 second intervals) between 5 or 6 narrow passbands,
each 360 kHz wide, spaced over about 50 MHz near the "center frequency"
at 7850 MHz. The fringes are processed in each "channel" separately and,
if possible, averaged coherently with the phase reduced to this center
frequency. Ideally, there is no loss of sensitivity over a non-switched
observation. Instrumental dispersion must be calibrated by injecting a
coherent signal at the beginning of the receiver chain at each station
and processing these signals as if they were fringes. The "phase
calibrator" signal is injected continuously, but is weak enough not to
affect the system temperature, and, since it correlates at zero fringe
rate, it does not ordinarily interfere with the detection of the true
fringes. In the event of malfunction of the phase calibrator, the
fringes of a strong radio source can be used instead, assuming that the
instrumental dispersion is the same for the other observations as well.
If the instrumental dispersion information is lost, the amplitudes from

the individual channels must be averaged incoherently, with a corresponding loss in sensitivity.

It may one day be possible to use the extra (u,v)-plane coverage gained by frequency switching for the analysis of source structure. With the present system, the fringe amplitudes and phases do not change appreciably over the less-than-one-percent spanned bandwidth, and the increased sensitivity gained from the coherent averaging is considered to be more important. Both greater recording and spanned bandwidths are planned, however, for the future Mark III system. It may then be advantageous to treat each frequency channel separately in source structure analysis.

C. SCHEDULING

From the source structure point of view, (u,v)-plane coverage is the main concern; for any one source, it is desirabe to make measurements over as wide a spread in hour angle as possible. Given unlimited telescope time, or interest in only a few sources, and no geodetic requirements, the ideal schedule would have all the stations following one source at a time through its entire observable hour angle range. Only then is there a chance of obtaining the maximum amount of information about a visibility function that a given VLBI array can provide. This sort of scheduling, however, wastes observing time since some telescopes have to spend time waiting for sources to come up somewhere else.

Fortunately, most of the sources of concern to this program do not require such drastic measures. The visibility function can be expected to vary smoothly for a period of time dependent on the angular size of the brightness distribution. With the exception of 3C 84, the sources are small enough to allow gaps in the data on the order of an hour. The practical solution to limited observing time, then, is to move the antennas back and forth between a few sources in the sky, returning to each often enough so that the visibility function is "reasonably well determined". It should be noted that this sort of scheduling is also wasteful, in that large amounts of time are spent moving the telescopes. It does, however, better correspond to the geodesist's scheduling precept: the antennas should be cycling between at least three sources at

once.

A general knowledge of the expected visibility function for each source is necessary to make a schedule, as well as knowledge of the time scale of its variability (Which sources must be included in every experiment?). In addition to source structure, astrometry, and geodesy requirements, there are other headaches for the scheduler. For example, differential experiments (see Wittels 1975) tend to monopolize large blocks of time, causing gaps in the data for other sources. And there is usually a list of "trial" sources to be allotted a few runs each during the session. Also, it takes any normal human 30 seconds to change a tape, not counting rewind time. Some telescopes, typically Goldstone, are not available for the whole experiment. Different telescopes move at different rates about different axes. (A particularly tricky situation occurs when two sources near the same right ascension transit at Goldstone, one on the north side of the zenith and one on the south. This problem occurs with 3C 84 and 3C 120.) Telescope limit stops are all different. Cables must not be wrapped around the azimuth axis by more than their length. Extra time must be allowed for "peaking up" and for radiometry. Previous to the May 1974 session, Onsala had to be allowed two hours at regular intervals to replenish the cryogenic system. And so on, ad nauseum.

For these reasons, and more, efficiently scheduling the Quasar Patrol array has become an art which has never been completely computerized. The first approximation to a schedule, in fact, is often constructed with a celestial globe in hand, along with tables of rise and set times. Blocks of schedule may be lifted from previous experiments. One day's schedule should, as far as possible, be complementary to the previous day's in sidereal time, to fill in the gaps in the sampling. Extra runs may be inserted for the fast-moving stations while the slow ones are still changing source. The proposed schedule is then checked, to make sure that all the stations can keep up with it, by an ingenious not-so-little computer program (Vandenberg 1974). After a suitable number of iterations, the scheduler may be blessed with a "final" schedule, which is sure to be changed at the last minute over the telephone. The same computer program then prints multiple copies of fill-in-the-blank observing logs for each station.

D. SETTING UP AND RUNNING THE EXPERIMENT

As the appointed time approaches, the experimenters disperse themselves among the various stations and begin setting up for the experiment. Since the Mark I VLBI regime represents a major perturbation on the normal operation at most stations, this process can take as much as a day or more.

The hardware requirements for both astronomical and geodetic VLBI have been described so many times (see e. g. Hinteregger 1972, Whitney 1974) that it hardly seems necessary to add more words. A block diagram of the Green Bank station, however, is included (Figure II.2). The other stations, and even Green Bank on occasion, may have differed in detail from this example, but the general principles must remain the same or there are no fringes.

A few restrictions were put on the source structure effort by the requirements of the others, and benefits were reaped as well. One of the most far reaching in effect was the choice of the NRAO Mark I recording system, over the Mark II system. The Mark I's narrower recording bandwidth (360 kHz) restricted the sensitivity and limited study to the brightest dozen or so compact radio sources. Three advantages, however, emerged from its use. The first was that a great deal of care had been taken to account for all losses in correlation, so that it was possible to calibrate the fringe amplitude scale without appealing to unresolved sources, which may or may not exist. The second windfall came from the care the geodesists have taken to preserve the meaning of fringe phase, making it relatively easy to construct the so-called closure phase, on which much of the following analysis depends. Lastly, the Mark I system is more reliable than the Mark II.

Of particular interest here are the aspects of the hardware which affected the fringe amplitude calibration. Discussion of these, however, is best understood in the context of the data processing and will be postponed to a section on that topic.

The actual running of a VLBI session can be, with luck, extremely dull. When everything is working, the duties of the observer consist of changing the tapes, cleaning the heads, making the tape labels, keeping the logs, making sure the antenna operator points the antenna at the right place at the right time and takes the calibration data, and other even less exciting chores. The long periods of boredom are sometimes

-9-

-9-

Figure II.2. Block diagram of the Green Bank VLBI receiver.
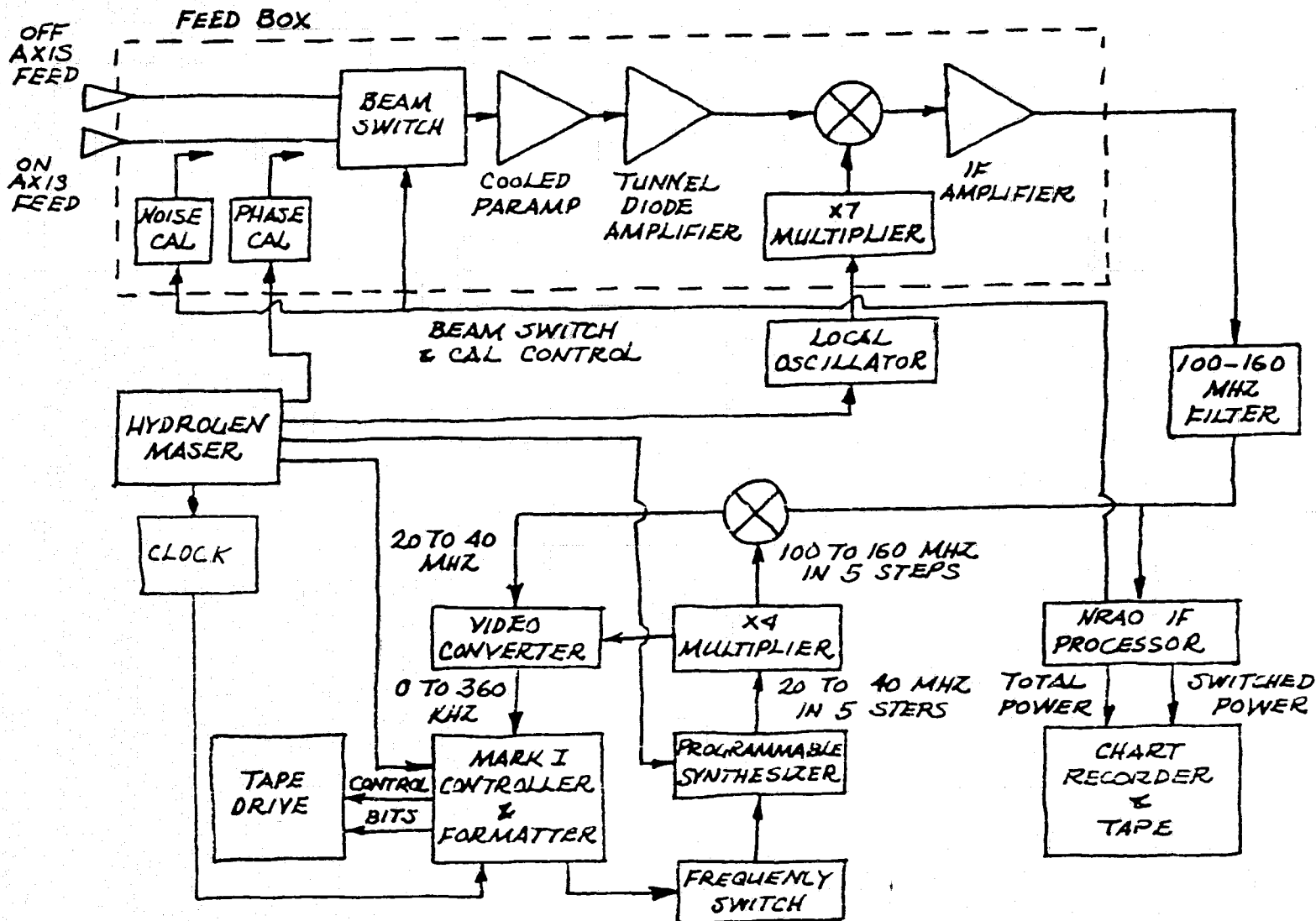
broken, however, by moments of intense panic, during which data is usually being lost. It then becomes the observer's responsibility to find and fix the problem, or find someone who can. VLBI suffers from the added complication that, although many checks on part or most of the system are run routinely, no overall check is available in real time. If fringes are not later found, it is not always possible to reconstruct what happened. Constant meticulous attention to detail and large amounts of faith are required of a VLBI experimenter. It is a tribute to the skill and dedication of the (large) Quasar Patrol team that so little data has actually been lost.

At the end of each session, the enormous pile of tape boxes outside the door at each station was shipped off to Haystack for processing.

E. DATA REDUCTION

In the case of VLBI, the term "data reduction" may be taken quite literally. In the first of two steps, the program "VLBI1" compresses on the order of 100 runs onto one output tape, which includes the complex correlation coefficients of each 0.2 second "record" of data for seven different delays. The program "VLBI2" further reduces the tape tonnage to 500 runs per output tape, by searching for and recording only the maximum (complex) correlation for each record. The 3 tons typically boil down to 4 or 5 VLBI2 output tapes. The inner workings of both these algorithms have been described in great detail by Hinteregger (1972) and Whitney (1974) in their theses, and in summary form by Vandenberg (1974), and will not be discussed further here. However, some description of the output format and of the corrections made to the fringe amplitudes is relevant to the calibration problem(s).

At this point, the data consist of, for each record, the complex correlation coefficient at the fringe rate and delay for which the fringe amplitude was a maximum. Corrections have been made for the effects of infinite clipping, nonzero residual fringe rate, etc., so that the amplitude gives the fraction of the recorded noise which was correlated. The Mark I system and the data processing programs were checked (see Wittels 1975) by simultaneously recording tapes including independent noise with a known amount of correlated noise added. The resulting correlations were always within 6 percent of that expected over a large

-11-

range of fringe rate and amplitude.

For an ideal, single-frequency run, the complex amplitudes could be simply averaged over the whole length of the tapes to increase the integration time. Because of the bandwidth synthesis, however, the records are not all taken at the same frequency. Instrumental dispersion and the change in resolution with frequency cause phase rotation. The practice, in the multifrequency case, is to rotate each channel to the center frequency, using the phase calibrator to determine the instrumental dispersion and the observed group delay to correct for the resolution difference. It should then be possible to average the complex correlation coefficients coherently through the whole tape. Problems, however, arose in practice. Some caused only headaches and others significant loss of data.

Because we are forced to work with the amplitude of the fringes, irrespective of phase, noise causes a positive correlation even when there are no fringes. Whitney (1974) has worked out a theoretical estimate of the expected correlation in the no-signal case (for clipped, band-limited data sampled at the Nyquist rate):

$$\sigma_\rho^2 = \frac{\pi}{4} \frac{1}{\Delta\nu\Delta t}$$

where $\Delta\nu$ is the bandwidth and Δt the integration time. Units are, again, fraction of the recorded noise. This figure serves as an estimate of the uncertainty in the estimation of the correlation coefficient in the case where there are fringes. With 360 kHz bandwidth and 3 minute coherent averages, the conventional 5 sigma detection limit becomes about 0.0007, or approximately 0.3 Jy on baselines involving the Goldstone antenna. The corresponding figure on HN is about 0.5 Jy, and for the Sweden baselines higher still.

Where there are fringes, it is possible to allow statistically for the additional correlation that the noise causes:

$$\rho^2 = \rho_0^2 - \sigma_\rho^2$$

where ρ is a better estimate of the correlation than ρ_0, which VLBI2 estimates. This correction is made to all the data, but is only significant for weak fringes, with correlation coefficients less that 0.0020. When there are no fringes, even the corrected fringe amplitudes are still positive, although small, and can systematically bias some of the amplitudes upward and perhaps affect the source maps.

If the system temperature is not the same in all the frequency channels, then corrections would have to be made to the amplitudes as well as the phases. We have found, however, that variations are negligible except when one channel is very near the edge of the receiver passband at some station. Rather than try to correct the amplitudes, we threw the data from the bad channels away.

Another, more recurrent problem, was phase noise due to somewhat less than coherent local oscillators. If a coherent average is made for a time longer than the time scale of the phase variations, the amplitude is systematically reduced by an unknown factor. Shorter coherent averages (normally 100 records or 20 seconds) were then used, with an ensuing sacrifice in integration time. The amplitudes from the individual 100 record "segments" were averaged incoherently to produce a whole tape average with a larger error bar.

Other equipment problems caused trouble, as well. Beginning with the August 1973 session a recurrent tape recorder problem at Green Bank and Sweden caused incredible numbers of parity errors and significant and variable loss of correlation. The error was almost completely compensated for in processing beginning in March 1974, but the two week-long, 4-station August and October 1973 sessions were left in shambles, most of the data tapes having been re-used before the cure was discovered. Large amounts of bad and doubtful amplitude data were thrown away, and many more were re-averaged using only records without parity errors. As a result, much of the data from these experiments is considerably noisier than the other sessions. The August session had calibration trouble as well, as we shall see shortly, so the loss was not as bad as it could have been.

During the March 1974 experiment an electronic problem at Green Bank caused a more or less uniform loss of correlation, the amount of which had to be determined empirically. This correction depends on the system temperature, but, to a close approximation, it can be assumed to be constant for any one source.

At this point, we again summarize the state of the amplitude data, now considerably "reduced". With luck, we have an estimate of the fraction of the recorded noise which was correlated, along with an error bar. These data must now be merged with the station radiometry to translate the amplitudes into units of flux density.

-13-

F. RADIOMETRY

To normalize the fringes, it is necessary to know the fractional contribution of the radio source to the total system noise temperature at each station. In practice, both the system temperature (T_q) and the contribution to it due to the source (T_a) are either measured or calculated individually. Both values can generally be expected to vary with antenna elevation, and with the weather, so that a more or less continuous record is virtually mandatory for a good calibration. Unfortunately, such a continuous record has not always been possible and it has been necessary to improvise some of the calibration.

The simplest radiometry scheme was that employed at both Goldstone and Haystack, where the (broadband) system temperature was measured using a noise-adding radiometer system. Measurements both on and off source were repeated, if possible, before and/or after each VLBI tape. This system is particularly effective at Goldstone, where the system temperature is very low, the effective aperture is very large, and the weather is usually very good. The Goldstone radiometry data has also been used whenever possible for determining total source fluxes for the times of the experiments. The source fluxes were scaled to total power observations of DR 21 and 3C 274 (Dent 1971, Baars and Hartsuijker 1972). The Haystack antenna is smaller, however, and the receiver and atmosphere noisier. It was not always possible to "see" the weaker sources in total power. The usual remedy, in such cases, was to compute the source temperatures based on an efficiency-versus-elevation curve determined from a stronger source and the source flux as measured at Goldstone.

At Green Bank, the system temperature was monitored by a manual version of the noise-adding radiometer scheme, with a measurement taken for every tape. The source temperatures were measured, however, in a beam-switching mode, which eliminated the effects of, among other things, the beautiful West Virginia clouds. As a result, the Green Bank calibration was second only to Goldstone's and was sometimes used for total fluxes.

As far as calibration is concerned, the "problem child" was definitely Onsala. The antenna itself is relatively small and was not intended for use at 7.8 GHz; the aperture efficiency was barely 15 percent. On top of this, no successful effort at calibration was made

until near the end of the experiment series. One attempt did occur in August 1973, when several measurements were made of Cassiopeia A to determine the antenna efficiency. All the data were recorded on a strip chart, which unfortunately had to be cut into a number of sections to get it off the malfunctioning recorder. The result looked too much like trash and was inadvertently thrown away before it could be analyzed. System temperatures for each observation, with the exception of August 1973, were measured with a "Y-factor" system, where a variable attenuator is used to compensate for an increase in system temperature due to a noise source. The attenuator setting (the "Y-factor") was recorded in the log. For sessions prior to May 1974, all the source temperatures were computed based on an efficiency of 12 percent as measured in May 1973, on the assumption that pointing was perfect and that no elevation dependence was present. The former is probably not a bad assumption, except in high winds, whereas the second could cause large systematic errors. In May 1974, a new cryogenic system was installed, and the noise source temperature was changed and never measured accurately. A concerted effort was made to calibrate the new system in July 1974; much to everyone's surprise, 3C 84 (at 60 Jy) was discernable in the records. (The Y-factor attenuator was used to compensate for the increase in the noise temperature due to 3C 84, and the reading recorded.) During this particular session, the system temperature varied from about 105 K. near zenith to 120 K. at 15 degrees elevation, and increased rapidly below that. The scatter on the efficiency measurements was close to 20 percent; within that range, there was no evidence for any variation with elevation. The average value of 0.03 K/Jy, or about 15 percent, was adopted for both May and July 1974, even though some inconsistencies result (Wittels 1975). The scatter is much less in the correlation coefficients, indicating that most of the noise originated in the radiometry methods, rather than, say, pointing. The upshot of this discussion is that rather large systematic errors probably exist in the Onsala calibration. The overall scale could easily be off by 20 percent. In addition, a "skew" in the calibration scale, as a function of Onsala hour angle, might exist due to neglect of the elevation effects (especially in August 1973, when the system temperature had to be assumed constant). An intuitive estimate of the largest possible systematic error leads to a figure in the 20 to 30 percent range.

Estimates of the error bars for the radiometry have generally not

been too rigorous. In cases where the temperatures were measured or the antenna parameters well determined (in other words, H, N, and G), they were estimated from the scatter, which seems to be largely due to atmospheric effects, and is therefore time variable. When fringes are strong, most of the error in the final normalized fringe amplitude comes from the radiometry, so it is a stroke of luck that our best calibrated antennas determine the shortest baselines. Radiometry errors for Onsala were estimated from uncertainties in the parameters used to calculate the temperatures. Fringes were seldom strong on Onsala baselines and most of the error in the normalized amplitudes came from the uncertainty in the correlation coefficients.

Radiometry data and error bars having been determined by one means or another, it remained only to normalize the correlation coefficients to units of correlated flux density

$$S_c = S\rho \sqrt{\frac{T_{s1} T_{s2}}{T_{a1} T_{a2}}}$$

Here S is the total flux and S_c the fringe amplitude in Janskys. It has been customary to work with the fringe amplitude in these units because the maps may then be computed in brightness temperature units if desired. Error bars for the fringe amplitudes were computed from the correlation coefficient and radiometry error estimates, assuming all the contributions to be independent. In most cases the computed error bars agree reasonably well with the amount of scatter in the data, a fact which inspires confidence in the estimation procedure.

G. CLOSURE PHASE

To measure a source brightness distribution uniquely, we must know the complex visibility function. Amplitude data alone, no matter how much of the (u,v) plane it samples, cannot produce a unique solution. VLBI is not generally able to measure the fringe phase because the relative phase of the local oscillators at the two stations as a function of time, and atmospheric phase shifts as a function of time, are unknown. We are therefore forced to "make do" with the next best thing, the so-called "closure phase". The idea was first used by Jennison (1958) for early radio link interferometers, which were not phase stable, and has been applied in its present form to VLBI data by Rogers et al.

(1974). The closure phase is simply the sum of the observed fringe phase, including all of the error terms, summed around the triangle of baselines formed by three stations. All phase error common to only one station, including local oscillator and atmospheric phase errors, add twice with opposite signs and cancel. We are left with the sum of the visibility phases on the three baselines.

One minor complication is introduced because a triplet of stations (e. g. "HNS") is generally processed in the order HN, HS, NS. "Baseline 2" (HS) is backwards and the sign of its phase must be reversed for the sum.

Another minor complication comes from the fact that the earth rotates between the times of arrival of a wavefront at the different stations. Hence, by normal processing conventions, the delay (and hence the phase) on baseline 3 has been computed for a slightly different a priori time than on the other baselines. The baseline 3 phase must be rotated back in time to correspond to the arrival time at station 1 (in this case H).

Frequency switching remains a minor complication as long as the phase calibrator is working well. In that case, the individual channel phases can be rotated back to the center frequency, averaged, and summed to obtain a closure phase appropriate to that frequency. If the phase calibration is poor, this procedure will introduce extra noise into the closure numbers but will not produce any systematic effect. In no case is any of our data affected by more than about 20 degrees of phase due to poor phase calibration.

Phase noise does not affect closure phase, so long as the individual baseline coherent averaging is done over a time period shorter than the time scale of variation. If the coherent averages are longer, however, noise can be introduced, but again there are no systematic effects. To avoid the problem, closure phases were constructed for each 100-record segment and these were averaged incoherently for the whole tape.

Closure phase for runs severely affected by parity errors had to be recomputed, deleting all the bad records.

The error bars which were computed for the closure phase data points include only the uncertainty (σ_ϕ) in the phase estimation itself (see Whitney 1974):

$$\sigma_\phi = \frac{\pi}{2\rho} \frac{1}{\sqrt{2\Delta\nu\Delta t}}$$

The closure phase error bar is taken to be a quadratic sum of three of these, one for each baseline. This is appropriate when the fringes are strong. The size of the error bars increases rapidly with decreasing correlation, meaning that the closure phase is noisy when fringes are weak on any one of the three baselines. The additional noise due to poor phase calibration and phase noise has not been included; in some cases, then, the size of the error bars may be too low. Again, however, the error estimates agree reasonably well with the scatter in the data.

It should be pointed out that for a 4-station run, only three of the closure phase data points are independent. The fourth is a linear combination of the other three, and adds no new information to the solution.

H.   SUMMARY OF EXPERIMENTS

For convenience, a table (Table II.1) listing all the Quasar Patrol experiments has been prepared. Sessions have been included in the table whether or not they contain data on the sources under consideration here. The station abbreviations (H = Haystack, G = Goldstone, N = NRAO, S = Sweden, F = Fairbanks, Alaska) will be used throughout this thesis. Any problems which could have affected the accuracy of the data, such as problems with the weather, the frequency standards, or any of the other equipment, are listed. Unless otherwise stated, hydrogen maser frequency standards were used at all the observatories.

Table II.1   A List of Quasar Patrol Experiments.

Dates	Stations	Problems
14, 15 April 1972	H, G	
9, 10 May 1972	H, G, F	Rain at H
29, 30 May 1972	H, G, F	
3 June 1972	H, F	
6, 7 June 1972	H, G, F	
27, 28 June 1972	H, G	
3, 4 July 1972	H, G	Not frequency switched
29, 30 August 1972	H, G	
7 November 1972	H, G	
4, 5 February 1973	H, G	
30, 31 March 1973	H, G	
17-19 May 1973	H, G, S	Rb standard at G
22, 23 May 1973	H, S	
10-14 August 1973 Cs standard at G No S radiometry	H, N, G, S	Parity errors at N and S
12-16 October 1973 Rb standard at G	H, N, G, S	Parity errors at N
22, 23 January 1974	H, G, S	Scheduling problems
4-8 March 1974	H, N, G, S	Equipment problems at N
29 April-3 May 1974	H, N, G, S	Rain at H
8-12 July 1974	H, N, G, S	
27, 28 October 1974	H, N, G	
15-17 January 1975	H, N, G	
28 May 1975	H, G	
24 August 1975	H, G	

Chapter III

DATA ANALYSIS

Given seven boxes of cards, containing the amplitudes and closure phases and error estimates, the observer's next chore is to translate these into source maps. This is precisely the problem over which VLBI'ers have torn out hair ever since there has been enough data to even consider the possibility. It is not an easy one, for basically two reasons: lack of phase information and poor sampling in the (u,v)-plane.

Without any form of phase data, the solution for the brightness distribution is ambiguous. There are at least two solutions, namely the correct one and its mirror image, and probably many more. The use of closure phase provides at least a partial solution to the problem. Even with it, however, VLBI does not become true aperture synthesis. Because the phases on the three baselines must somehow be separated, it is not possible to work directly with the complex visibility function; the algorithms must be more devious.

Closure phase makes possible a better description of the visibility function at the points sampled, but it does nothing to improve the sampling. Only more and/or better distributed baselines can do that. Between the case where sampling is complete and the one where there is clearly not enough data, there lies the hazy region of "almost enough." VLBI with four or five stations, which is common enough now but constitutes a tremendous effort, lies in this hazy realm. Generally speaking, it is necessary to exchange some a priori information about the source for the missing data. A common form for this information is assumptions about the number and shape of the individual source components (see e. g. Purcell 1974). It may or may not be possible to represent a given set of data in this fashion, since sources seldom have true Gaussian brightness distributions. In this analysis, the assumptions have been made instead about the angular size of the source, the goal being to find the smallest source which can represent the data rather than the one with the least components. Before the mapping algorithm is described in detail, however, a short digression on the interpretation of closure phase is in order.

A. ON THE VISUALIZATION OF CLOSURE PHASE

It is easy to see that the closure phase for an unresolved source is identically zero, irrespective of the source's location in the sky. Therefore, closure phase is of no direct use in astrometry.

A symmetric source of any type produces a similar effect, since such a brightness distribution has a real Fourier transform. If all three visibility phases are equal to zero, the closure phase must be also. The real visibilty function, however, may be negative, which we interpret as a phase of plus or minus 180 degrees. Then the closure phase will be 0 degrees when an even number (including zero) of the baselines show a phase of 180 degrees, and will be 180 degrees when an odd number do. As a function of time, one would expect the closure phase on a given triplet to alternate abruptly between 0 degrees and 180 degrees as the amplitudes on the various baselines pass through sharp nulls.

Any deviation from 0 degrees or 180 degrees indicates that the brightness distribution is not symmetric, and also indicates the direction of the asymmetry. This becomes clear when we recall that inverting the brightness distribution reverses the sign of the visibility phases, but leaves the amplitude unaffected. The closure phase therefore determines the orientation of the source, a piece of information which is not available from amplitude data alone.

As a simple example, let us consider an equal point double brightness distribution on the equator, to be observed by three east/west baselines. Its visibility function would look like Figure III.1.a. In the region where the amplitude is negative, we measure a positive amplitude with a phase of 180 degrees. At time A, the beginning of the track, all baselines are within the first null and have 0 degree visibility phase; hence, the closure phase is 0 degrees also. At time B, however, baseline 1 (the longest) has crossed the null and its phase is now 180 degrees, while the other two phases are still 0 degrees. At time C, all the phases have returned to 0 degrees. The behavior of the closure phase as a function of time would look like Figure III.1.b. The same "excursion from zero" effect can also be produced by a triplet containing two long baselines which cross the same null one after the other. In the case of equal point doubles, the closure phases are
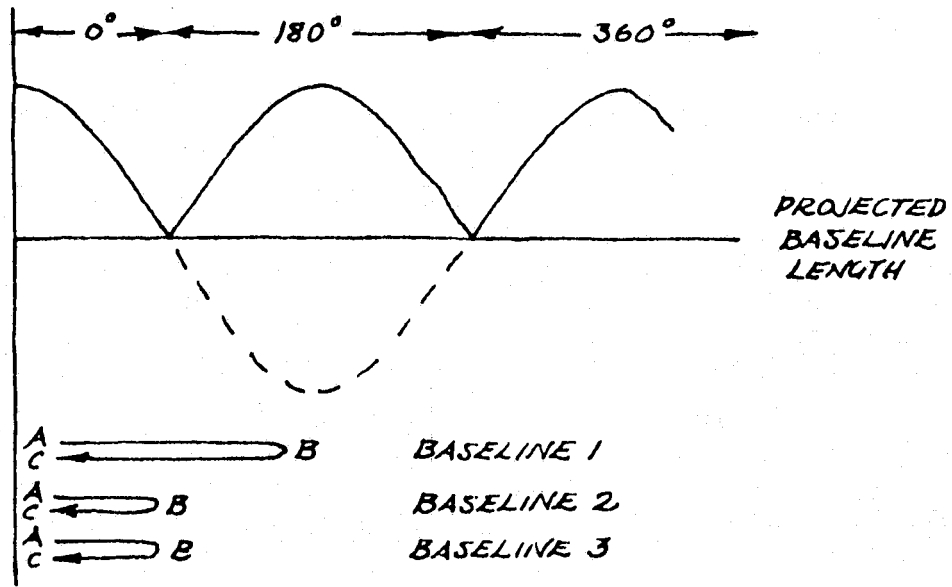
Figure III.1.a. Visibility function for an equal point double source in one dimension.
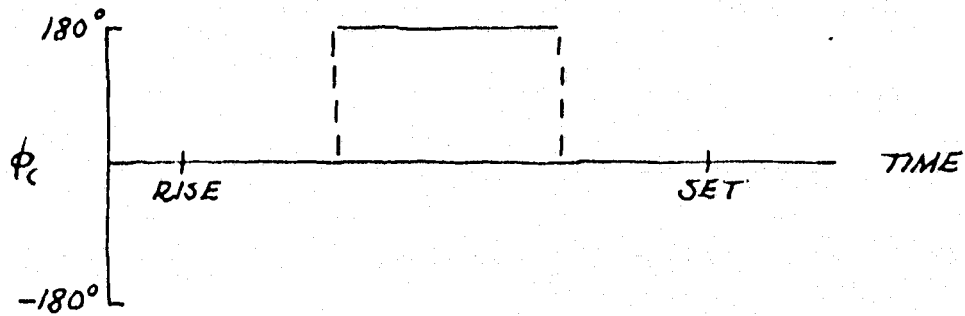

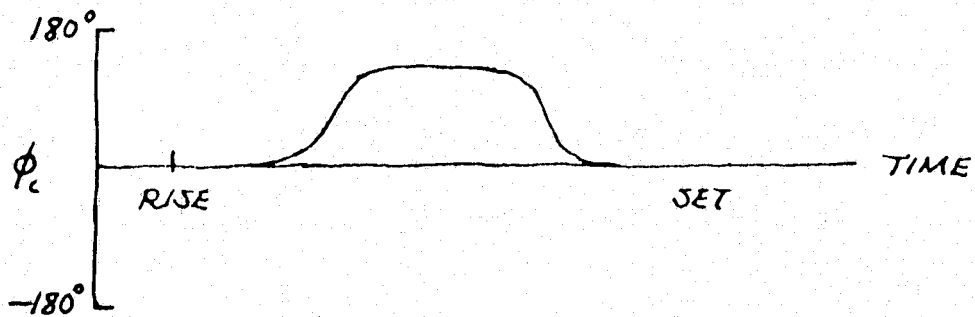Figure III.1.b. Closure phases of the above visibility function observed by the triplet shown.

Figure III.1.c. Closure phase of an unequal ppoint double source observed by the same triplet.

-22-

relatively easy to visualize. If the source components were not points, but had the same shape, the source remains symmetric and the phase behavior is similar.

If the point components were unequal in flux, the sharp nulls would disappear and the phase jumps would be more gradual and would not reach 180 degrees. If the same array of east/west interferometers were to observe such a source, the closure phase jumps would also be more gradual (see Figure III.1.c). It is easy to see how quickly the closure phase curves become complicated when all the baselines are crossing minima!

It is instructive to think of a double source with extended components as if it were a point double with each component having a power equal to the correlated flux the true component would have at the current resolution. We have, in effect, a point double whose flux densities change as a function of resolution. This is strictly true if the visibility function for each component has 0 degree phase, for example, if it is symmetric and is being observed inside the first null. Otherwise, the component positions as well as their powers are functions of resolution.

Although this system of graph-paper Fourier analysis may seem a bit artificial, the author has found it very useful in deciding what to expect in analysis of a given source. It has saved a substantial amount of computer time, if nothing else.

B. MAPPING

The more or less traditional method of source structure analysis in VLBI is model-fitting (see e. g. Purcell 1974). In this technique, the brightness distribution is assumed to consist of a small number of individual circular or elliptical Gaussian components. The parameters of the components, relative positions, fluxes and sizes, etc., are then fit to amplitude data by some sort of iterative least-squares technique. The same process can be applied with closure phase data, used simultaneously with the amplitude data, with some improvement. The closure phase determines the orientation of the brightness distribution, and simply adds more data. Model-fitting, even with closure phase, however, has its difficulties. For one thing, the initial guess at the model from which the iterations begin must be quite close, a fact which makes the

procedure frustrating, at best. In addition, the models are confined to a relatively small number of simply shaped components. The actual source may or may not be representable to within the errors by the chosen model. Furthermore, except for very simple cases, it is virtually impossible to evaluate the degree of uniqueness of a model, once it is found.

We would like to have a method of producing a map or maps of the brightness distribution. A map, in this context, would refer to any regular grid of hypothetical point sources whose flux densities are such that the observed visibility amplitudes and (closure) phases are reproduced. Let us assume, for the moment, that the source has been completely resolved on the longest baseline (u_{max}); the fringe amplitude is zero there and beyond. Then the well-known sampling theorem of Fourier transforms (see Bracewell 1965) tells us that such a grid representation is possible and that the spacing of the grid should be $1/(2u_{max})$. Larger grid spacings will not reproduce the data and smaller spacings extract no new information. The map grid may be as large as desired, but it need only be as large as the brightness distribution.

The technique adopted here has been to least squares fit the flux densities of these hypothetical point sources to all the data, amplitude and closure phase, simultaneously. A little thought will show that this is equivalent to fitting for the coefficients of the (complex) Fourier series coefficients of the visibility function. Unfortunately, because the amplitude and closure phase are nonlinear functions of these coefficients, iterative methods are necessary. Specifically, a gradient expansion search for minima in χ^2 space, "Marquardt's algorithm", has been employed. The solution can be expected to be well determined provided that the brightness distribution is restricted to be small enough that most of the corresponding sampling cells in the (u,v) plane contain data points. If this requirement is not satisfied, the (u,v)-plane coverage is deemed insufficient to map a source of the required size.

Complications arise in cases where the visibility function is not yet zero on the longest baseline (see Figure III.2). This is the case for virtually all Quasar Patrol observations since the sources are picked to show fringes on all the baselines. Some sort of spatial frequency filter must be applied to force the visibility function to zero beyond u_{max}, or in other words, the source brightness distribution must first be smoothed to a resolution appropriate for the antenna array before being
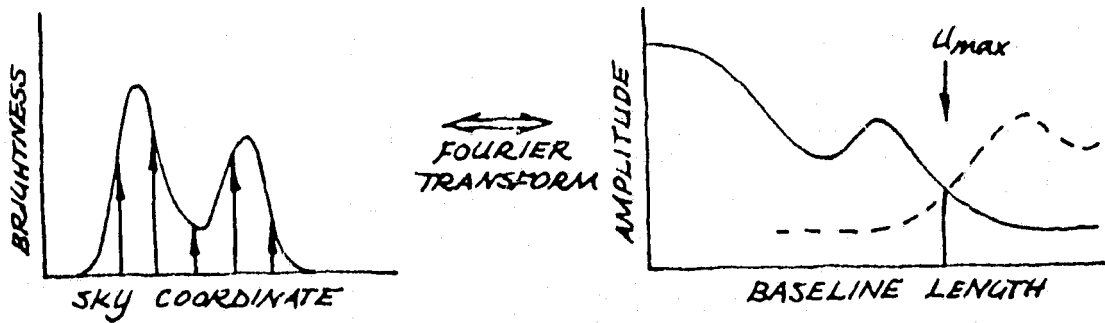
Figure III.2.a. The sampling of a one-dimensional source whose
visibility function does not go to zero beyond the maximum observed
spacing. Power is aliased into the observed part of the visibility
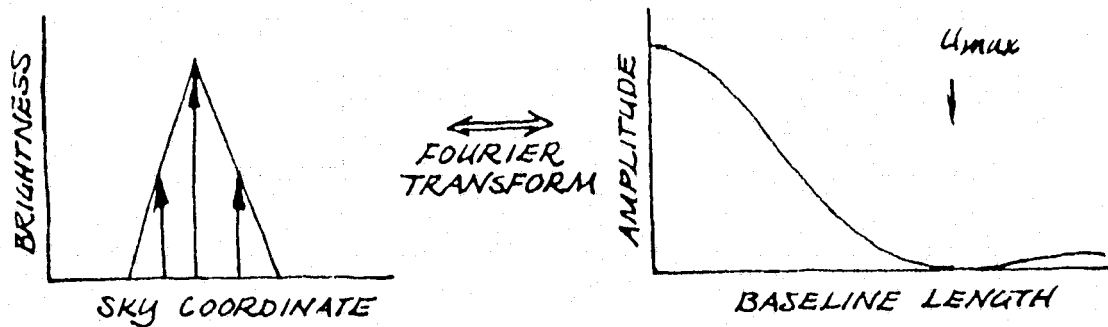function from the adjacent image.

Figure III.2.b. One-dimensional convolving function and spacial
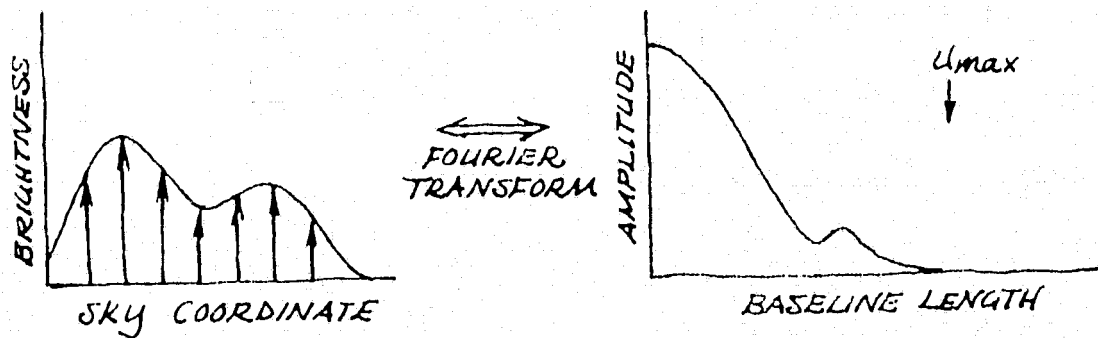frequency filter.

Figure III.2.c. Smoothed brightness distribution and filtered visibility
function.

sampled. The smoothing function is arbitrary, but if the necessary grid
is to be kept as small as possible there can be no sidelobes. The
function that has been chosen is the "rectangular triangle function"
whose Fourier transform is

$$T(u,v) = sinc^2\left(\frac{u}{u_{max}}\right) sinc^2\left(\frac{v}{v_{max}}\right)$$

This choice is made over an elliptical function on the basis of computer
time considerations; the Fourier transform of the "cone function"
involves integrals of Bessel functions. The observed fringe amplitudes
are multiplied by $T(u,v)$ before fitting. We are guaranteed that at most
one more grid row will be necessary on each side of the brightness
distribution, because of the convolving function. The maximum error
possible due to overlap with the next image in the (u,v) plane is about 5
percent and if the source is well resolved it should be much less. In
order to avoid setting any hard-won data points entirely to zero, and
hence jeopardizing the least-squares solution by doing the same to the
error bars, u_{max} has been set 10 percent beyond the highest resolution
actually sampled.

In exchange for such a "clean beam", one sacrifices resolution. In
this case, however, where we have very little knowledge of the source
structure to begin with, the absence of confusing sidelobes should be
considered enough of a blessing to justify the loss in resolution.

Fitting in the sky domain in this way allows the enforcement of
another physical restriction: the source brightness must be everywhere
positive. The volume of parameter space which must be searched is
thereby reduced by a factor of 2^N, where N is the number of grid points.
Practice has shown that this procedure is usually necessary. Evidently
the noisy and incomplete data distribution can allow unphysical solutions
to have lower values of χ^2 than the desired one. The convergence of the
algorithm is slowed in the process.

The use of any sort of iterative technique always brings up the
question of initial parameter values. Here the gridding method shows its
character as the model fitting technique that it is. There is no a
priori way of knowing what initial grid will allow convergence along a
"clear path" in χ^2 space to the deepest minimum. Through experience,
however, it has been found that a detailed initial approximation is
usually not necessary. It has generally been adequate to begin with all
the parameters zero except for one point, which is set to some small

value. If the point has been selected so that the source will fit on the grid with a peak in the brightness at that position, the solution will generally converge. A number of trials may be necessary to find such a starting point, but the approach is systematic and requires no detailed knowledge of the brightness distribution other than its overall size. It is also possible, however, to input a better initial approximation. For sessions with relatively little data on a given source, it is sometimes convenient to begin the iterations with a source map from some other, better determined, set of data (or from any other suitable form of lucky guessing).

For presentation purposes, the sky grids were all convolved with the transform of $T(u,v)$ and formed into contour plots.

C. ERROR ANALYSIS

We now assume, for the moment, that the form of the fitting function allows a reproduction of the data for some parameter values. In other words, the data contain no systematic errors and the grid is large enough. Three considerations then arise in the error analysis. Assuming that a minimum has been found, we need to evaluate the purely statistical effect on the solution of the error bars on the data points, and also the intercorrelation between the parameters. We also need to know something about uniqueness; how many other similar minima exist within reasonable value ranges of the parameters?

These different effects will be evaluated as well as possible in this section, but first a fairly detailed description of the least-squares fitting technique is necessary. The algorithm works in parameter space, which has as many dimensions as there are fitting parameters. The function χ^2, or the mean square deviation of the computed curve from the data, is a continuous function of position in parameter space. A typical χ^2 minimum should be somewhat ellipsoidal in shape near the "bottom". Inside the minimum, χ^2 may be evaluated at various points and a parabolic curve in each dimension fitted, which can then be used for a quick and accurate location of the extremum. Such a procedure is completely equivalent to linearization of the fitting function by means of a Taylor series and subsequent use of linear least squares fit techniques to find corrections to the parameters (see

Bevington 1971). Standard error analysis techniques appropriate to linear problems may be applied. Such a method works well, however, only so long as the starting point is already inside the minimum. In a search for the minimum, it is more efficient to simply increment along the perhaps circuitous path of steepest descent of χ^2. The Marquardt algorithm allows a continuum of variation between these two modes, depending on the texture of χ^2 space, by the addition of a self-scaling constant to the diagonal terms of the normal matrix. The computer code first searches for a minimum by moving along the direction of largest negative gradient and then, once inside, solves for the exact location of the minimum through parabolic interpolation. Restrictions on the allowable values of the parameters are implemented by simply preventing the search from proceeding past the limit stops.

Once inside the minimum, where the linear approximation to the fitting function applies, both estimated errors for the parameters and inter-parameter correlation coefficients can be simply calculated from the inverse of the normal matrix. Except in cases where one or more walls of the minimum are formed by numerical limit stops, so to speak, the error bars thus obtained have been "reasonable". In other words, the power contained in the noise in both the sky plane and the (u,v) plane is about the same.

The parameters, however, are often very highly correlated. Correlation coefficients anywhere between nearly zero and well above .8 have been observed. This means, in general, that the estimated errors on the parameters do not provide a complete picture of the uncertainties in the map. Such high degrees of correlation, it might be added, are not unexpected. Since there is no positional information contained in the closure phase, the brightness distribution can "slide around" on the grid, to the extent that it will reproduce, and still reproduce all of the data equally well. An even more fundamental problem derives from having performed the fit in the sky plane, as opposed to the (u,v)-plane. Although the grid points are uncorrelated, according to the sampling theorem, for the highest resolutions, as far as the majority of lower resolution data points are concerned, flux could equally well be redistributed between many of the grid points. Within the context of sky-plane gridding, and model fitting in general, there is no way to improve the parameter independence.

Since, therefore, the error bar estimates do not mean very much, we

are more or less left to our own devices to decide how much faith to put in the computer output. Although the numerous trials that can be necessary to find a solution may be a bother, they can help here by putting a handle of sorts on the uniqueness problem. If essentially the same maps emerge from different initial grids, one may have some faith that the distribution is well determined by the data. If different maps emerge, one should be wary. Experience has shown that, in most cases of decent data distribution, the maps are repeatable. We would like, however, to inspire some degree of confidence by mapping otherwise known sources. That is the subject of the next section.

D.   PERFORMANCE ON TEST DATA

We need a source whose brightness distribution is known in advance to try the algorithm out on. None exist on the millisecond of arc scale in the sky, so one has been created in the computer. This source (Figure III.3), known as "XXXXXXXX" for lack of a better name, consists of three circular Gaussian components of various sizes and flux densities. Note that since the Gaussians never truly go to zero outside of any finite grid, a certain amount of error is introduced by truncating the grid. This is, however, realistic, because the same thing would happen for any actual source with a halo.

Source "XXXXXXXX" has been "observed" with the same (u,v)-plane coverage that was achieved on 3C 84 (declination +42 degrees) during the July 1974 session using all 4 stations (Figure V.2). Generation of the "data" in this way is somewhat unrealistic. In actual data, the distribution of closure phase points is affected by the fringe amplitudes, there not being any when the fringes are below the detection limit on any baseline. There is not, however, much closure phase data missing, and simplicity dictates that the test source data be generated in this way. The source was also "observed" with the sampling obtained on 3C 120 (declination +5 degrees) during the same session, to illustrate the case of poorer (u,v)-plane coverage.

A number of computer runs were performed. First, the system was checked on perfect data, the no-noise case. Following that, noise on the 15 percent level was added to both amplitudes and closure phases. Since it is possible, or even probable, that the Onsala calibration scale is in
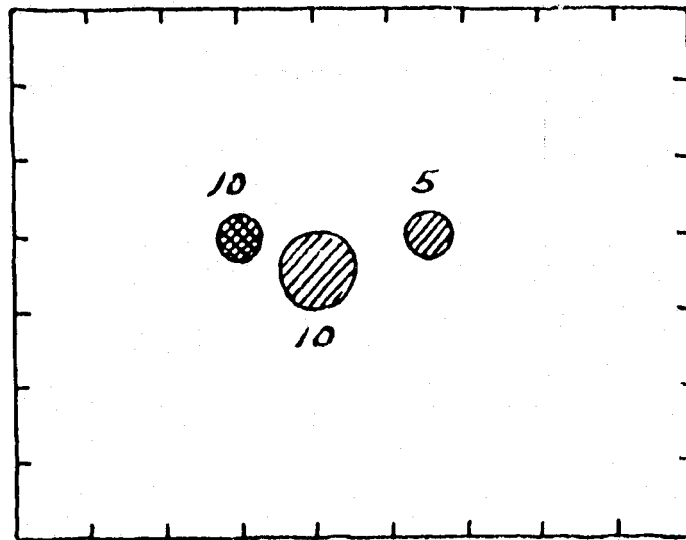
-29-

TEST SOURCE

Figure III.3. The computer-generated test source, consisting of three circular gaussian components with the half-width shown. Component fluxes are given in Jy. The angular scale is in milliseconds of arc.

error, two runs were made with all amplitudes on the Onsala baselines too high by 20 percent, and too low by 20 percent. An attempt was also made to simulate the lack of elevation corrections at Onsala by skewing the calibration scale up and down by multiplication with a parabolic function of Onsala hour angle. The amount was 20 percent at hour angle 6 hrs. These maps of source XXXXXXXX are presented in Figure III.4. It is fairly clear that errors on this (reasonable, in practice) level have little effect on the appearance of the map, although some of the details are changed. In general, the algorithm seems to do what one would expect; for example, if the scale of the highest resolution is adjusted downward, the map is appropriately broadened.

The cases of perfect and noisy data were also tried on the test source at the declination of 3C 120 (Figure III.5). As we see in the next chapter, only the H, N, and G stations were used for 3C 120, so only these were used in the test as well. the larger and more elongated beam obscures the structure. The result resembles some of the actual 3C 120 observations.

An infinite number of different runs on realistic and unrealistic test sources could be constructed. In view of the success shown here, however, we quit and proceed to real sources.
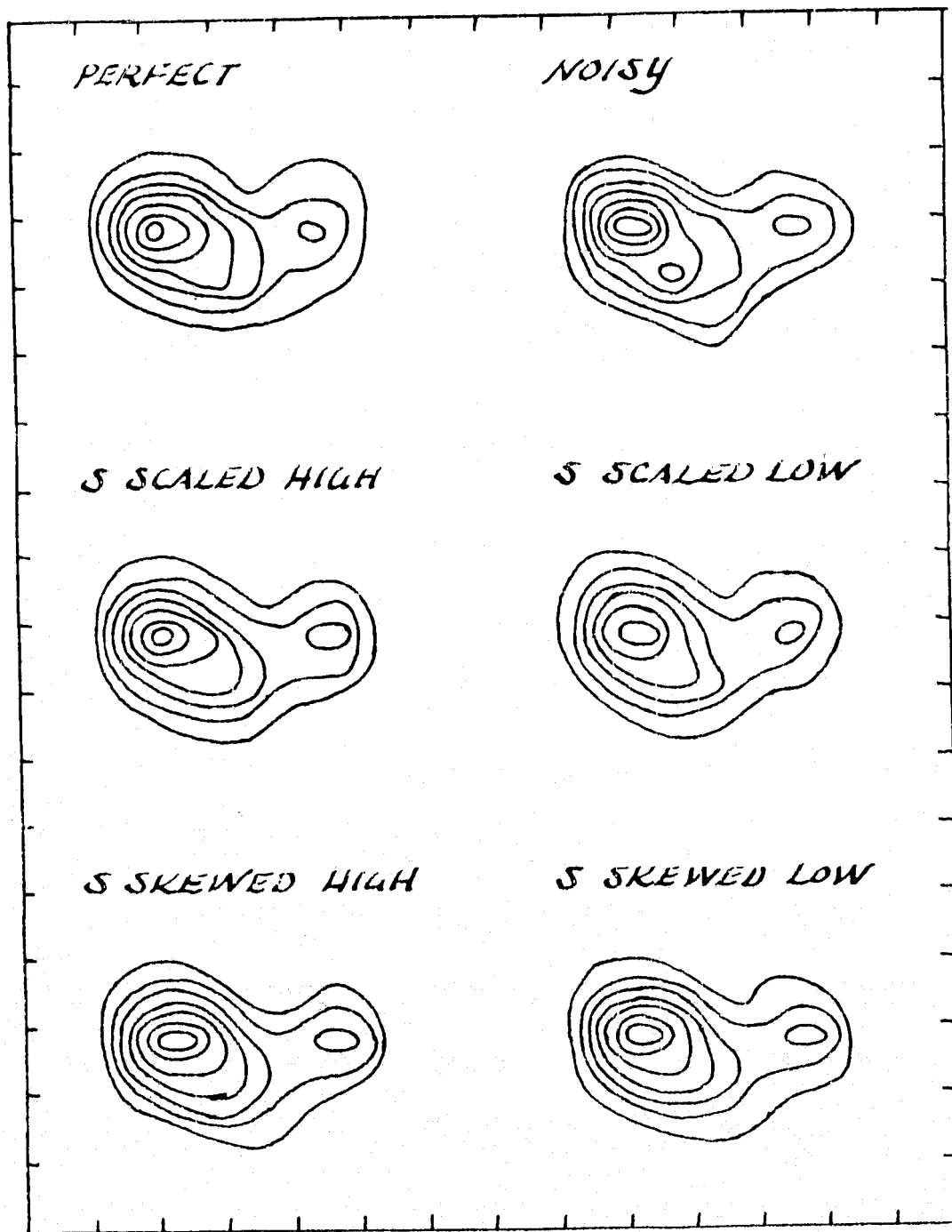
Figure III.4. Results of mapping tests on the test source as explained in the text. Baselines used were HN, NG, HG, HS, NS declination assumed was +42 degrees.
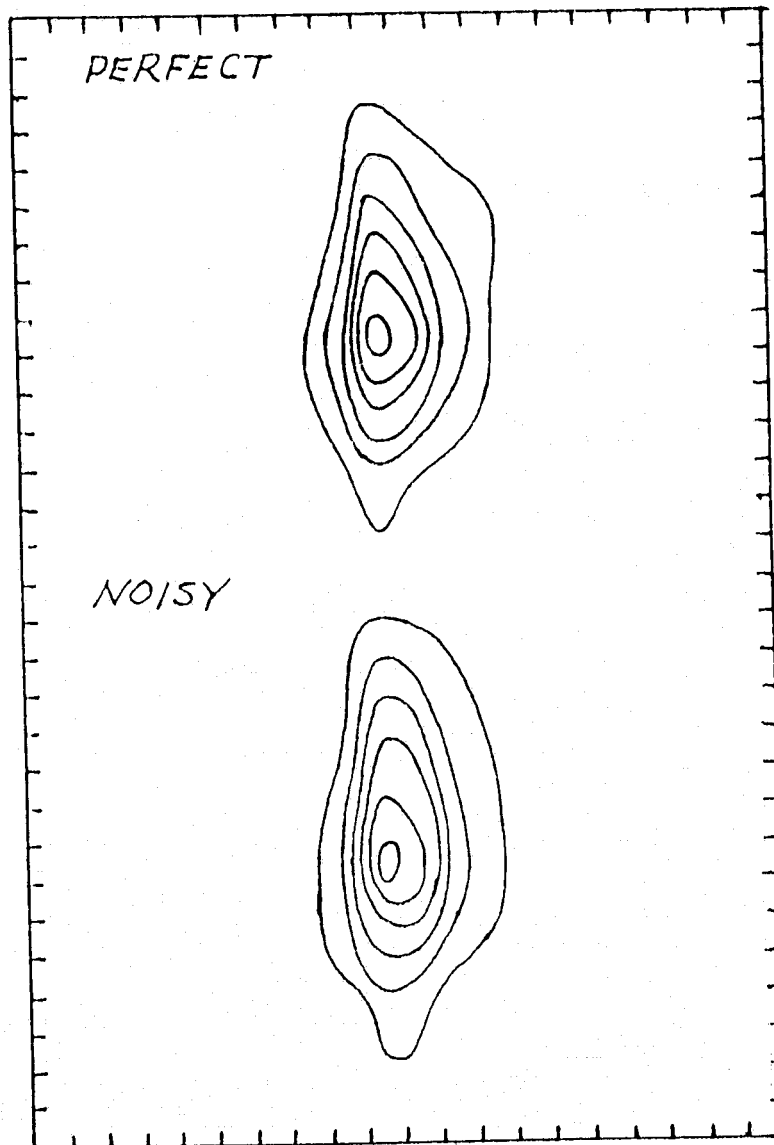
Figure III.5. Results of mapping tests with an assumed declination of +5 degrees. Baselines used were HN, NG, HG.

3C 120

In spite of the poor (u,v)-plane coverage that it generally displays for earth rotation synthesis (being at a declination of only +5 degrees), 3C 120 has been a favorite target for numerous VLBI experiments (Kellermann et al. 1971; Shaffer et al. 1972; Kellermann et al. 1973; Shapiro et al. 1973; Wittels et al. 1975; Schilizzi et al. 1975). Outbursts happen fast and often, so that observations bear fruit after a small number of years. Like 3C 273B, 3C 279 (Whitney et al. 1971), and 3C 345 (Wittels et al. 1976), it exhibits motion of its amplitude minima, and it lends itself to the same numerous sorts of explanations. It is particularly important to distinguish between actual apparent motion and a succession of stationary outbursts that mimic such motion. In previous experiments, lack of (u,v)-plane coverage and phase data have made it impossible to reliably make the ditinction. The addition of closure phase data now opens up that possibility.

A. 3C 120 IN A NUTSHELL

3C 120 has a Seyfert-type spectrum (Burbidge 1967; Sargent 1967; Arp 1968), of Class 1 (Khachikian and Weedman 1974) with broadened permitted lines but narrow forbidden lines. It is remarkable for its unusually strong helium lines (Shields, Oke, and Sargent 1972; Shields 1974), for its power in the infrared (e. g. Rieke and Low 1972), and for its rapid optical (e. g. Kinman 1968) and radio (e. g. Medd et al. 1972) variations.

Its optical appearance (Arp 1968) is of "a bright starlike nucleus with spikes of nebulosity radiating from the center out into an oval-shaped region". Electronographic observations (Walker, Pike, and McGee 1974) show, in addition, an extended nebulosity of elliptical outline, possibly an underlying elliptical galaxy.

The radio source is complex (Clark et al. 1968b). It contains one extended component with a normal radio spectrum, one that becomes optically thick near 20 cm, and one that is optically thick in the

centimeter range and is variable. The flux density of the variable
component has been well monitored at several wavelengths (e. g.
Kellermann and Pauliny-Toth 1960; Medd et al. 1972; Dent and Kojoian
1972). The behavior seems to be dominated by separate and distinct
outbursts, each of which fits very well to predictions made on the basis
of an adiabatically expanding cloud of relativistic electrons in a
magnetic field (van der Laan 1966; Pauliny-Toth and Kellermann 1966,
1968). This apparent harmony between theory and observation has earned
for 3C 120 a reputation, whether it is deserved or not, as the "source
that works". Figure IV.1 presents the total source flux as a function of
time during the period covered by the Quasar Patrol, as determined from
the Goldstone total power measurements.

B.   THE DATA

In general, 3C 120 is rather well resolved by the Quasar Patrol
array. This fact, combined with its relative weakness, conspired not to
produce fringes on the Onsala baselines. Therefore, only the data from
the HNG triplet have been used. Quasar Patrol data exist on these three
baselines for seven sessions between August 1973 and January 1975, and
before that, for six sessions with HG only. Two HG data sets also exist
for May and August 1975.

The most striking feature about this data set is the steady motion
(see Figure IV.2), from November 1972 through July 1974, of the minima of
the visibility function inward in the (u,v) plane. Such behavior can
only be explained as an effective increase in the extent of the
brightness distribution. The orientation of these minima indicate
extension along a position angle of about 65 degrees.

C.   THE MAPS

Fits to the spatially filtered data were obtained for all seven
sessions (Figure IV.3). Details are given in Table IV.1, and the maps in
Figure IV.4. All of these were obtained by initialization to a single
point. The unknown NRAO calibration factor in March 1974 was fixed at
the crossing point between the HG and NG baselines. Any ambiguities that
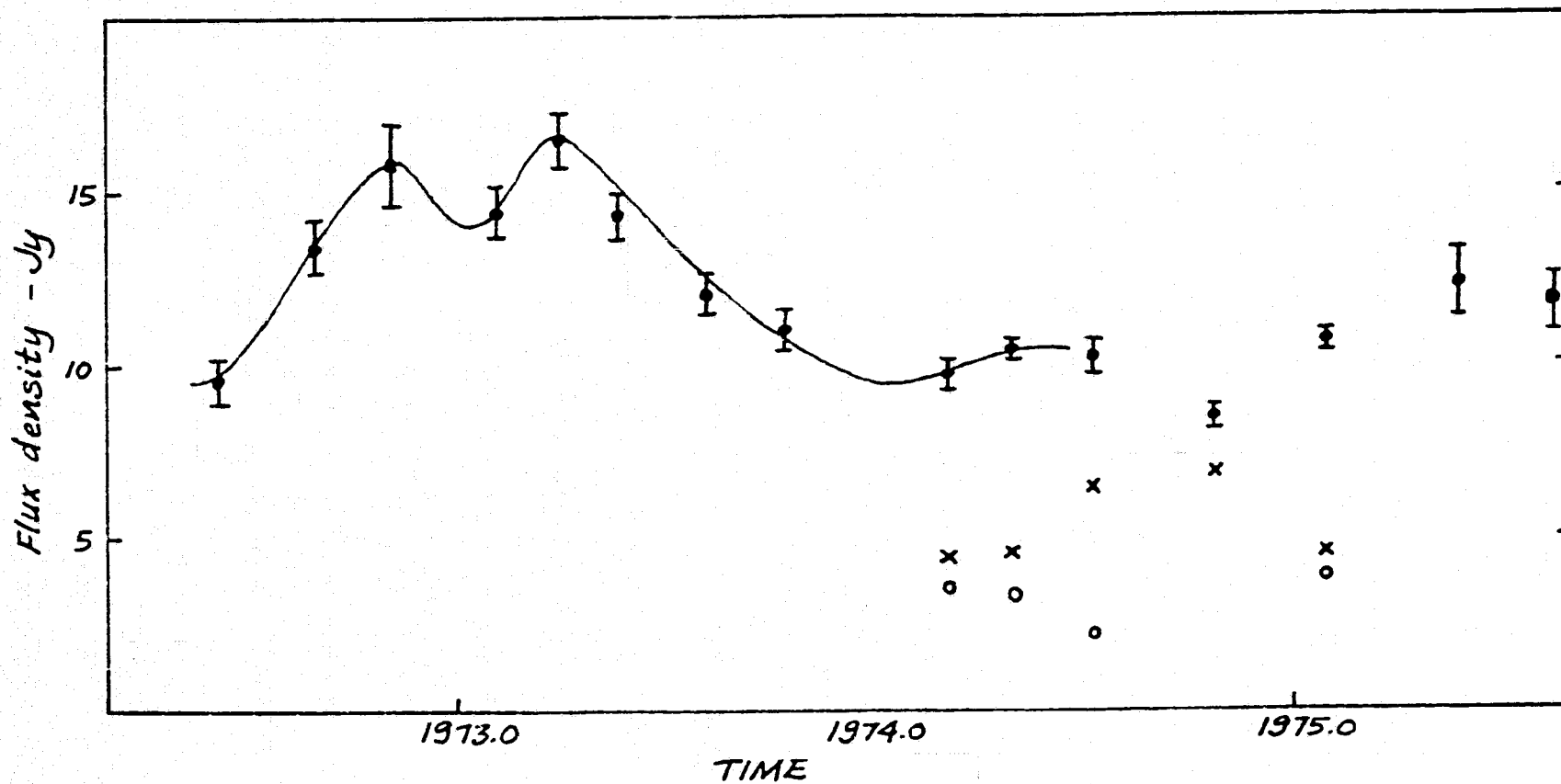
Figure IV.1. Total flux variations of 3C 120 from the Quasar Patrol
    total power measurements (●). Individual source component fluxes
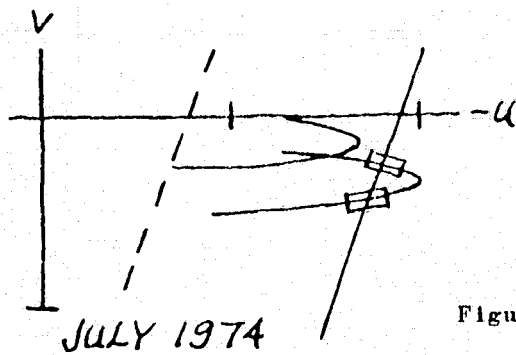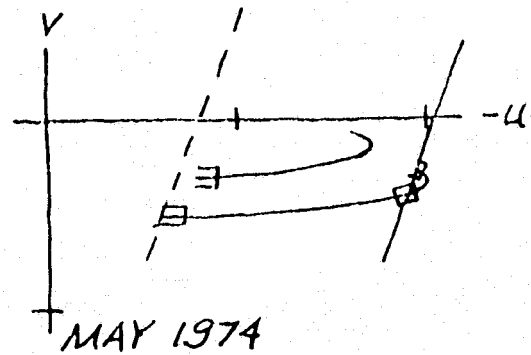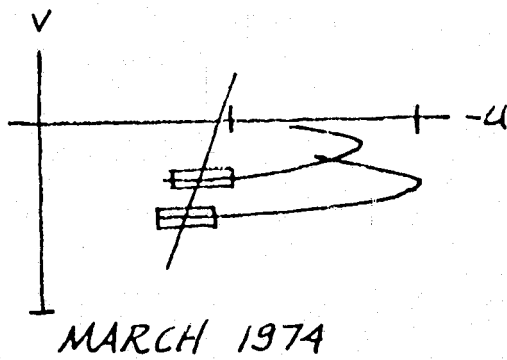   are also shown (X, O).

MARCH 1973

MAY 1973

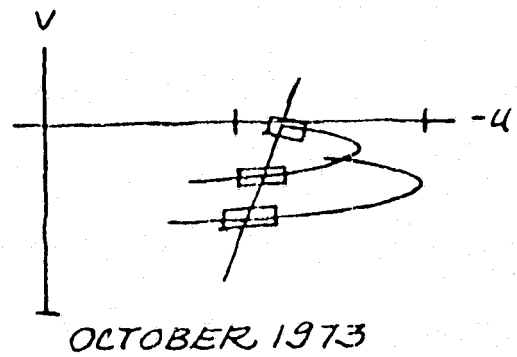AUGUST 1973

OCTOBER 1973

MARCH 1974
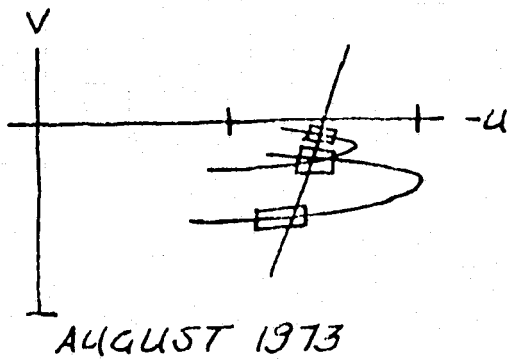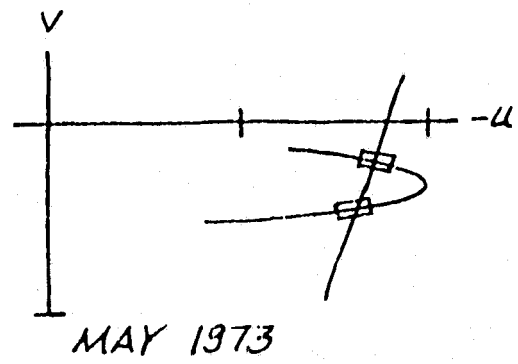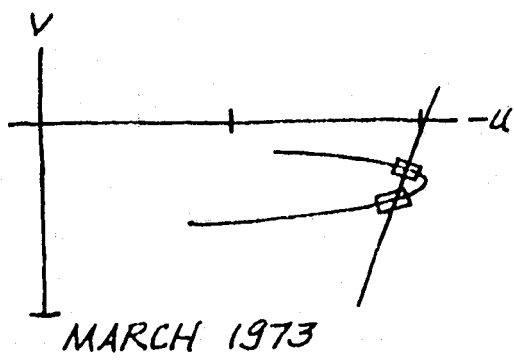
MAY 1974

JULY 1974

Figure IV.2. Motion of the visibility
nulls for 3C 120 as observed on the
HG and NG baselines.

-37-

Table IV.1. Summary of 3C 120 solutions

Session	Half-power beam E/W	Half-power beam N/S	Data A	Data ϕ	Grid E/W	Grid N/S	$\sqrt{\chi^2}$	Peak T_b	Map Flux	Total Flux
Aug 73	1.86	7.60	89	23	6	4	1.06	8×10^9	10.1	12.1
Oct 73	1.86	7.50	83	28	9	4	1.87	4×10^9	10.8	11.0
Mar 74	1.86	7.50	75	22	8	4	0.73	8×10^9	8.0	9.7
May 74	1.86	7.54	53	17	8	4	1.36	4×10^9	7.8	10.4
Jul 74	1.86	7.44	89	29	8	4	5.12	4×10^9	8.5	10.2
Oct 74	1.88	7.72	60	12	8	4	1.22	4×10^9	6.8	8.4
Jan 75	1.86	7.68	74	24	7	4	0.99	6×10^9	8.4	10.8
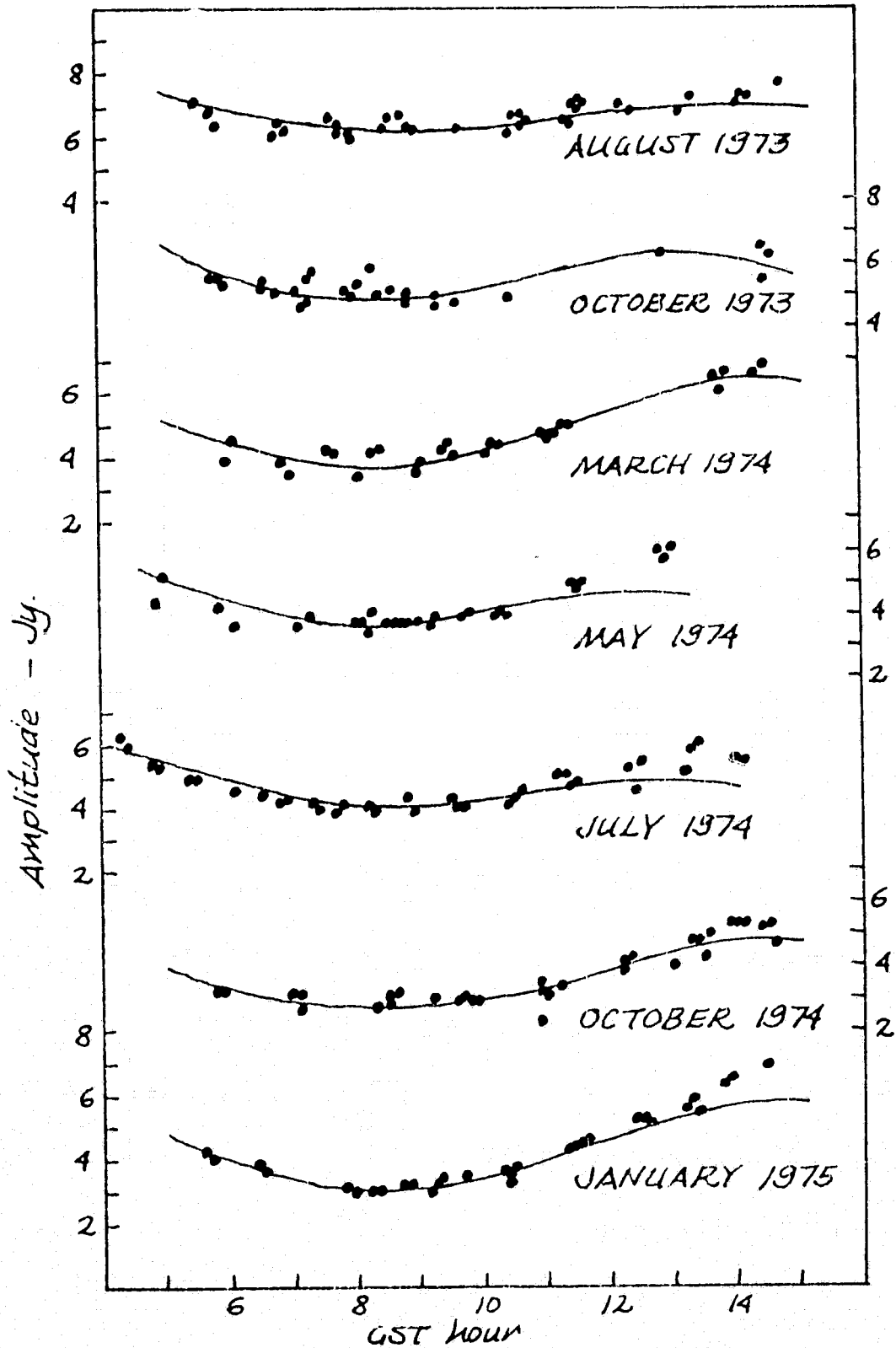
Figure IV.3.a. Fits to the filtered HN baseline amplitudes on 3C 120.

BASELINE NG
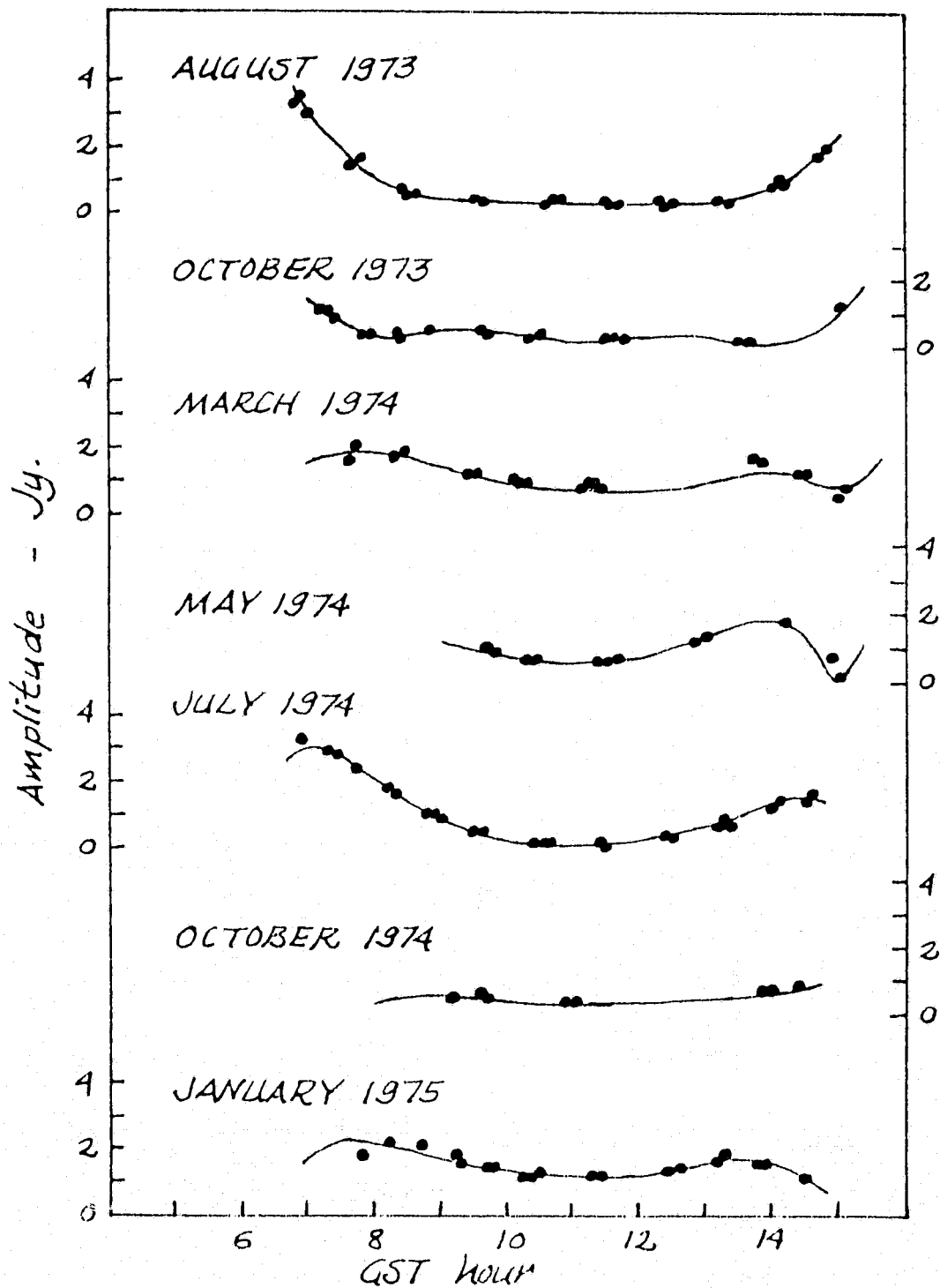
Figure IV.3.b. Fits to the filtered NG baseline amplitudes on 3C 120.
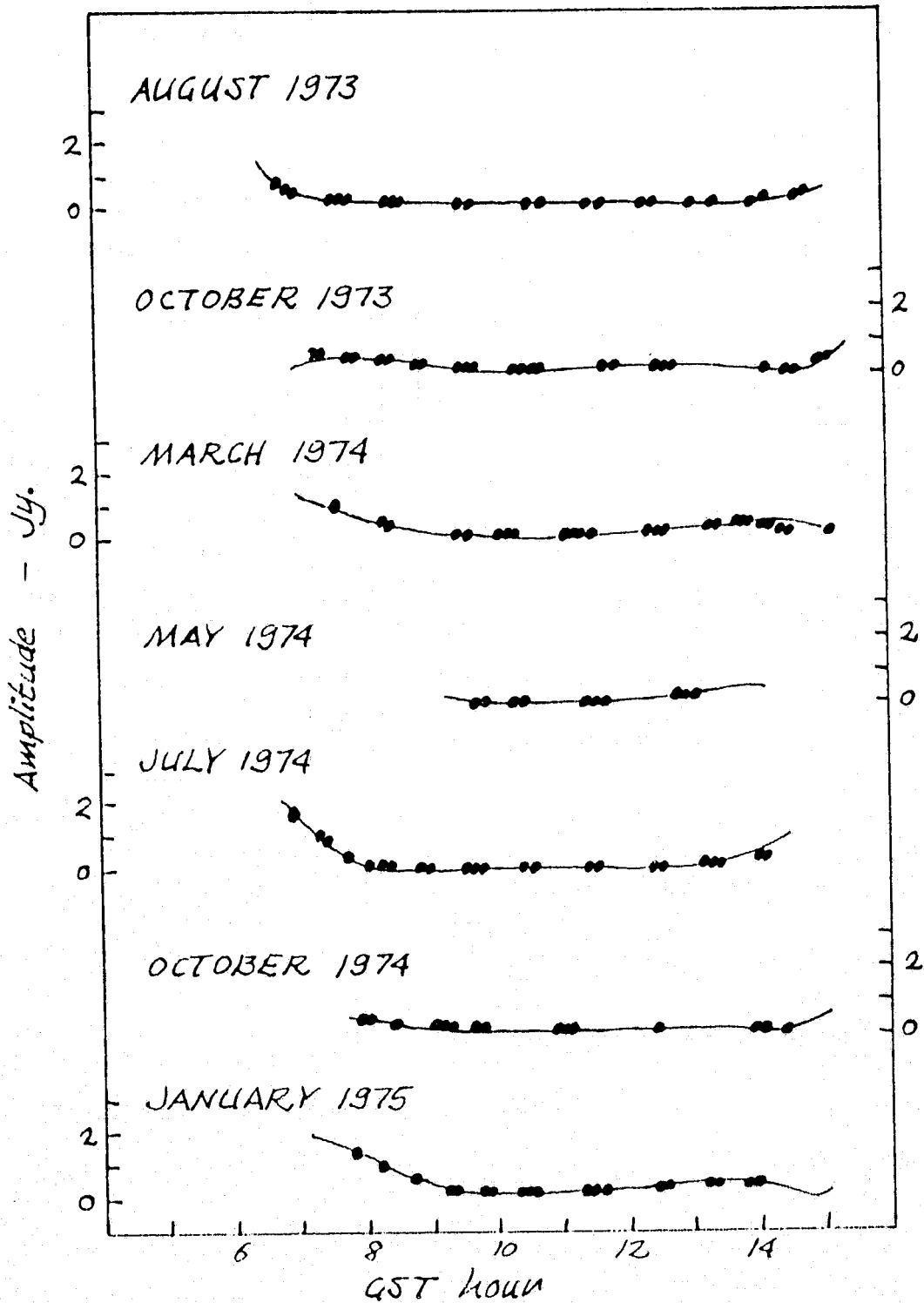
Figure IV.3.c. Fits to the filtered HG baseline amplitudes on 3C 120.
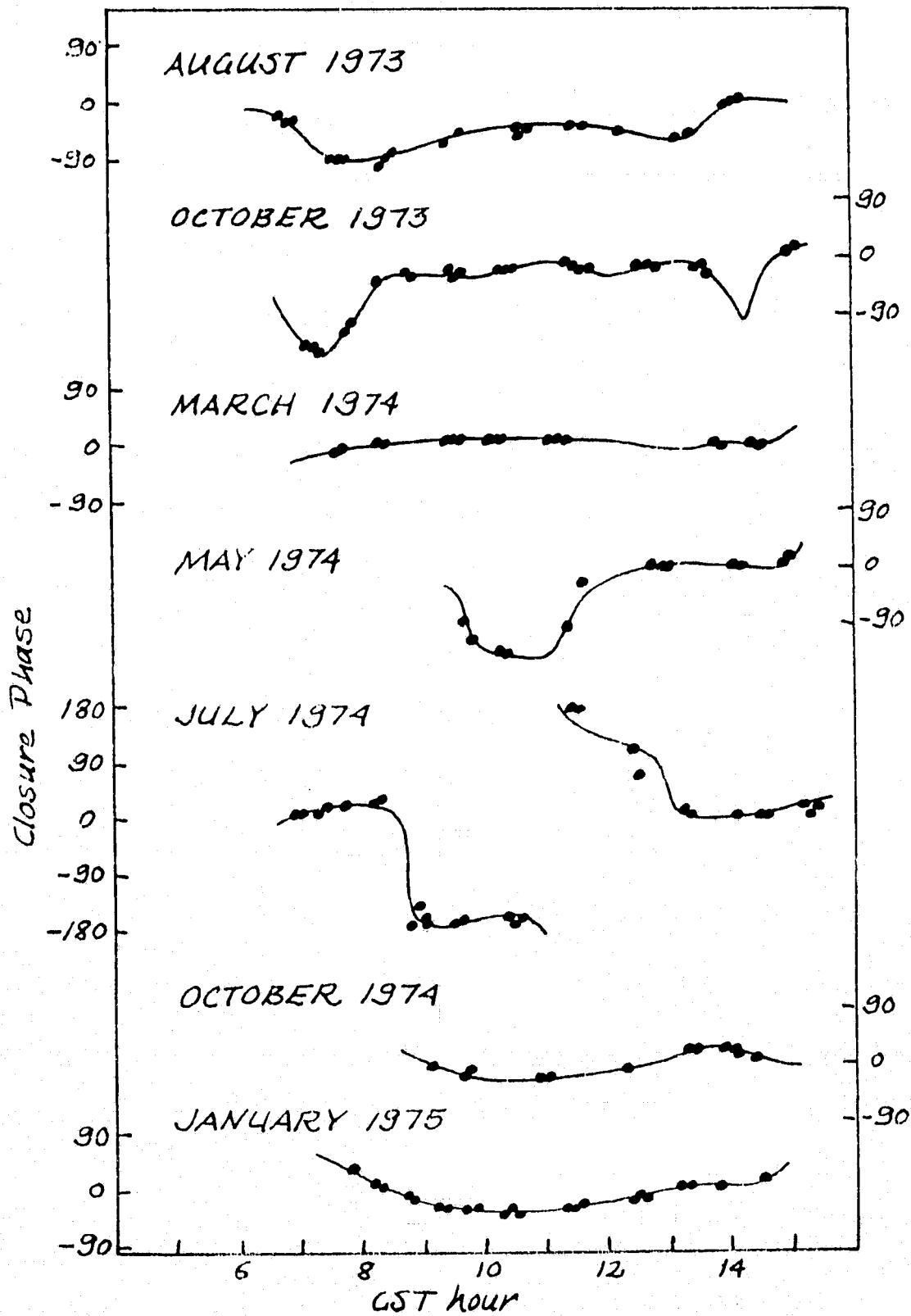
Figure IV.3.d. Fits to the HNG closure phases on 3C 120.
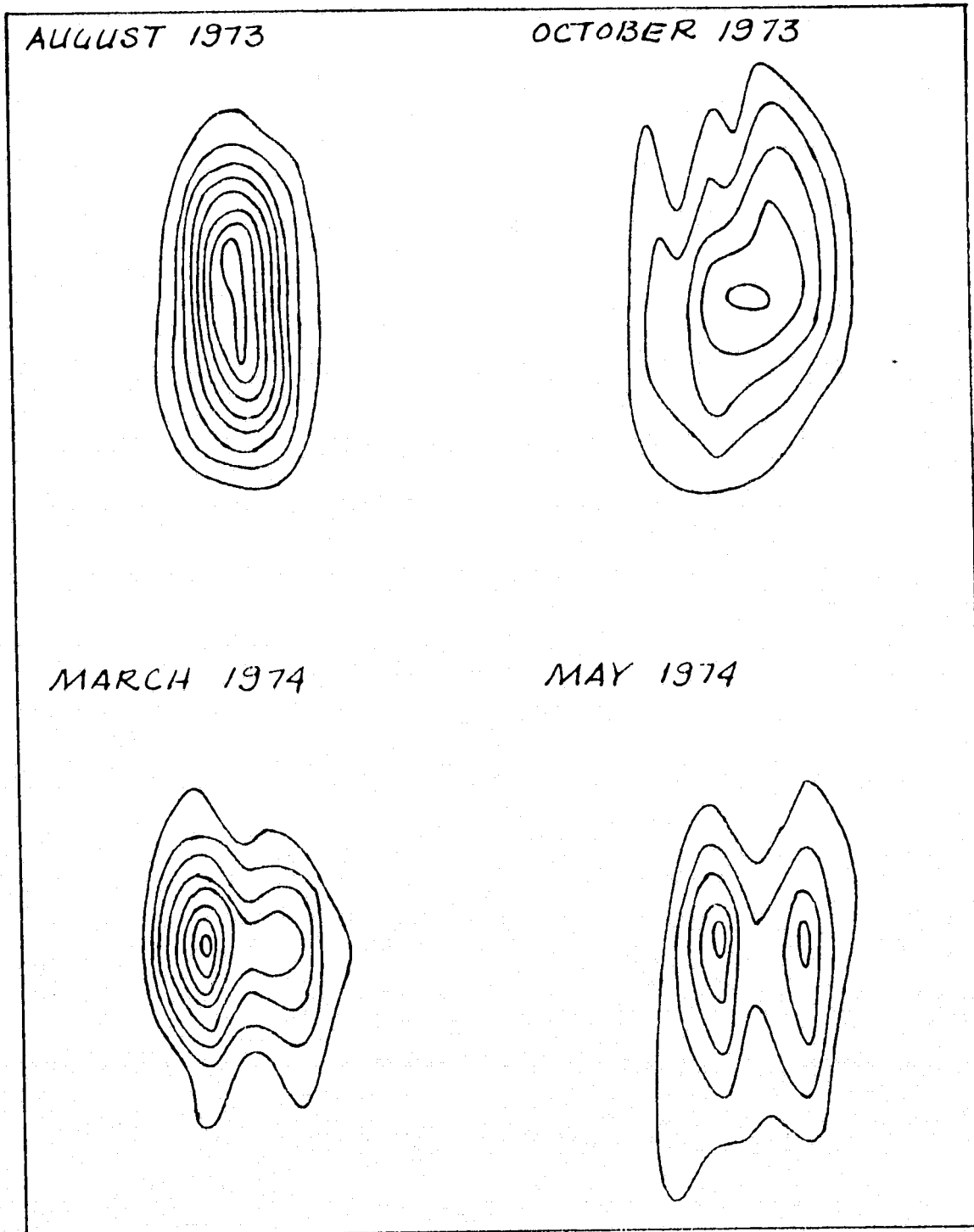
Figure IV.4.a.   3C 120 maps for the August and October 1973, and March and May 1974 sessions.   The scale is in milliseconds of arc.   North is at the top and east to the left. The contour interval is 0.05 Jy/square msec of arc, or 1.1×10^9 K.
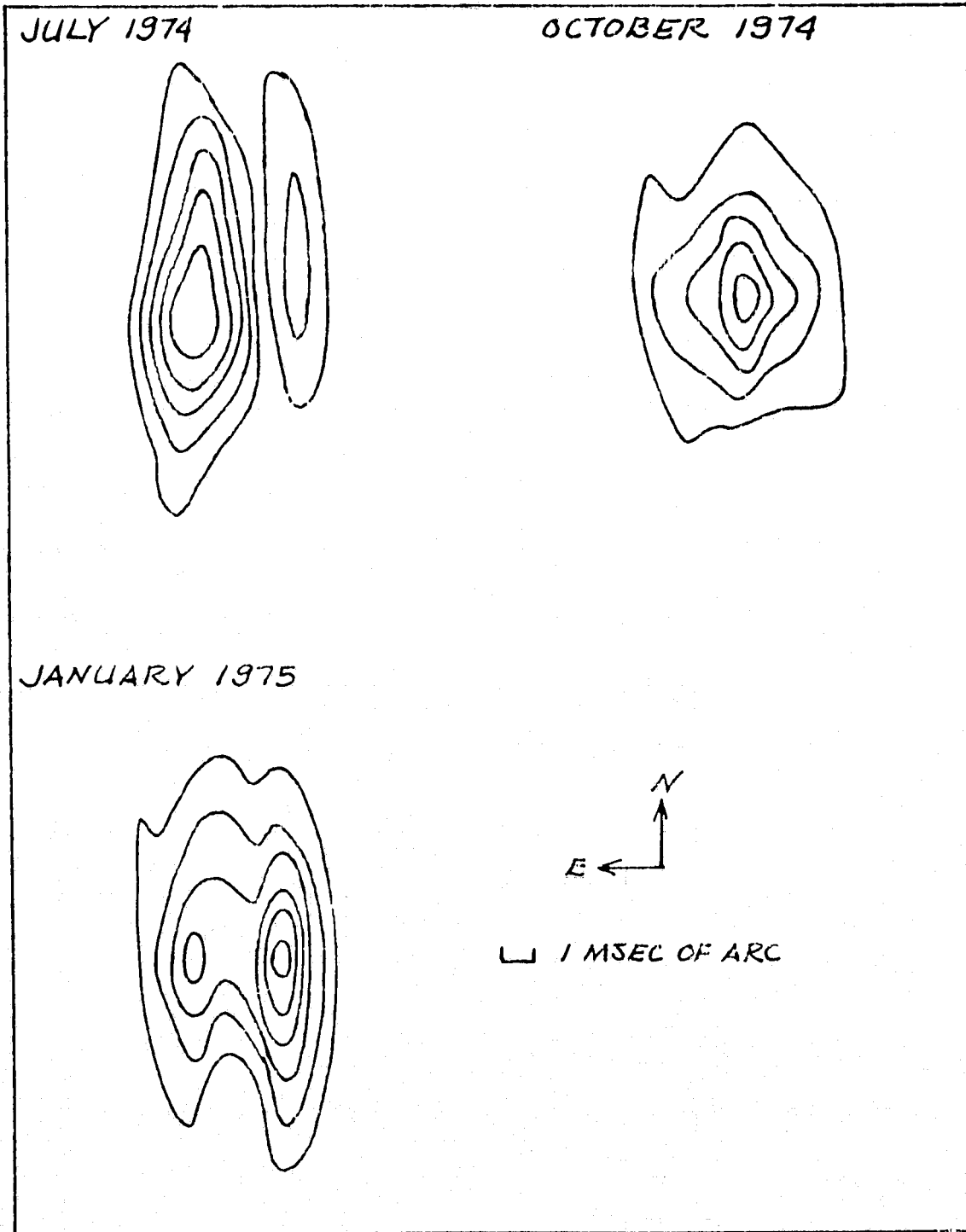
Figure IV.4.b. 3C 120 maps for the July and October 1974, and January
1975 sessions. The scale is in milliseconds of arc. North is at
the top and east to the left. The contour interval is 0.05
Jy/square msec of arc, or 1.1×10^{9} K.

were discovered showed significantly poorer fits than the ones shown. The contour interval is 0.5 Jy per square msec of arc, or 1.1×10 K.

The models account for all but 1.9 ± 0.2 Jy, which is taken to be coming from a more extended halo component. The fact that this number is apparently constant, rather than proportional to the total flux, speaks for its being truly due to undetected power rather than a calibration error in the VLBI system. The halo must be larger than about $0\overset{''}{.}01$, but perhaps not much larger. There has been some difficulty in fitting the amplitude points of the very lowest resolution. Flux for the halo may come from the decimeter component in the spectrum or from a superposition of past outbursts, or these two may be synonymous.

A few general comments concerning the quality of the maps are probably in order. The one for October 1973 is probably not worth very much, and the data may be at fault. That experiment was one of the ones severely affected by parity errors and there is always the possibility that the editing is incomplete. Even for the others, however, the lowest contours are irregular and variable in shape. This is certainly not a real effect. Extended structures depend almost solely on the single HN baseline, which shows a relatively condensed track in the (u,v) plane. The double structure, when it shows, however, is determined by the positions and heights of the maxima and minima and is no doubt real.

D. DISCUSSION

In cases where the source components are easily separable on the maps, individual component fluxes have been computed and added to Figure IV.1. The map was simply divided along an arbitrary line about equally spaced between the components and the flux summed on each side. Whatever part of the halo power that appears in the map has therefore been included. The uncertainty is due mostly to the difficulty in dividing the power properly between the components. A range of approximately plus or minus 1 Jy is allowed in the division of flux. This number is taken to be the error bar on the component fluxes.

Now that the reality of the double structure has been established, component separations can be easily and accurately estimated from the positions of the minima in the (u,v) plane. The individual component sizes are not involved, since, if the minima are observed, there is no

need to perform a least squares fit to all the data. As long as the
internal structure of the components remains poorly resolved, the
computed separation should correspond to the distance between centroids.
This separation has been computed (Figure IV.5) for every session where
nulls or minima were observed or inferred to lie just off the end of a
(u,v) track. In every case where the position angle of separation can be
determined, it is near 65 degrees. We have therefore constrained it to
this value for the less obvious cases as well. The range of permissible
values is determined mainly by the distribution of the data. One
baseline experiments where minima were visible, namely March and May
1973, January 1974, and May 1975, have also been included. One baseline
data also exist for August 1975; it shows only a single poorly resolved
component. Although the flux ratios are not well determined by these
observations, they are consistent with the division suggested by Figure
IV.1. For all sessions through March 1974, the first minimum is the one
observed. In May and July 1974, it is the second. There may be a
systematic difference between estimates made from the first and those
made from the second null, in that the latter may yield larger
separations. This difference might be explained by internal asymmetry in
the components, for example, if one or both were brightened toward the
outer edge. In January 1975, the first minimum was inferred to lie just
inward of the NG track. The indicated rate of apparent expansion is
between 1.1 and 1.5 msec of arc per year or about 4 times c.

From the maps, which unfortunately cover only a short time span on
the scale of the flux changes, and the associated separation plot we
believe we can make the following four generalizations.

First, each total power flare is the result of flux variations in a
single spatial source component.

Second, source components move with respect to one another in such
a way that the overall size of the source increases with time. As we
shall see shortly, internal expansion within each component is also
sometimes observed.

Third, the overall expansion has been observed to be more or less
continuous and linear over a time period of several flares. The
expansion is linear to within the error bars through July 1974. The
separation in January 1975 is slightly less, but by no means is it as
small as during 1972 and 73. This suggests that the new components are
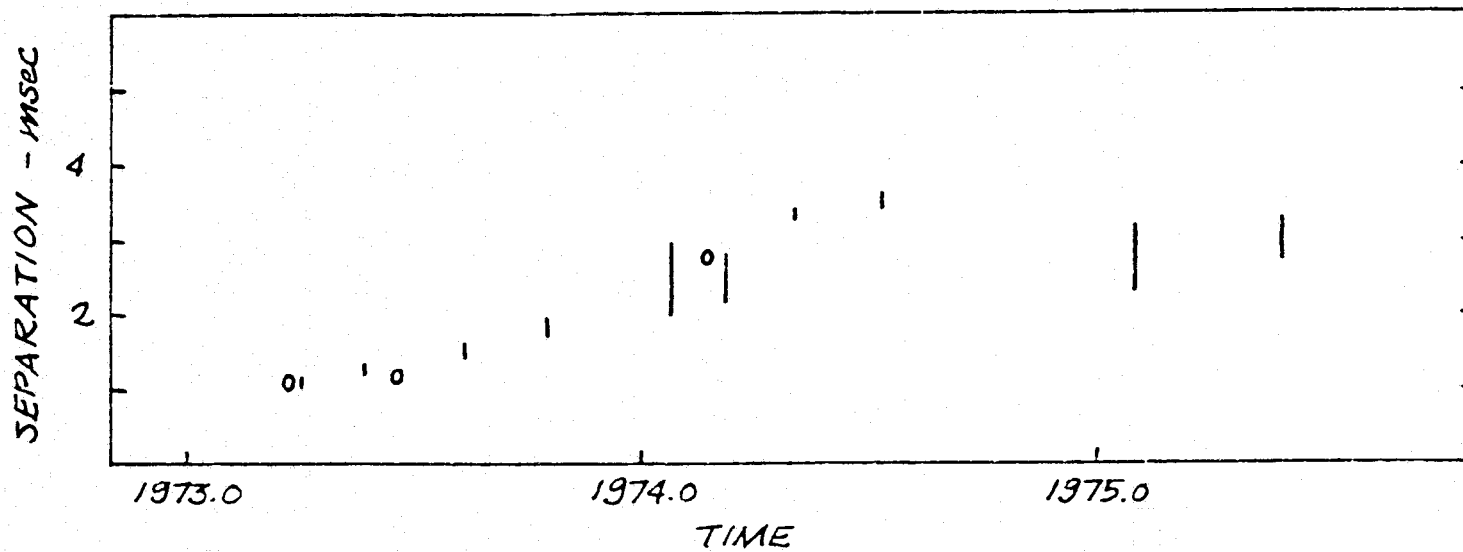appearing on or near the outer edges of the radiating region rather than

-46-

Figure IV.5. Equivalent point double separation, in milliseconds of arc, for 3C 120 as a function of time. The circles are separations at 2.8-cm wavelength taken from Schilizzi et al. (1975).

recurrently in the center.

Fourth, the same preferred postion angle of 65 degrees is
maintained through the whole time period.

We begin to suspect the possibility that physical outbursts are
rarer than the total flux curves would suggest, an "outburst" actually
involving the delayed production of a number of total flux peaks. In the
light of this possibility, let us briefly examine earlier data, VLBI and
otherwise. The 1972-73 flares were the strongest ever recorded (see Medd
et al. 1972; Andrew, unpublished). Prior to that, nothing comparable had
occurred since 1967-68. The intervening period was occupied by a series
of smaller flares. The earliest 3.8-cm VLBI data, in February and
November 1971 (Shaffer et al. 1971) on Goldstack only, showed structure
on the 1 to 2 msec of arc scale, presumably involving one or more of
these minor events. The two data sets are not on adjacent flares (see
Seielstad 1974) and are considered to be too widely separated in time for
much sense to be made of the variations. April 1972 data (Kellermann et
al. 1973), also on HG alone, showed a point source of about 3.7 Jy. In
all probability, this is the first observation of the rising 1972 flare.
An unresolved component was also observed on 8 August 1972 (Kellermann et
al. 1973) at 6.3 Jy and on 29, 30 August 1972 (Shapiro et al. 1973) at
7.1 Jy. This rate of increase is believable considering the total power
changes, for the rise of the 1972 burst. Meanwhile, however, some
variation in the amplitudes was observed in June (Kellermann et al. 1973;
Shapiro et al. 1973), meaning that either the April and August point
sources are not the same one or some remnant of the old structure flared
up enough to produce structure. By October (Kellermann et al. 1973) and
November (Shapiro et al. 1973), the source is no longer unresolved. From
thence proceeds the expansion which we have observed on the three
baselines.

We note that, on the rising side of the flare, the component in
question was unresolved. Later observations definitely show observable
component sizes. Size estimates (see Kellermann et al. 1973; Shapiro et
al. 1973; Seielstad 1974; Wittels et al. 1975) are model dependent, but
apparent super-relativistic velocities are indicated. Internal expansion
is also necessary to explain the complete invisibility, on our array, of
older components.

Unfortunately, interpretation from the amplitudes of only one
baseline is difficult. If a minimum is observed, a separation may be

computed, provided that there is enough data to specify which minimum it is. If the components of the supposed double are dissimilar, the component ratio is resolution dependent, and an estimate of it based on the depth of the minimum can be misleading. Care must be taken not to overstate the conclusions.

Some data exist at other frequencies. Schilizzi et al. (1975) discuss three observations in 1973 and 1974. Although, except for the first session, they are based on relatively few measurements, the separation estimates agree well with ours (see Figure IV.5). The same components appear to be observed at 2.8 and 3.8-cm wavelengths. This is to be expected since the frequency difference is not great.

Shaffer and Schilizzi (1975) present observations from May 1974 on the Green Bank/Owens Valley baseline at 18 cm. Their resolution was comparable to HN at the present frequency (maximum resolution 18.5 million wavelengths), and the visibility curves show strikingly similar variations. The general size and orientation of the compact source must therefore be similar at the two frequencies, this time somewhat more than a slight difference. It accounts for between 60 and 70 percent of the total flux. Even at this relatively long wavelength, more than half the power emanates from the compact radio source.

In brief summary, we have observed the expansion of a series of individual outburst/components that comprise 3C 120. The expansion appears to be continuous over a number of total power flares. Also, available evidence suggests that the compact source has the same or similar structure over at least a moderate range of frequency.

Chapter V

3C 84

The 3C 84 radio source is similar in size and spectrum to 3C 120.
It is much stronger, however, so that sensitivity is less of a problem.
It is situated at about +40 degrees declination so the (u,v)-plane
coverage is better. And it changes, in both total flux and correlated
flux, much more slowly. In fact, our problem in this case is not to make
sense of the evolution based on our brief "snapshots", but rather to see
the changes at all.

A.   3C 84 IN A NUTSHELL

3C 84 (otherwise known as Perseus A) is closer than 3C 120 and
therefore better studied optically. It is identified with the Seyfert
galaxy (Seyfert 1943) NGC 1275, the most prominent member of the Perseus
cluster of galaxies. Assuming a value of H = 50 km/s Mpc for the Hubble
constant, it lies 110 Mpc distant ($z=0.018$) Unlike other Seyfert
galaxies, NGC 1275 is not obviously a spiral. It has a bright,
elliptical-looking central part and numerous absorption clouds and
emission filaments outside (Burbidge and Burbidge 1965; Lynds 1970).
These filaments lie all around the galaxy, but the maximum extension
occurs near 0 degree position angle. However, although the cluster
contains a large proportion of ellipticals, its most prominent member
does not appear to be one; the stellar component dispays an A-type
spectrum (Minkowski 1968). The nuclear spectrum, of Seyfert Class 2
(Khachikian and Weedman 1974), has line widths of several thousand km/s.
In addition, many of the filaments show sharp lines at a velocity 3000
km/s greater than the redshift velocity, which normally would suggest
expulsion of material from the nucleus. To confuse things, however, this
high velocity system may be seen in 21-cm absorption against the nucleus
(DeYoung, Roberts and Saslaw 1973). The nuclear optical continuum
appears to contain a nonthermal component (Oke 1968), and optical
polarization has been detected (Walker 1968). The nucleus also appears
strong in the infrared (e. g. Rieke and Low 1972). X-ray emission from

the Perseus cluster is complex in spatial distribution and appears to contain a point source component centered on NCC 1275 (Wolff et al. 1974).

The associated radio source 3C 84 consists of a number of spectral components of a variety of physical sizes (see e. g. Ryle and Windram 1968). There is a component with a normal power law spectrum, and an angular size of a few minutes of arc. There is also a peak in the spectrum attributed to a component which becomes optically thick near 800 MHz. VLBI observations (Clarke et al. 1969; Purcell quoted by Pauliny-Toth et al. 1976) show this component to have structure on the scale of 0.05 and to be elongated along a position angle near 0 degrees. The third component, the one of concern to this VLBI study, becomes optically thick near 10 GHz. The angular structure of this presumably nuclear source will be discussed shortly.

The centimeter wavelength component shows flux variations at all frequencies where it can be observed. A particularly long history exists near 8 GHz, where Heeschen (1961) recorded it at 10 Jy in 1959. Since that time, it has shown a more or less linear increase (e. g. Dent 1966; Medd et al. 1972; Dent and Kojolan 1972). During the later of the experiments discussed here, in early 1975, the flux density at 7.85 GHz exceeded 60 Jy. This is a remarkably large, but also rather slow, flux variation. There is some indication that the increase may be irregular (e. g. Medd et al. 1972) with a suggestion of superposed outbursts. The increase is barely discernable in the Goldstone total power measurements (Figure V.1).

B.   THE DATA

Inspection of the amplitude data reveals that 3C 84 must be about the same angular size as 3C 120 at its largest. Overall, the source is very well resolved. At the lowest resolution on HN, about 85 percent of the total source flux is correlated, while the amplitude on the GS baseline never rises above 5 Jy.

The amplitude curves are filled with a whole range of peaks and valleys of different heights and depths, in apparent confusion. If the amplitude data are projected onto the (u,v) plane, a reassuring feature becomes evident, however; what once was chaos falls reasonably well into
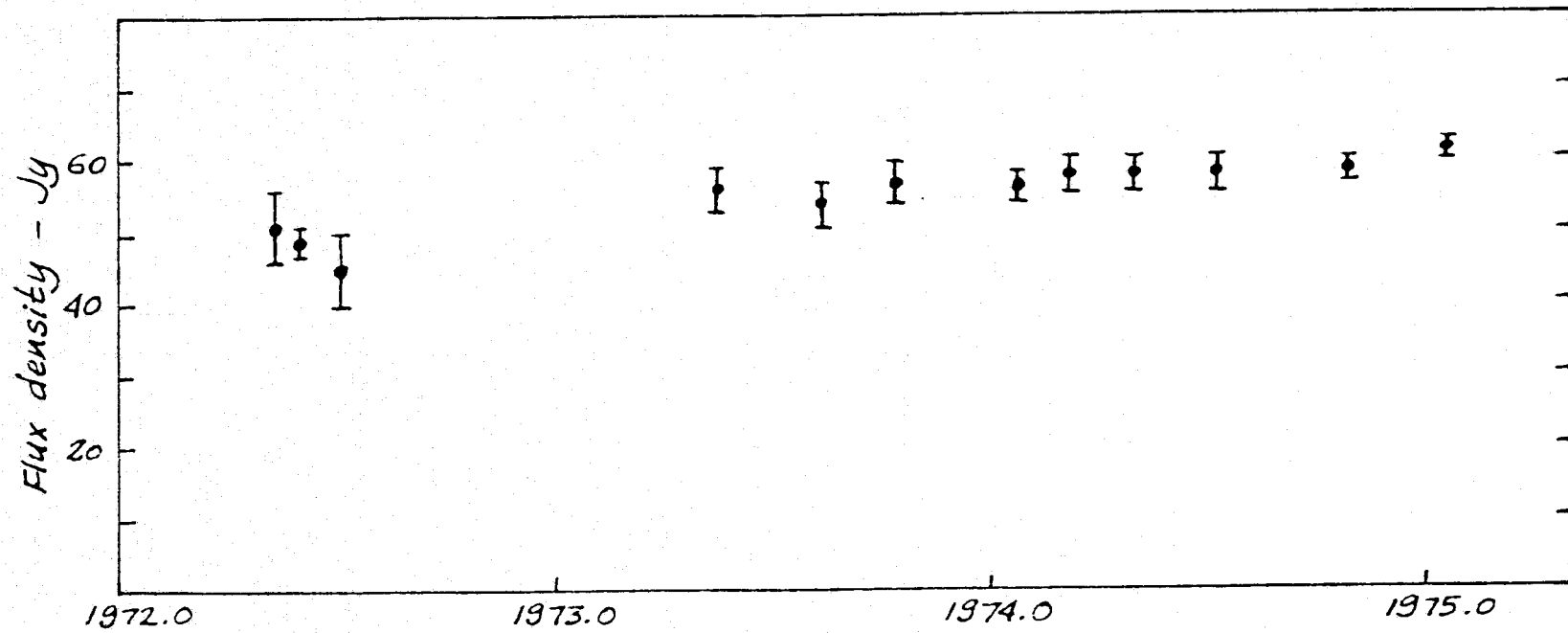
Figure V.1. Total flux variations of 3C 84 from the Quasar Patrol measurements.

a row of parallel ridges (Figure V.2). This suggests that the brightness distribution is elongated along a position angle near -10 degrees, and has a prominent separation of about 5 msec of arc. The maxima and minima vary widely in height and depth, however, and the simplicity seems to break down on the intercontinental baselines. The components of the source must therefore have a complexity of their own.

Because the amplitudes on the HN baseline reach almost 50 Jy (out of a total of about 60), we should expect to account for most, if not all, of the flux in the map. Indeed, the spectrum suggests that small components should dominate the power at 7.85 GHz.

Evidence for changes in the brightness distribution is discernable in the data, although it is slight. The heights of the maxima and depths of the minima can be seen to change slowly with time, and some changes can be seen in the closure phase. These changes are larger than any possible error in the data, including systematic errors, but only, slightly. We can expect the changes to be difficult to isolate in the maps.

C. "LOW RESOLUTION" MAPS

Because we have a longer time series of data for the HNG triplet only, and longer still for HG alone, a series of "low resolution" maps using only these baselines would be of interest. Of these, the HG baseline is the longest: 100 million wavelengths. The half width of the beam is 2.06 msec of arc east/west and 2.61 msec north/south. The second maximum in the basic amplitude pattern is just reached by the HG baseline. At this resolution, the brightness distribution should be relatively simple.

The fits to the (filtered) data appear in Figure V.3 and the maps in Figure V.4. All were obtained with a 5 by 10 point grid oriented due north/south. The July 1974 solution was obtained after initialization with several different single points. As all the amplitudes and closure phases change only slightly with time, all the rest of the solutions were initialized with the map output by the July 1974 solution. Most of these have also, at one time or another, been grown from a point source. The correction for the scaling problem for the NRAO baselines in March 1974 was adjusted so that the level of the HN amplitudes is the same as it was
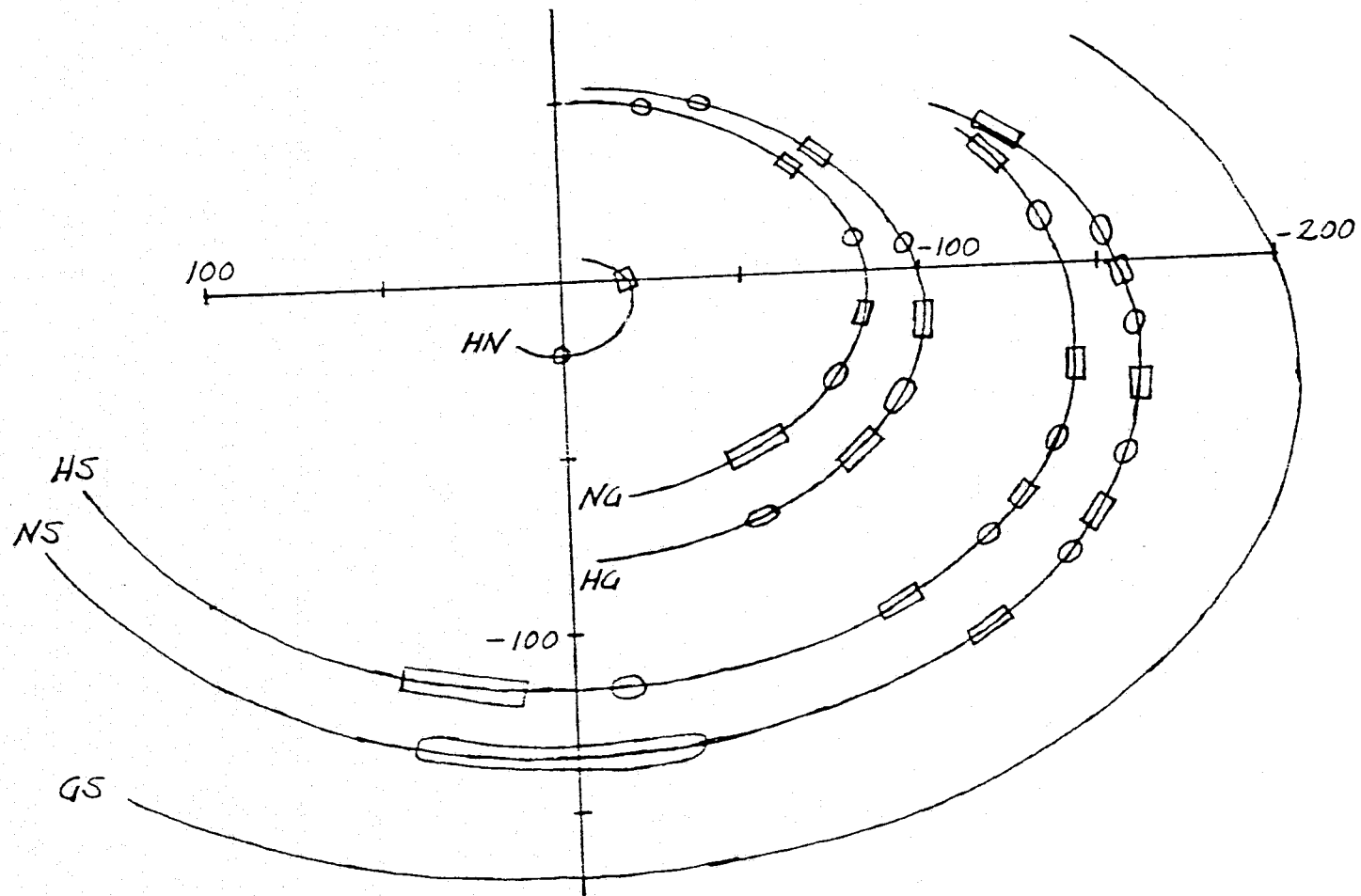
Figure V.2. Prominent pattern of amplitude maxima in the visibility function of 3C 84. Squares indicate amplitude maxima and circles minima. u and v are in millions of wavelengths.

Table V.1. Summary of low resolution 3C 84 solutions

Session	Half-power beam E/W	N/S	Data A	ϕ	Grid E/W	N/S	$\sqrt{\chi^2}$	Peak T_b	Map Flux	Total Flux
1972	1.86	2.38	90	0	5	10	2.44	8×10^{10}	40.1	50.0
May 73	1.86	2.50	74	0	5	10	9.46	8×10^{10}	47.7	54.2
Aug 73	1.86	2.52	66	11	5	10	2.04	9×10^{10}	43.4	54.4
Oct 73	1.86	2.38	134	41	5	10	3.38	9×10^{10}	47.9	57.0
Mar 74	1.86	2.38	183	40	5	10	5.96	1×10^{11}	53.3	57.9
May 74	1.86	2.20	167	24	5	10	3.50	9×10^{10}	51.2	57.8
Jul 74	1.86	2.38	230	49	5	10	3.45	9×10^{10}	53.7	57.9
Oct 74	1.86	2.38	105	29	5	10	6.97	9×10^{10}	52.3	61.5
Jan 75	1.86	2.38	105	29	5	10	6.97	9×10^{10}	52.3	61.5

BASELINE HN
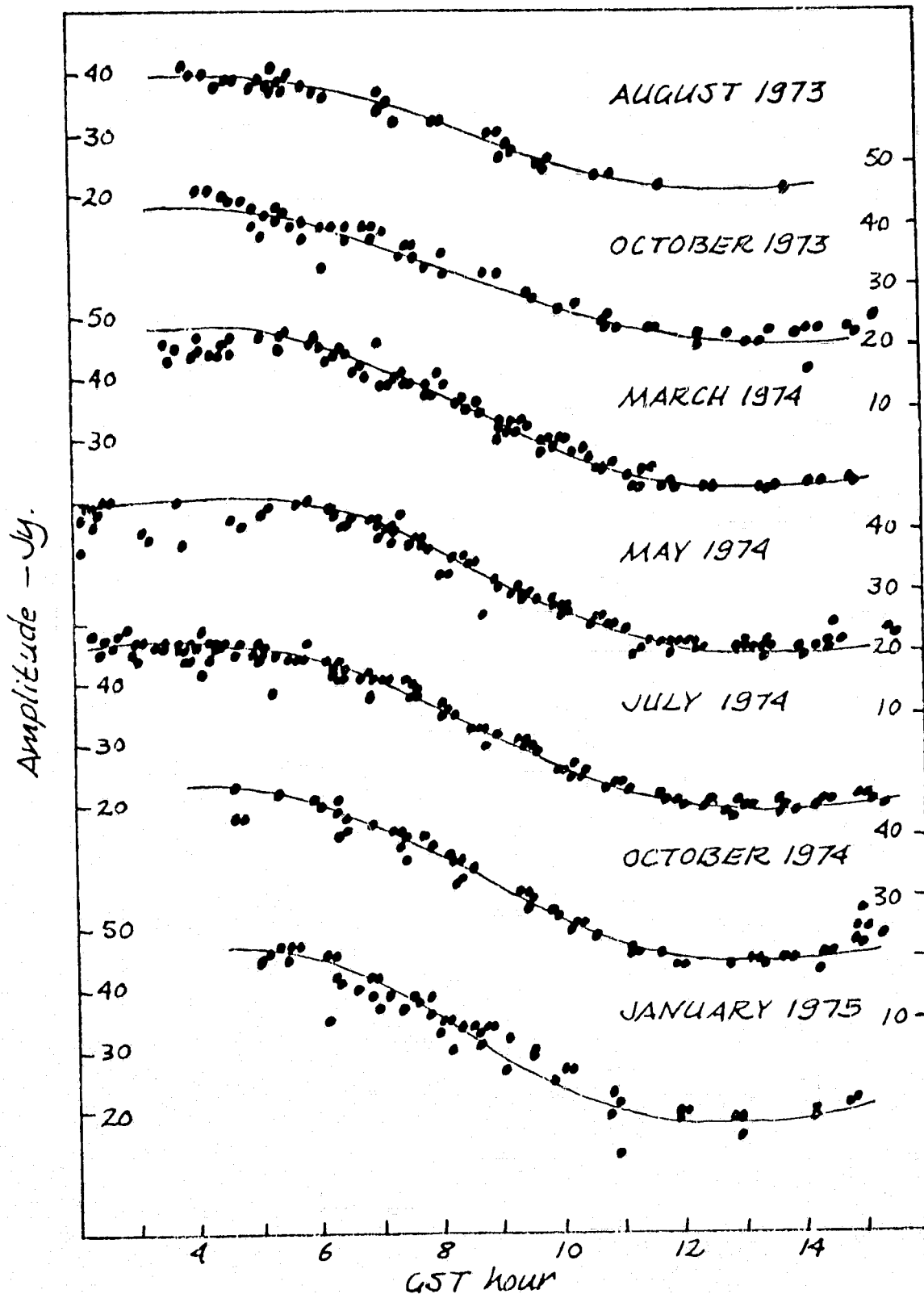
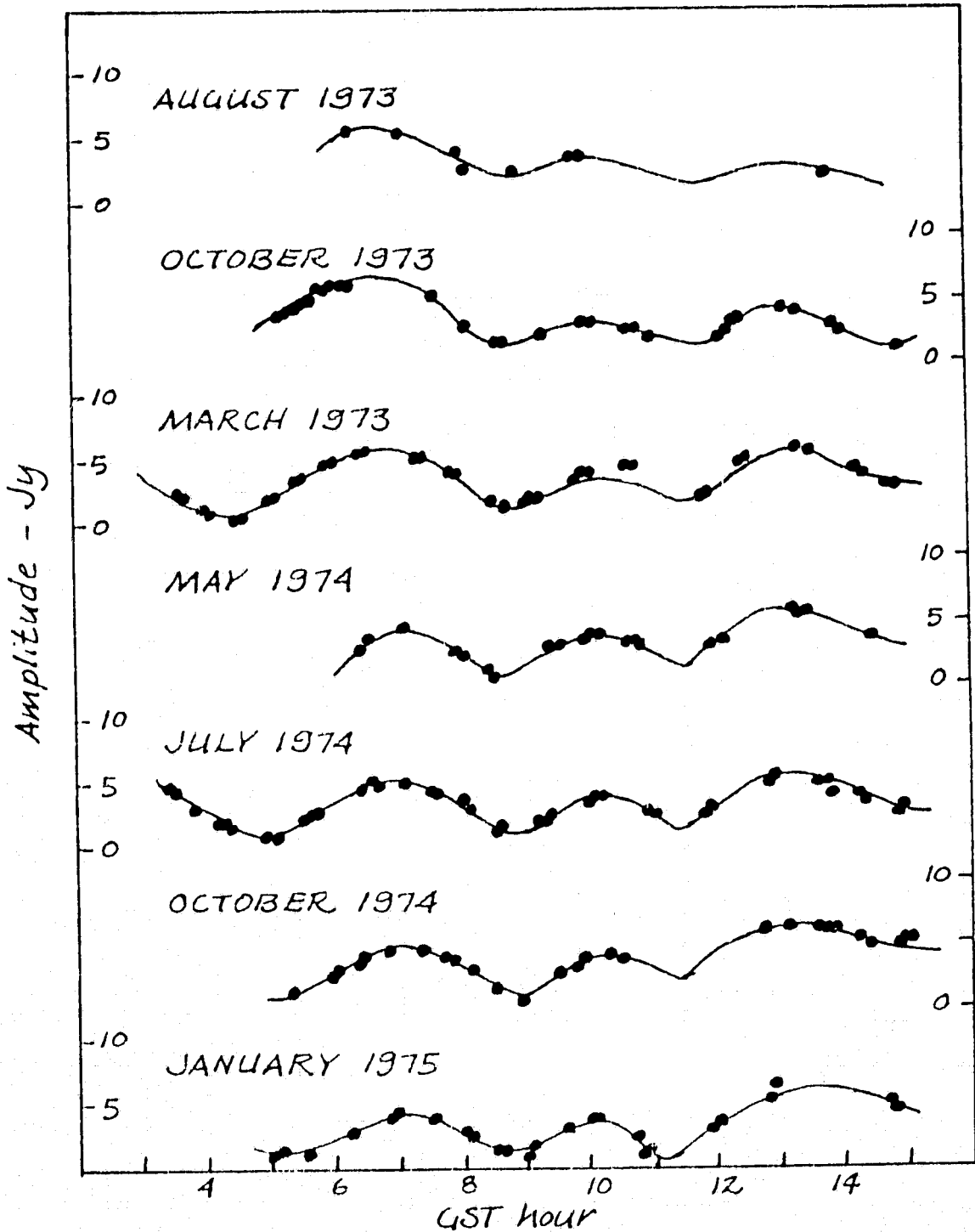Figure V.3.a. Fits to the filtered HN baseline amplitudes for the low resolution series of maps of 3C 84.

Figure V.3.b. Fits to the filtered NG baseline amplitudes for the low resolution series of maps of 3C 84.

BASELINE HG

AUGUST 1973

OCTOBER 1973

MARCH 1974

MAY 1974

JULY 1974

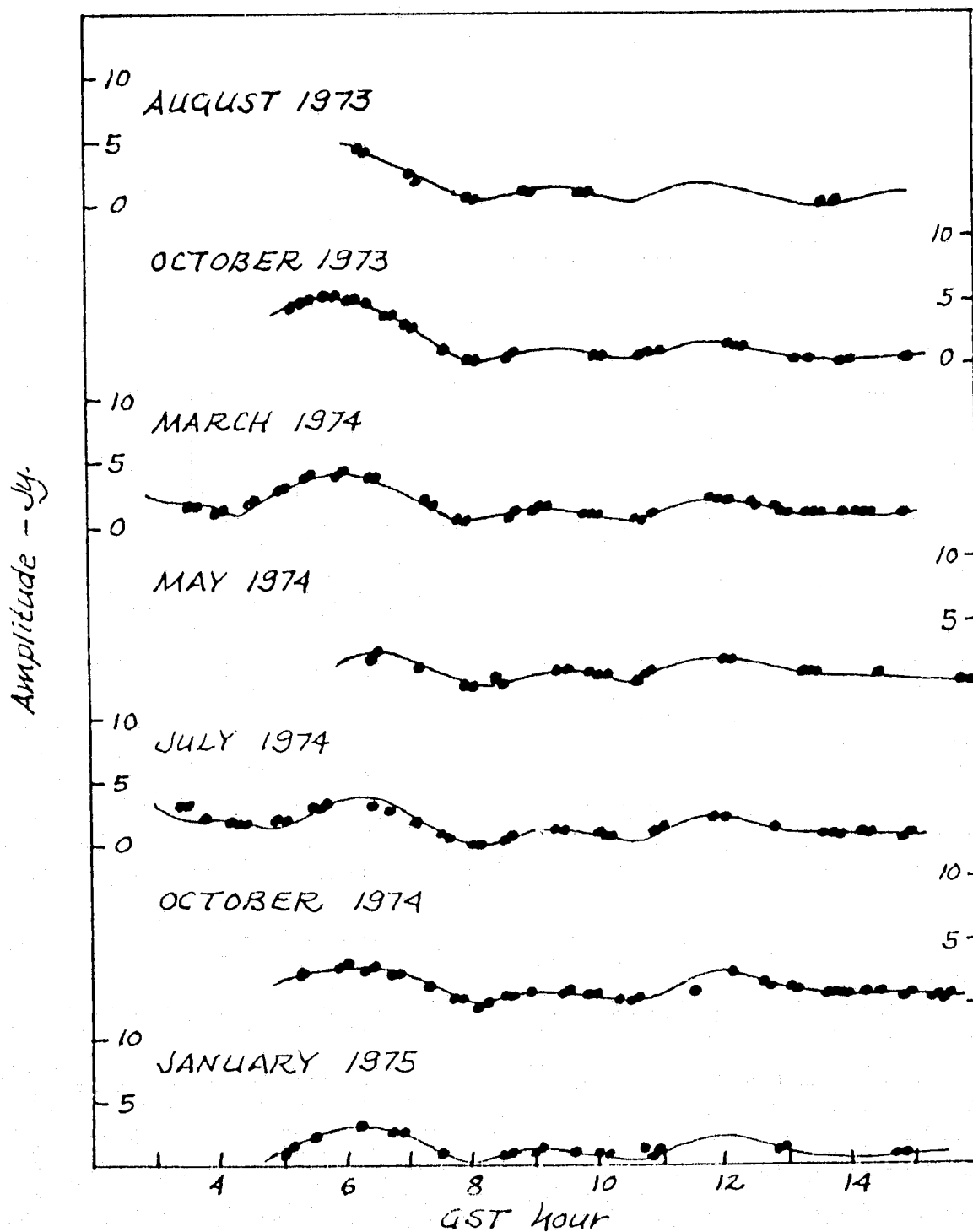OCTOBER 1974

JANUARY 1975

Amplitude – Jy.

GST hour

Figure V.3.c. Fits to the filtered HG baseline amplitudes for the low
resolution series of maps of 3C 84.

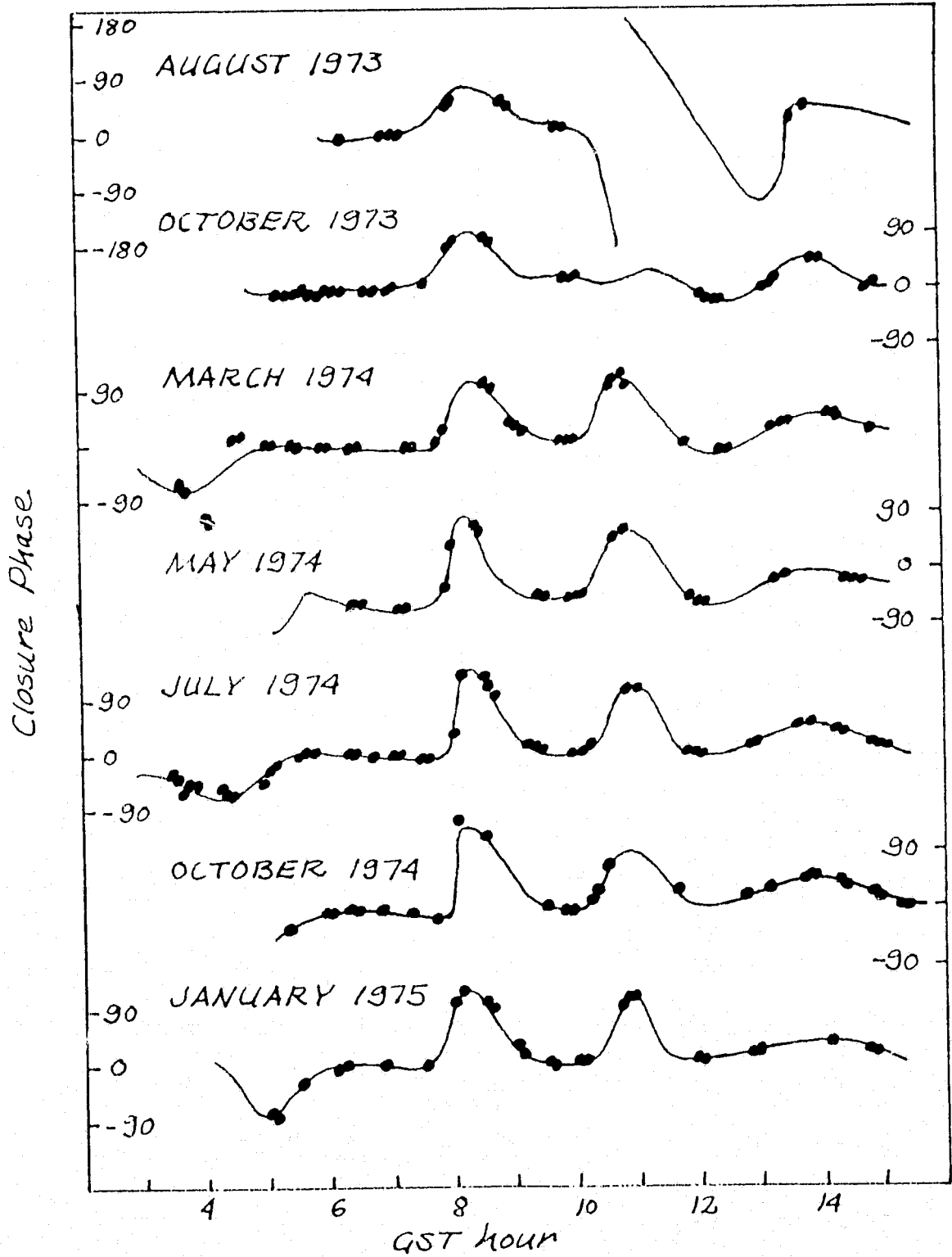TRIPLET HNG

Figure V.3.d. Fits to the HCN closure phases for the low resolution series of maps of 3C 84.
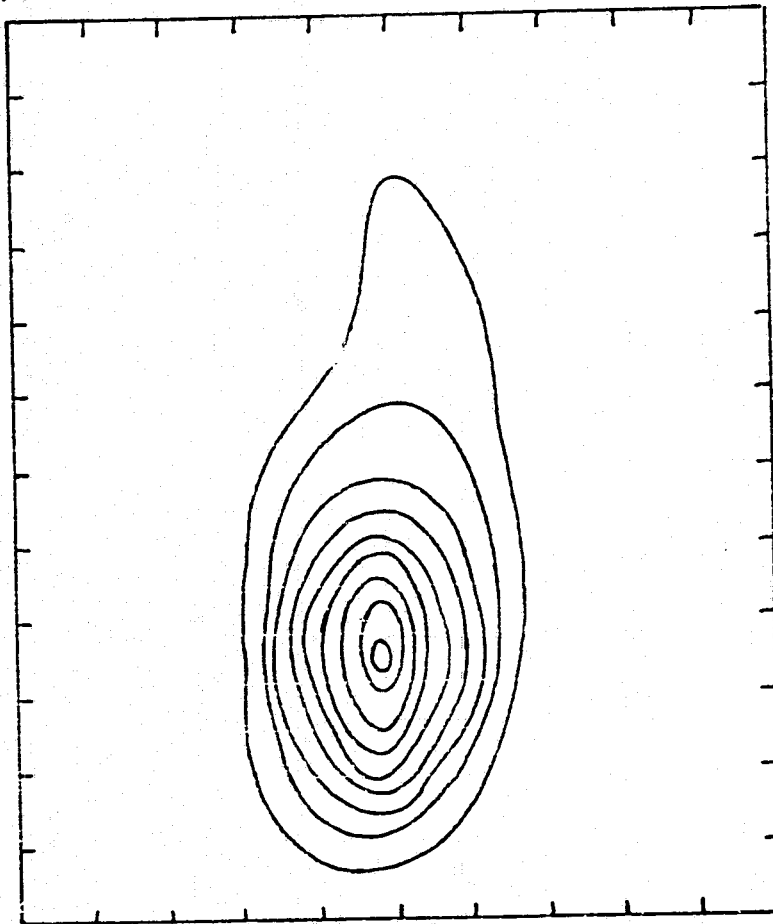
AUGUST 1973   OCTOBER 1973

Figure V.4.a.   Low resolution maps of 3C 84 for the August and October
     1973 observing sessions.   Contour interval is 0.5 Jy/square msec or
     1.1×10^{10} K.

MARCH 1974

MAY 1974

Figure V.4.b. Low resolution maps of 3C 84 for the March and May 1974
observing sessions. Contour interval is 0.5 Jy/square msec or 1.1
x 10^{10} K.

JULY 1974

OCTOBER 1974

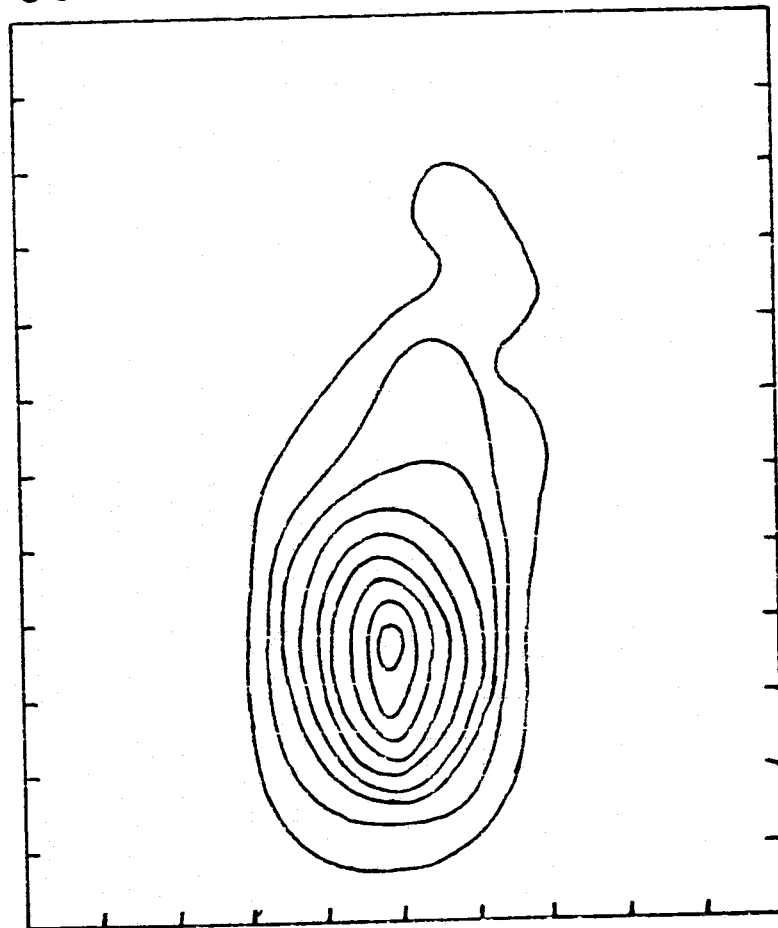
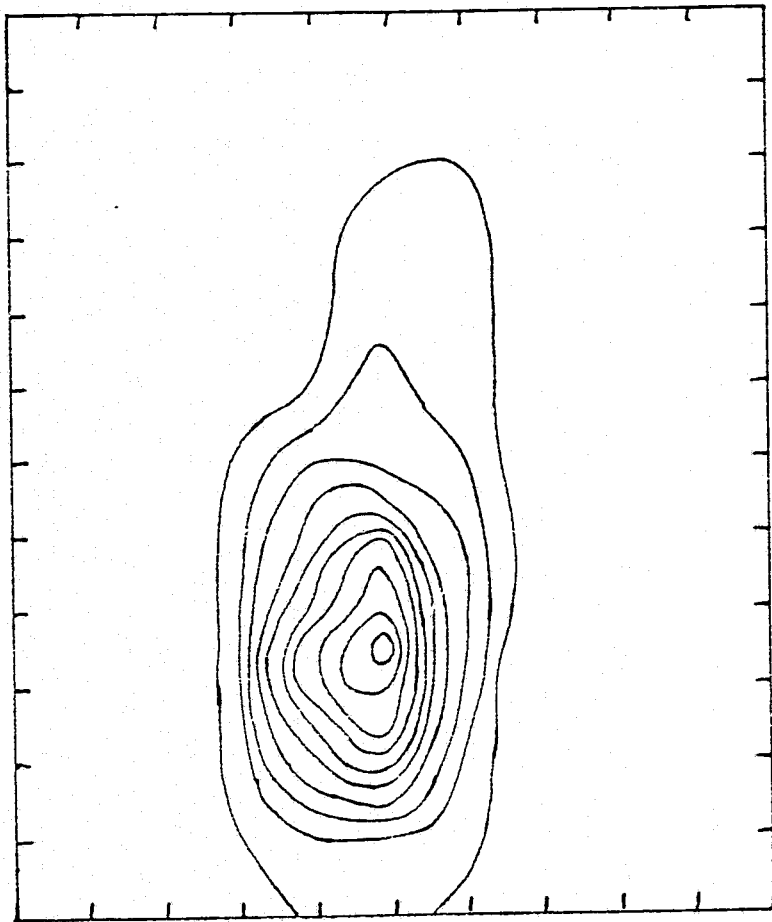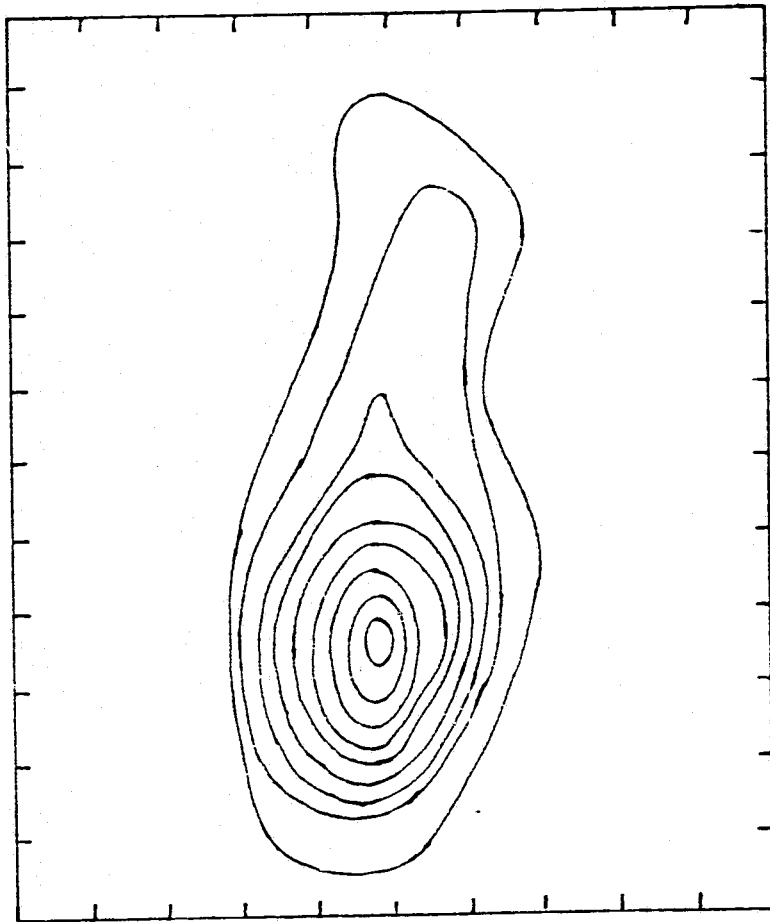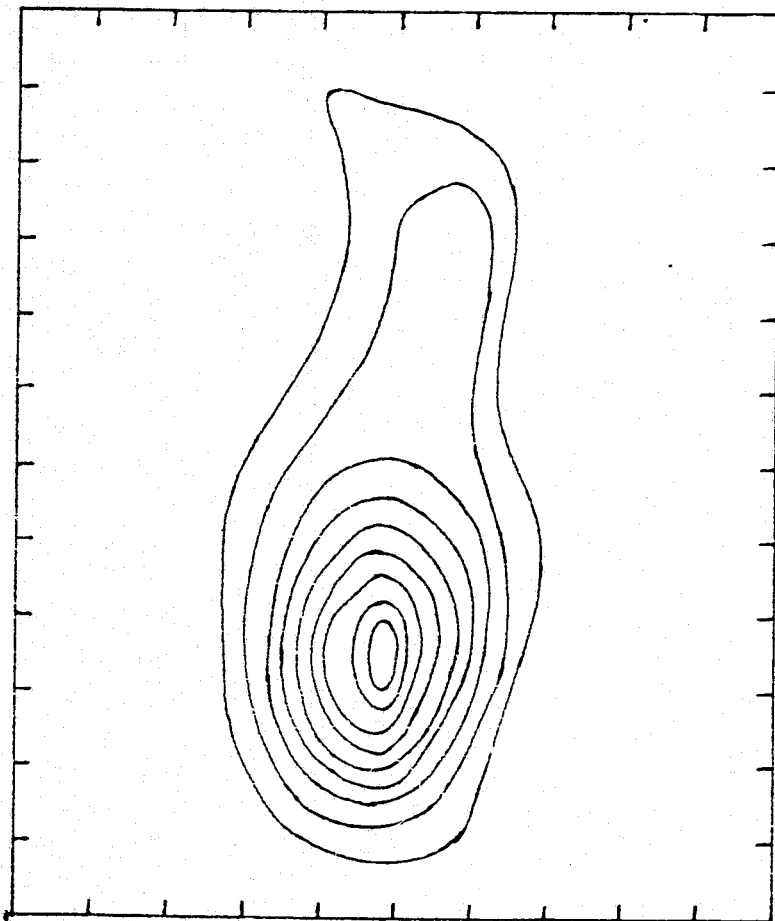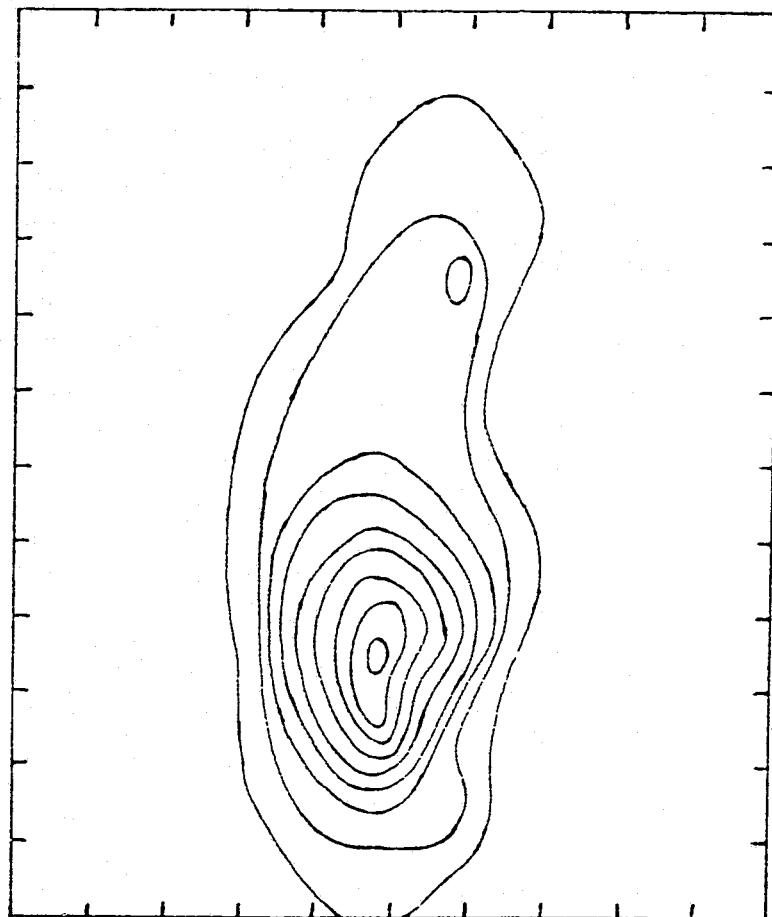
Figure V.4.c. Low resolution maps of 3C 84 for the July and October 1974
observing sessions. Contour interval is 0.5 Jy/square msec or 1.1
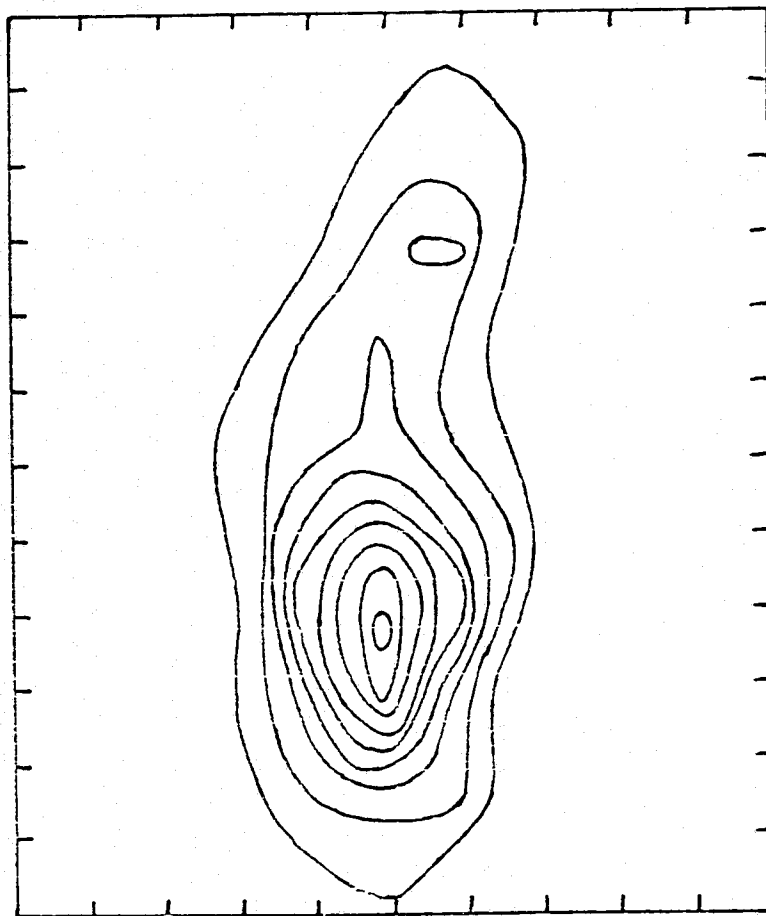x 10^{10} K.

JANUARY 1975

Figure V.4.d.   Low resolution map for the January 1975 observing session.
Contour interval is 0.5 Jy/msec or 1.1×10^{10} K.

for the sessions adjacent in time.

With the exception of August 1973, all curves pass through the data points well and in a consistent manner from session to session. The August 1973 solution, which is poorly determined because of the sparse data, shows a good, but different fit. Although the map looks similar, the solution cannot be considered very reliable.

Table V.1 summarizes the solutions.

Most of the flux appears to come from the southern end of the source. This large blob is what is responsible for the great power in the HN amplitudes. The expected elongation does appear in the map, at the expected position angle. In the NG and HG range, the southern component is well enough resolved so that its effective flux is comparable to the northern component(s), and the observed deep nulls are produced.

As expected, it is difficult to locate the source of the brightness changes. It appears to be related to a flux increase in the central or northern part of the source, or perhaps both. The southern component appears to be unchanged; at least, it reaches the same brightness contour in all solutions. The appearance is of a migration of emission to the north with time.

One baseline (HG) data also exist for three sessions in 1972 (May, June, and July), and for May 1973. This is not enough in itself for a map, but a possible solution has been reconstructed in the following way. Since the HN amplitudes changed very little with time when observed, the August 1973 HN points were added to these data sets, after being scaled with the total flux changes, and the grid was initialized with the October 1973 solution. One solution was done for the combined 1972 data and one for May 1973. These are not considered to be unique brightness distributions, but rather those which require a minimum of modification from the better-determined closure phase solutions. The two maps (Figure V.5) seem to continue back in time the trend that was just noted. The northern section of the source has been brightening with time. A further data set in 1969 at 5-cm wavelength on HN alone also shows the possibility of a similar structure. The overall size and orientation must at least be similar. Cohen et al. (1971) present an HG amplitude curve at 3.8 cm that could well be similar to our 1974 curve at 3.8 cms.
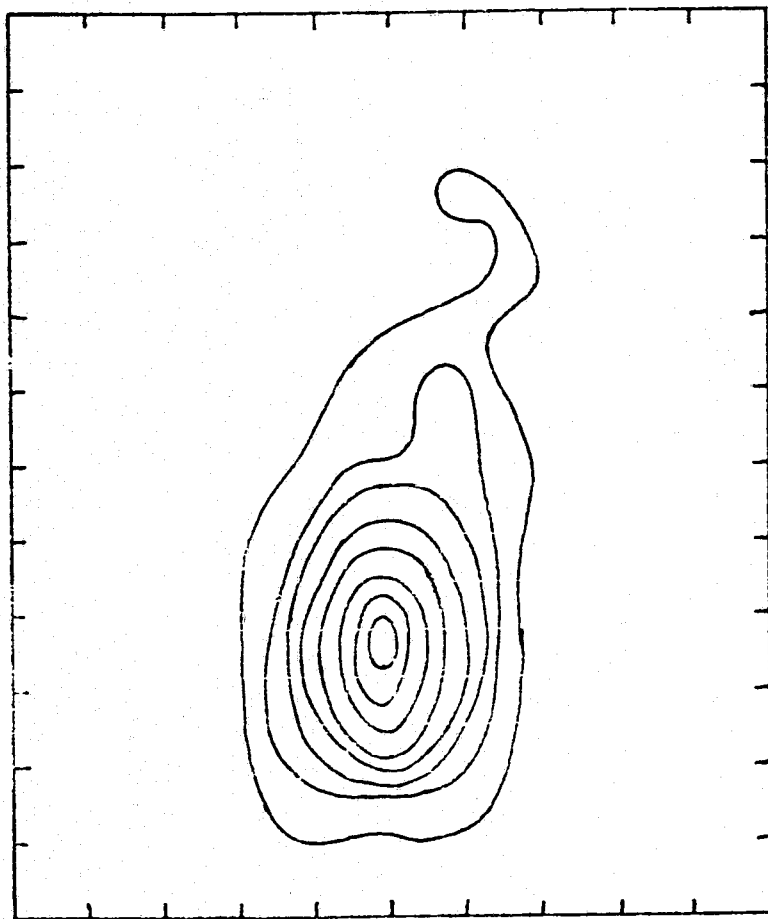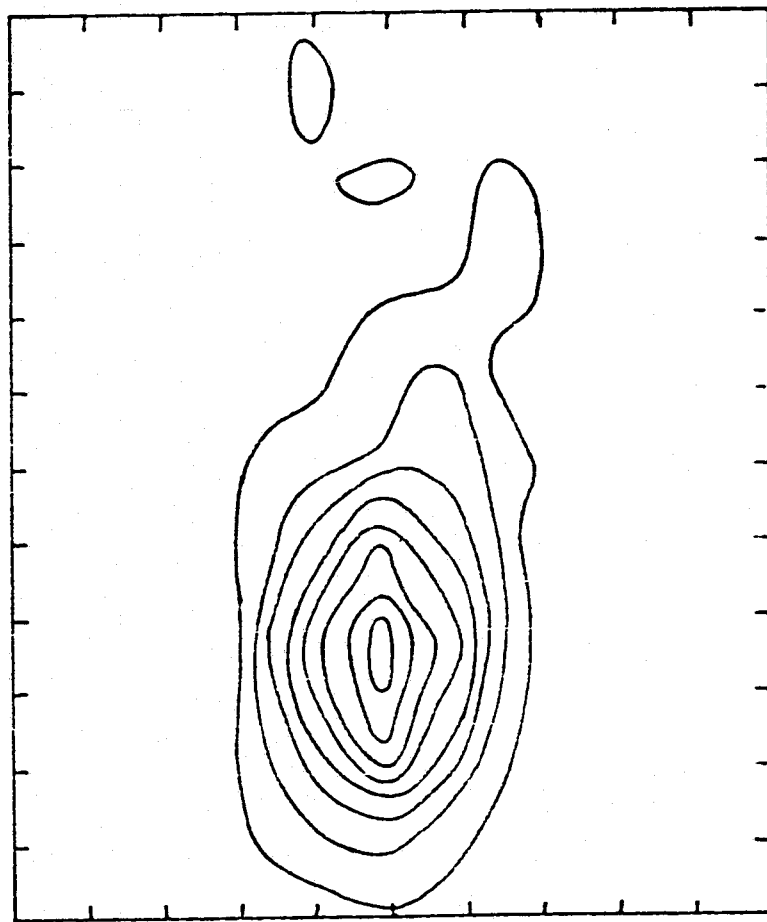
COMBINED 1972 DATA   MAY 1973

Figure V.5.   Possible maps of 3C 84 for some of the other 3C 84 data.
The combined 1972 data was taken during May, June and July.

D. HIGH RESOLUTION MAPS

Clearly, the full resolution of the array is necessary to see exactly what is happening. Because the lines of maxima and minima do not continue outward as entirely straight lines to the length of the Onsala baselines, we can expect the structure to be more complex at higher resolution.

Certain problems arise with the addition of Onsala. First, the GS baseline sweeps with remarkable speed across the complexities in the (u,v) plane. The density of the data points along the track is unequal to the task of following them. The data on GS are sparser than on the other Onsala baselines because the Goldstone station was generally only available for one day during each session. The longest baseline, therefore, adds relatively few data points to the solution. It does, however, add parameters in abundance, because the grid must be more finely spaced to accommodate the resolution. It also worsens the problem of interparameter correlation. For this reason, the GS baseline was not included in any of the present solutions, nor any of the closure phase data sets containing it.

Solutions were obtained for the October 1973, and for the March, May and July 1974, sessions. The grids consisted of 7 by 14 points, for a total of 98 fitted parameters. All were initialized with an interpolated version of the low resolution May 1974 solution. In addition, the May 1974 run was also successfully started from a single point source. The details are summarized in Table V.2. The fits to the data are presented in Figure V.6 and the maps in Figure V.7. This contour interval is 2.2×10^{10} K., twice that of the low resolution maps. Not enough data was available from the August 1973 session to attempt a solution.

These fits are not, overall, as good as the low resolution ones. Most of the deviation appears in the closure phase data involving Onsala, where the data are rather sparse and noisy. Some of the problem may come from power lying outside the grid. More likely, however, it is due to mutually contradictory data points, perhaps caused by calibration errors in Sweden. Recall that the scale is uncorrected for variations in system temperature, and the 3C 84 data is collected over a very large range of elevations. The source never sets in Sweden and, at the end of the track, is skimming the northern horizon in lower culmination. Since the

Table V.2. Summary of high resolution 3C 84 solutions

Session	Half-power beam E/W	N/S	Data A	ϕ	Grid E/W	N/S	$\sqrt{\chi^2}$	Peak T_b	Map Flux	Total Flux
Oct 73	1.16	1.40	280	116	7	14	3.36	1×10^{11}	48.1	57.0
Mar 74	1.16	1.40	406	140	7	14	3.81	2×10^{11}	55.0	57.9
May 74	1.16	1.40	352	102	7	14	2.94	1×10^{11}	52.4	57.8
Jul 74	1.16	1.40	545	150	7	14	3.37	2×10^{11}	53.7	57.9

BASELINE HN
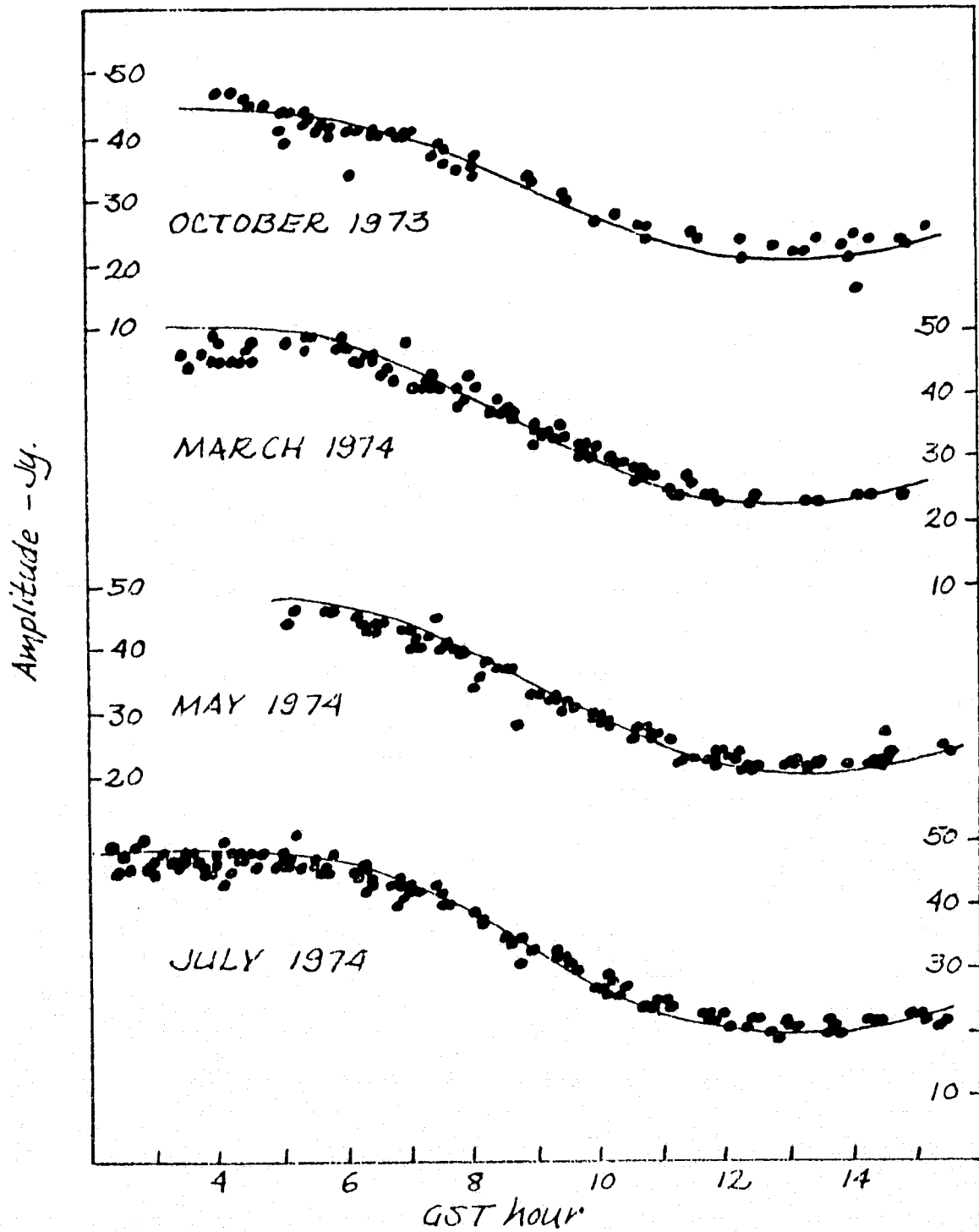
Figure V.6.a.   Fits to the filtered HN baseline amplitudes for the high
resolution 3C 84 maps.
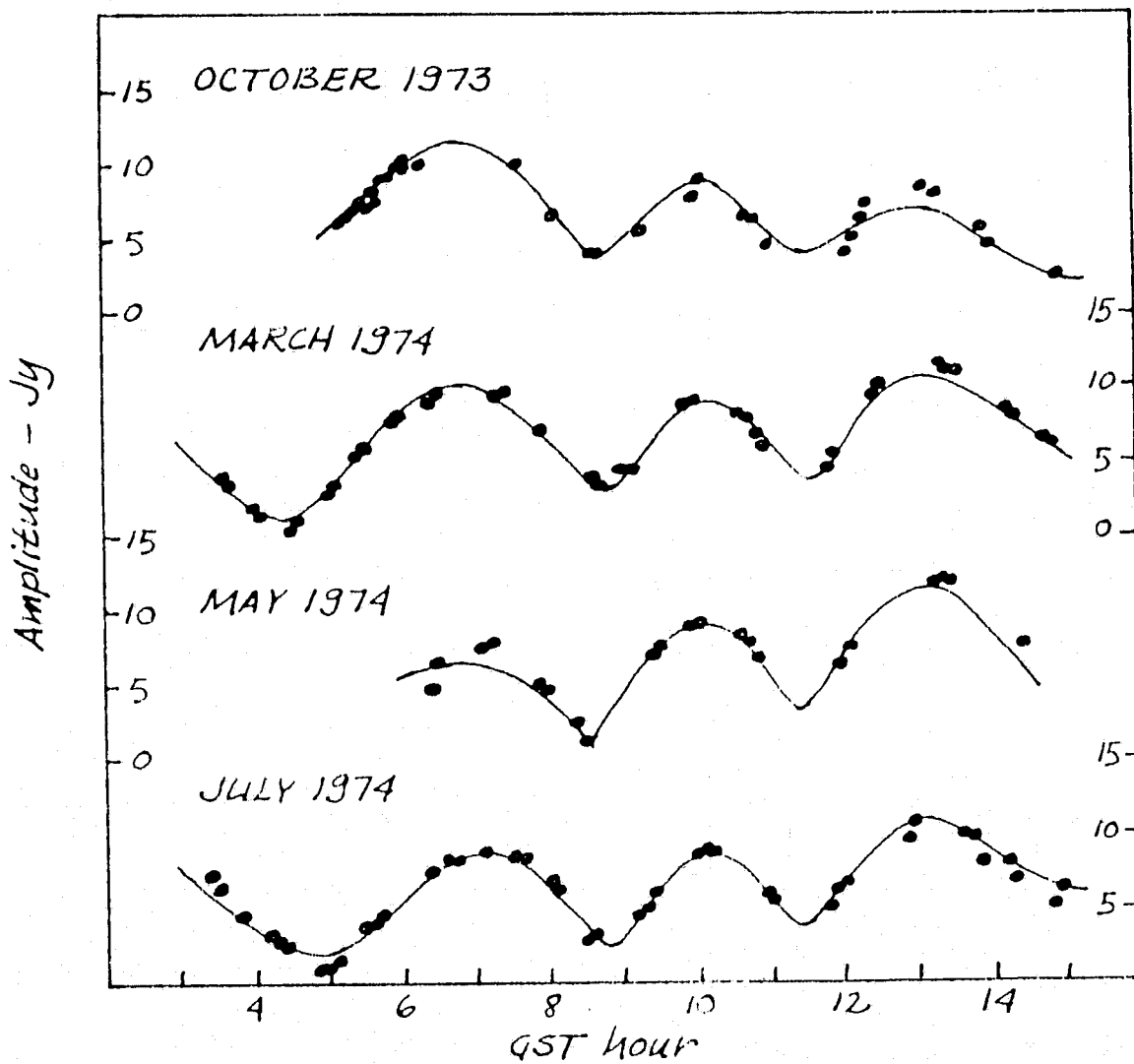
Figure V.6.b. Fits to the filtered NG baseline amplitudes for the high resolution 3C 84 maps.
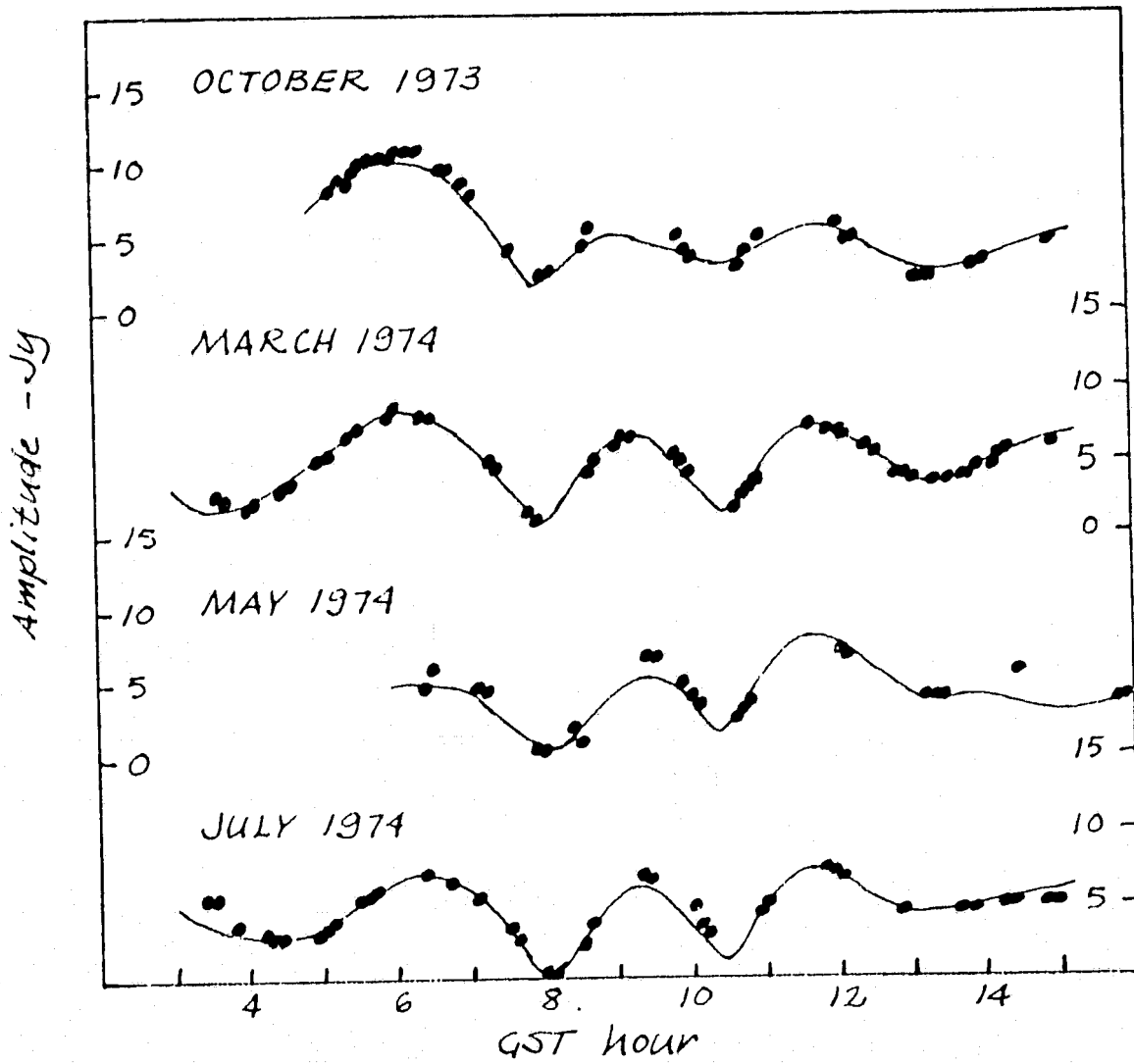
Figure V.6.c. Fits to the filtered HG baseline amplitudes for the high resolution 3C 84 maps.

Figure V.6.d. Fits to the filtered HS baseline amplitudes for the high resolution 3C 84 maps.

Figure V.6.e. Fits to the filtered NS baseline amplitudes for the high resolution 3C 84 maps.
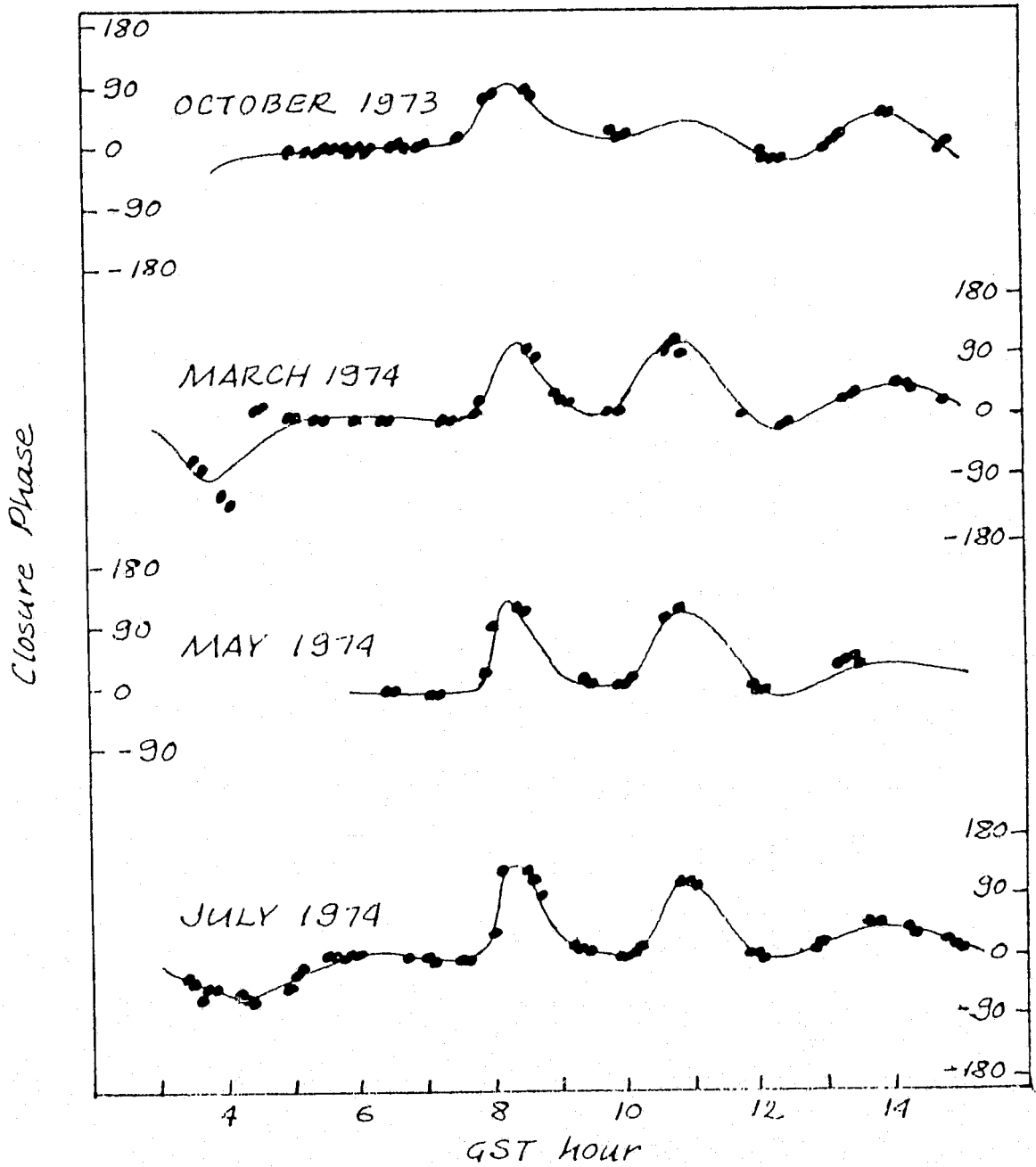
TRIPLET HNG

Figure V.6.f.   Fits to the HNG triplet closure phases for the high
resolution 3C 84 maps.
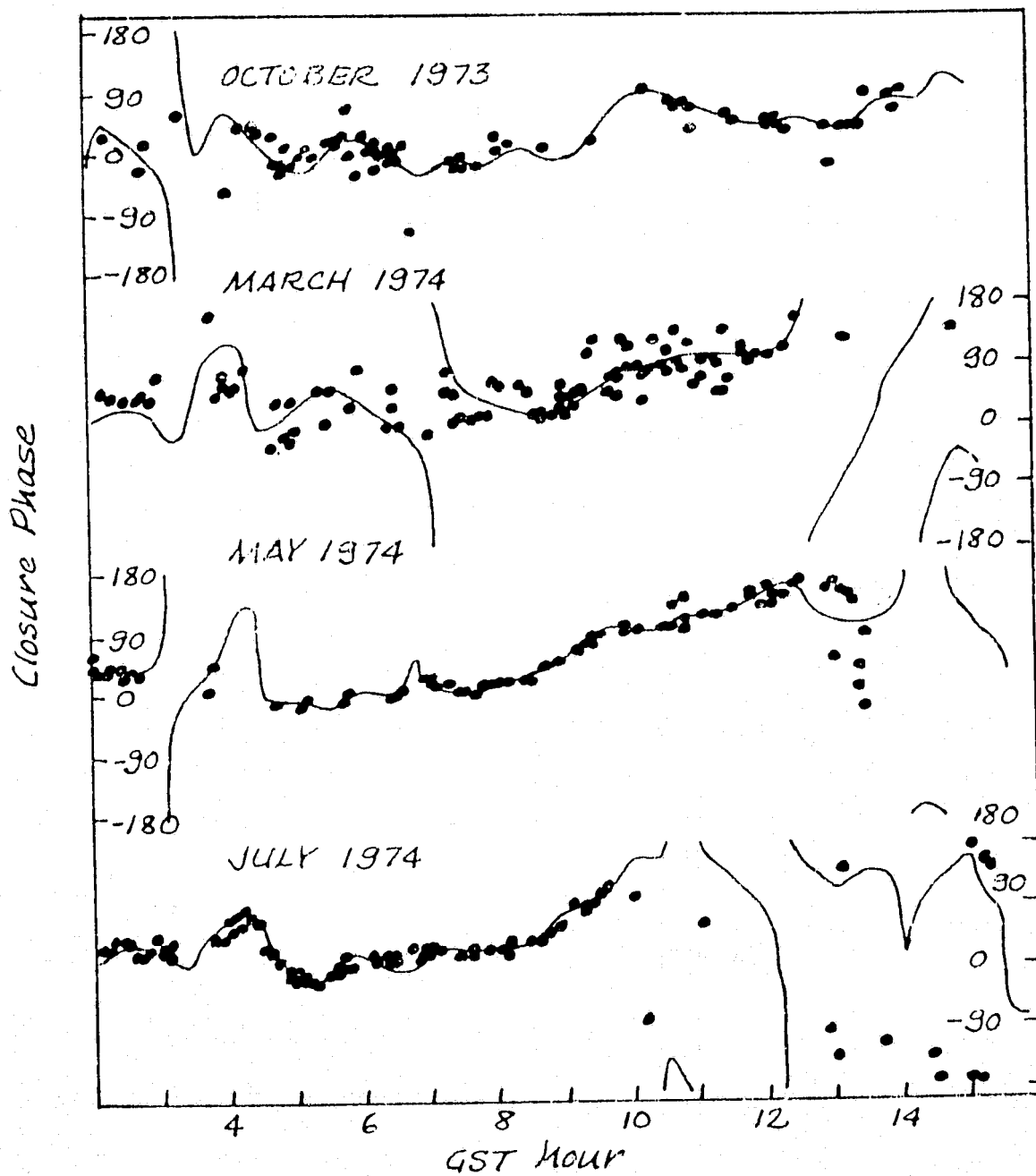
Figure V.6.g. Fits to the HNS triplet closure phases for the high resolution 3C 84 maps.

OCTOBER 1973
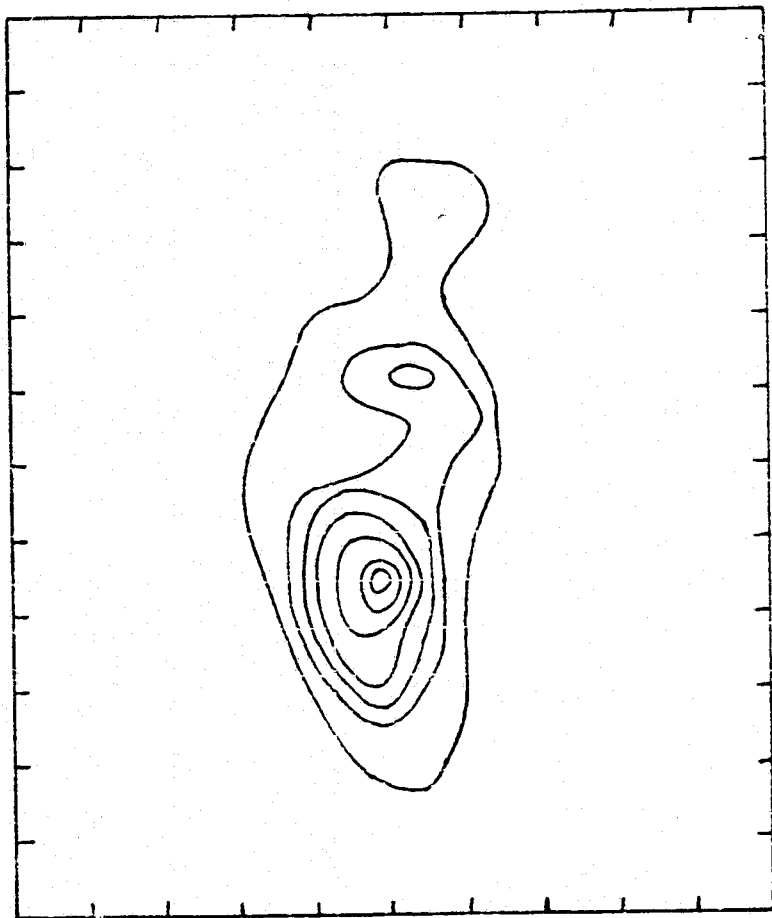
MARCH 1974
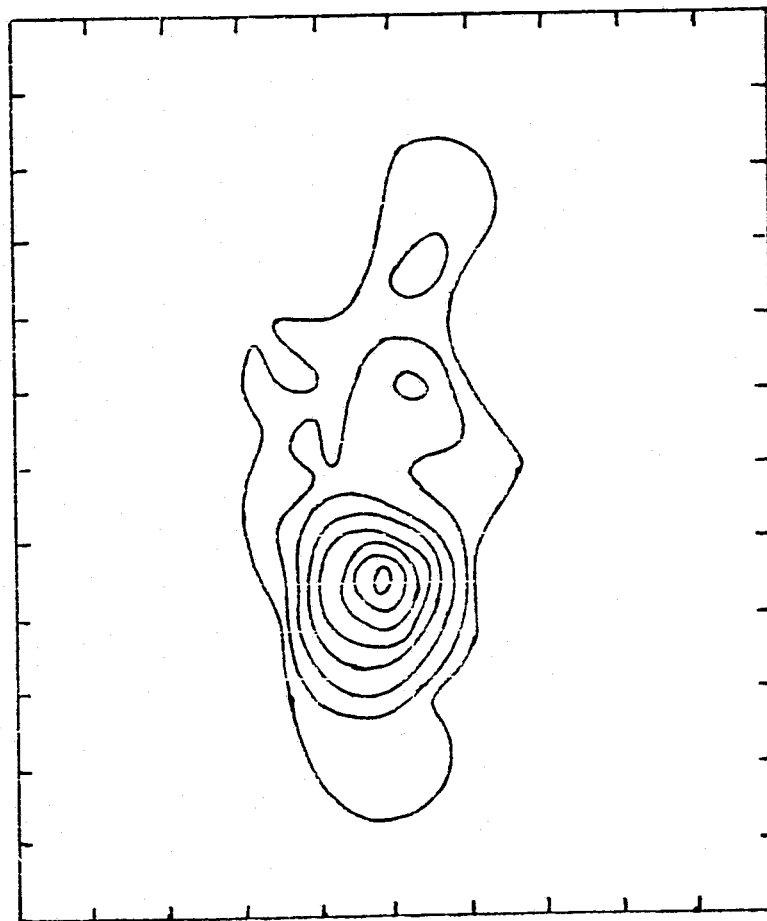
Figure V.7.a.   High resolution maps of 3C 84 for the October 1973 and
        March 1974 observing sessions.   Contour interval is 1.0 Jy/msec or
        2.2 x 10^{10} K.
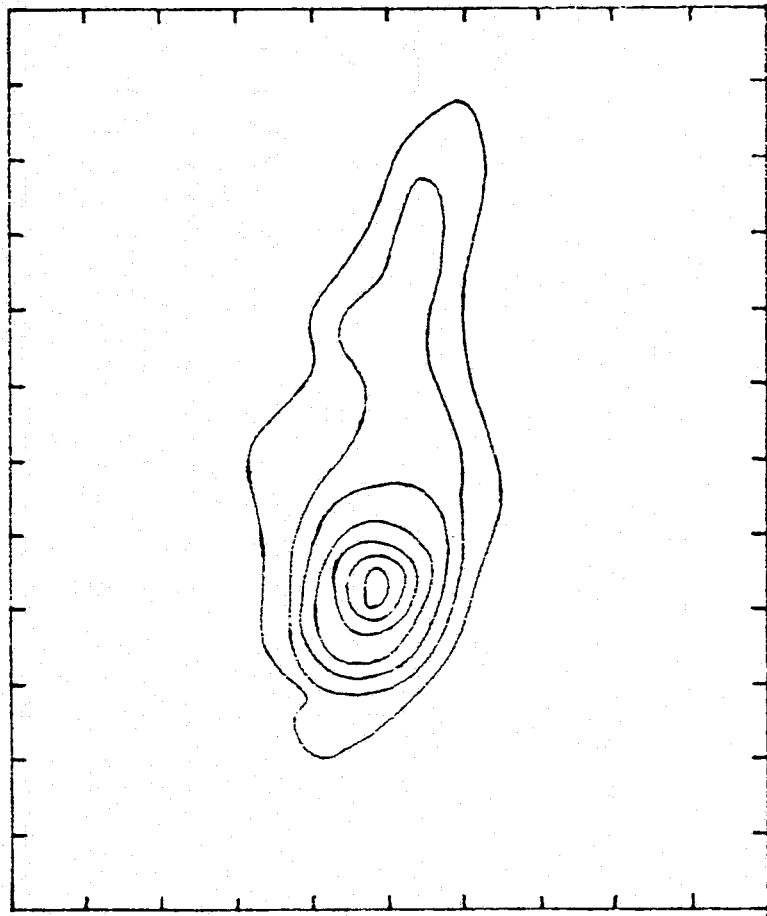
MAY 1974   JULY 1974
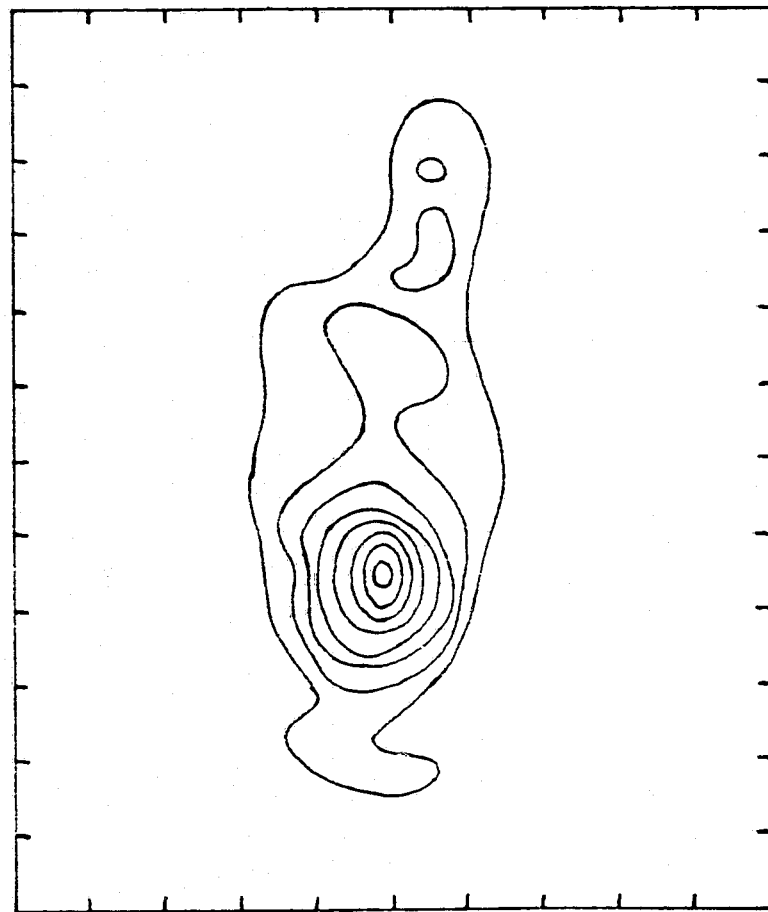
Figure V.7.b.   High resolution maps of 3C 84 for the May and July 1974
     observing sessions.   Contour interval is 1.0 Jy/msec or 2.2 x 10^{10}
     K.

general variations in the high resolution data are reproduced, we can expect the main features of the fine structure to be real. We might, however, beware of the details.

These maps will reproduce the trend in the GS amplitudes, but not the exact form of the wiggles. Since the wiggles and scatter are almost indistinguishable without better sampling, we can only say that the structure is consistent with GS as well.

Although the time span is much shorter for these maps, changes with a consistent trend are visible. There appear to be two components to the north of the strong one. During this time period, the northernmost component brightened while the central one dimmed, creating the impression of power migrating to the north without any actual motion of the "hot spots". As before, the brightness of the southern component reached nearly the same value in each session.

E. DISCUSSION

Conveniently, our perhaps best set of data was spaced not more than one week in time away form a four station run at 2.8 cm using the Bonn dish with Fort Davis, Texas, NRAO, and Owens Valley in the United States (Pauliny-Toth et al, 1976). This data set contains no closure phase information, but the coverage was relatively good on six baselines out to 290 million wavelengths. The author's adaptation of Pauliny-Toth's map and ours are presented side by side in Figure V.8. The 2.8-cm map has been arbitrarily inverted, to put the power at the proper end of the source. It has about twice the resolution that ours does. Like ours, Pauliny-Toth's map is composed of a string of components more or less aligned along the same position angle. Beyond that, however, there appear to be major differences. It would perhaps be possible to blend Pauliny-Toth's two southern components to form our one. But our central component occupies the space of a large blank in Pauliny-Toth's map.

These differences might be caused by real structure changes with frequency. Although the frequency difference is not great, the spectral region in question is near the synchrotron self-absorption peak. If different parts of the source became optically thick at different frequencies, one might expect rather drastic changes over relatively small differences in frequency.
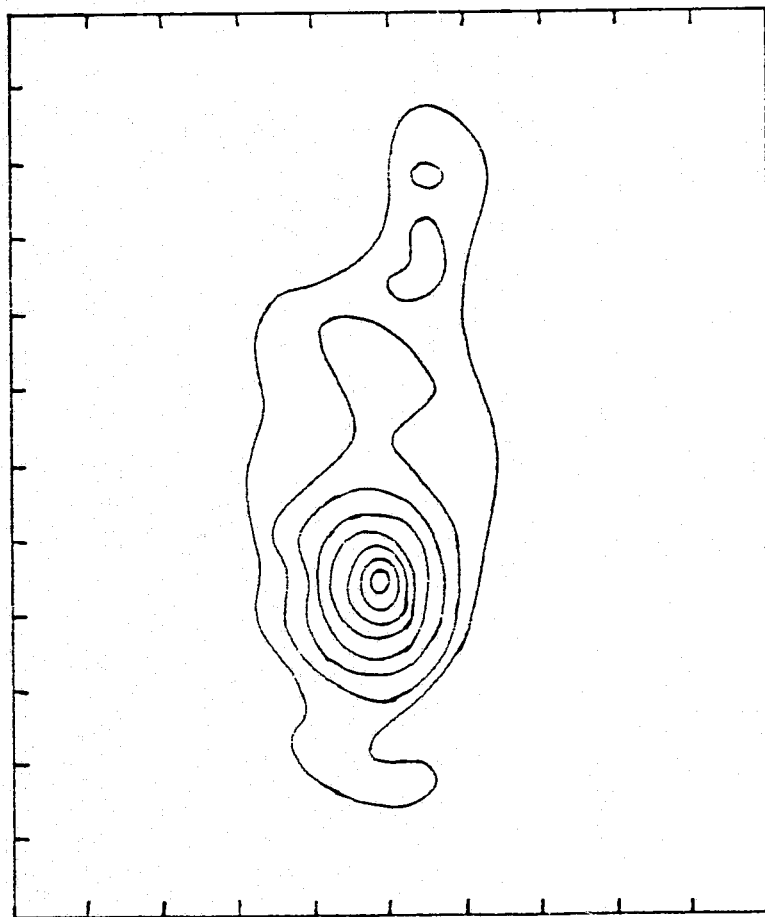
3.8 - CM MAP   2.8 - CM MAP
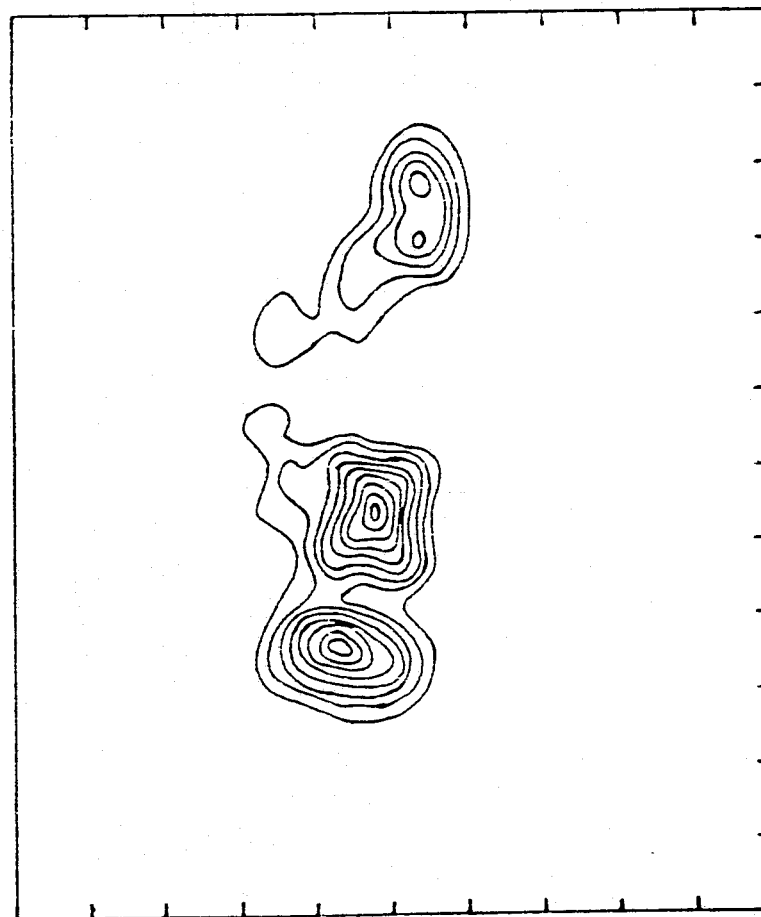
Figure V.8.   Comparison of the present results with the author's
             hand-sketched adaptation of the Pauliny-Toth et al.(1976) 2.8-cm
             map.

Alternatively, ambiguities caused by the mapping procedures or by differences in the (u,v)-plane coverage could be responsible. To test this possibility, our map was used to generate visibility curves on the "FOG" baselines. The Bonn baselines are all longer than our maximum resolution, so no useful comparison can be made with them. The reproduction was good to within a maximum deviation of less than 10 percent in isolated spots in the (u,v) plane. This suggests that our map is applicable to the 2.8-cm data as well with only minor changes. There is no evidence for large scale changes in structure with frequency in this resolution range. This result suggests that the Pauliny-Toth map is not the proper solution and might not fit closure phase data if there were any. This conclusion is reinforced by the appearance in the VLB Array Report (Cohen et al. 1975b), in the course of its evaluation of VLBI modeling problems, of another possible map based on the Pauliny-Toth data. It looks much like our present results.

Our mapping procedure has also been confirmed by means of a two-dimensional version (Hutton, unpublished) of the Fourier series analysis routine developed by Rogers et al. (1974), and by a semi-model-fitting technique developed by Cotton (see Wittels et al. 1976). Both were, of course, done on the 3.8-cm data. In addition, a map for early 1973, again at 2.8 cm, obtained by a method developed by Fort and Yee (1976) is presented in the VLB Array Report. It also closely resembles our map. The Fort and Yee algorithm has also been applied to some of the older, and probably inadequately sampled, Quasar Patrol data, producing several possible maps (Fort 1976). The shortest baseline used here was HG so that the larger scale structure is totally undetermined. With the addition of a little imagination an even older Canadian model (Legg et al. 1973) fit to some 2.8-cm data can also be made to resemble the present results.

We conclude that the construction of a spectral index map of 3C 84 should wait until phase data becomes available at other frequencies, or until grids initialized from an adequately sampled closure-phase solution can be least squares fitted to the amplitude data where this is not possible.

Fringe amplitude data have also been taken on 3C 84 at 2 cm (Niell et al. 1975) and at 18 cm (Shaffer and Schilizzi 1975) but no models have been fitted. The features of the amplitude curves are consistent with a similar structure.

We observe no motion of nulls. None of the source components appear to move, during the October 1973 to July 1974 time period, by more than about 0.2 msec of arc. The corresponding velocity limit is 0.3 msec of arc per year or 0.5 times c. There appear to be only changes in the relative power of the components. They change, at least during this time period, however, in such a way that power migrates northward, in the direction that might mimic apparent expansion if it were to continue long enough

Chapter VI

CONCLUSIONS

We now draw conclusions, on the performance of both the computer algorithm and the radio sources.

A. THE ALGORITHM

One important point can be made in favor of the sky-grid fitting operation; it was successful. It succeeded in exchanging information about the size of the brightness distribution for whatever information might be missing about the visibility function. Apart from the size restriction, which could be set arbitrarily, it allowed a completely general brightness distribution. The maps were constructed with no confusing sidelobes. It was possible, also, to implement reasonable physical restrictions on the maps; for example, that the source be positive. Furthermore, the procedure was less sensitive to initial model input than is usual for VLBI mapping or modeling.

The generality, however, required huge numbers of fit parameters, and hence huge amounts of computer time. The complicated nature of spaces with huge numbers of dimensions further slowed convergence by introducing complicated correlations between the parameters. We were, therefore, thrown out on our own, so to speak, for error analysis. Our evaluation of the procedure rests, then, on artificially generated test sources, on comparison with other methods and data sets, and consistency of different results on the same source.

We must conclude that, when the information is present in the data, and this is a question of coverage, the sky-gridding algorithm is capable of extracting it, given computer time.

B. THE SOURCES

In two optically similar galaxies, we find somewhat divergent radio behavior. In 3C 120, whose total power variations are rapid, we also

-81-

observe rapid changes in the structure. Each of the total power flares is seen to arise from a distinct structural component and the components are seen to separate at superrelativistic velocities. This separation has continued more or less linearly over a series of separate flares, along virtually the same position angle. In 3C 84, on the other hand, the individual components also change in intensity but do not move measurably. The time scale of the variations is somewhat slower.

Let us first consider 3C 120.

In the first, chronologically, instance of apparent super-relativistic motion (Whitney et al. 1971), nine possible explanations were suggested, all perhaps "almost as dubious as the like number of lives of the proverbial felines". The first suggestion (numbered i) was that the poor (u,v)-plane coverage was not sufficient to specify the brightness distribution, and that the double structure was an illusion. However, it has withstood the test of additional data, some of it with closure phase, on five sources: 3C 120, 3C 273B, 3C 279 (Whitney et al. 1971; Kellermann et al. 1974; Marandino, unpublished), BL Lac (Clark et al. 1973), and 3C 345 (Cohen et al. 1976; Wittels et al. 1976). Now is the time to re-examine, maps in hand, the other eight suggestions.

Explanations (vii), that the Hubble constant is totally wrong, (viii), that our notions of cosmology are totally wrong, and (ix), that the source components consist of tachyonic material, are too drastic for even this many-fold increase in the amount of data to justify. Explanation (vi), that the quasar redshift is not a distance indicator, seems less viable when applied to galaxies. Explanations (iii), the so-called "Christmas tree" model where components blink on and off randomly to mimic expansion, is eliminated by inspection of the 3C 120 maps (see also Wittels et al. 1976 for motion observed in 3C 345). We would also expect, if (iii) is the correct explanation, to see apparent contractions about half the time. None have been observed. The same objection applies to explanation (v), that multipath propagation phenomena are responsible. It would also seem difficult to produce expansion continuous over several flares.

That leaves the cat with only two of her lives. The apparent velocity of separation could represent a phase velocity, rather than a group velocity. Alternatively, actual motion of sources might be occurring. If the line of motion makes a small enough angle (less than about 30 degrees in the case of 3C 120's 4 c rate) with the line of

sight, special relativistic effects can cause rapid apparent motion
(e. g. Rees 1966; Cavaliere, Morrison, and Sartori 1971; Behr et al.
1976). Seielstad (1974) attempted to synthesize the flux history and the
existing VLBI data on 3C 120 in the light of a model proposed earlier by
Ozernoy and Sazonov (1969). Explosive events in the nucleus were assumed
to repeatedly eject pairs of synchrotron emitting plasmoids in opposite
directions. The plasmoids expand adiabatically as they travel outward.
If the velocities are assumed relativistic, the approaching component (A)
always appears further advanced in its evolution than the receding
component (B), because of the light travel time between the two. He
fitted a series of parameterized outbursts to the total flux history at
2.8, 3.8, 4.5, and 6.0 cm wavelengths, and divided them into pairs. He
then confirmed the existence of the multiple source components and
estimated velocities of separation and expansion from published VLBI
data. He concluded that the VLBI measurements, sparse though they were,
confirmed the model and, furthermore, that both separation and expansion
rates were relativistic. His analysis stopped in mid-1973, nearly at the
peak of the second member of the strong outburst pair. Our multiple
baseline data began with this pair.

The logic of the pairs of ejecta in the Ozernoy and Sazonov model
is based on the prominence of double structure in many radio sources,
among them the giant doubles, and on the suggestion of duplicity in the
total flux curves of a few variable sources (Andrew 1973; Seielstad
1974). Equally as striking as the double outburst phenomenon in the
appearance of the 3C 120 total flux curve is the rarity of the really
strong outbursts. Prior to the ones in 1973, the last were the
"classics" of 1967-68 that contributed so much to the theory of variable
radio sources (see Kellermann and Pauliny-Toth 1968). The smaller peaks
in between seem by comparison to be only afterthoughts. Although our
observations cover less than even one full cycle, they may contain some
relevant evidence. Only during the strong flares is there evidence that
the source and the components are consistently very small. Both become
larger and more complex during the later flares. A modification of this
simple ejection model might be made to fit the observations if it were
allowed that true physical outbursts occur less frequently than
originally proposed and that the ejecta do not fade uniformly as
adiabatically expanding clouds as they pass outward. It is interesting
that, although these minor flares do show the characteristic behavior

with frequency which suggests optical depth changes, Aller, Olsen, and
Aller (1976) have polarization data that shows a more complex model to be
required. In particular, they believe the flares never become completely
optically thin at these frequencies. They also observe continuity of the
position angle of polarization over several total power peaks, although
a possible change occurred in early 1974 at the time of one of the peaks.

Any model wheih involves relativistic ejection of any substantial
amount of matter involves formidable kinetic energy requirements. Also,
relativistic ejection generally predicts a large power difference between
approaching and receding components due to the redshift difference. For
symmetrical ejection, the case considered by Seielstad, it is not
possible to produce the 4 c apparent expansion without an apparent flux
ratio greater than 10 between the two components at their peaks.
Clearly, the receding component should not be seen at all.
Alternatively, one of the observed components might be the central site
of the ejection of the other, in which case there should be some
observabe difference between the two, or all of the components that we
observe are approaching by along different angles to the line of sight.
Ejection of multiple components in a plane which we are viewing edge on,
for example, would preserve the preferred position angle. Any ejecta
moving in directions too far removed from the line of sight might not be
blueshifted enough to be observable. Note that this model does not put
the Earth in a preferred position, because if the line of sight did not
lie near the plane, no superrelativistic expansion would be observed.
Alternatively, a model where stationary source components are
"turned on" by the passage of a moving excitation front might have some
advantages. The kinetic energy problems disappear and, since the
radiating material would not be moving, so do the redshift problems.
Travel time and phase velocity related phenomena are still available to
produce superrelativistic apparent motion.

A different sort of phase velocity model has been put forward by
Sanders (1974). In this model, the apparent motion depends on
observation of different parts of a dipolar magnetic field as synchrotron
radiation from electrons constrained to move along the field lines is
beamed toward Earth. A pair of light spots which separate linearly with
time is predicted for a perfect dipolar field. One would expect that the
complexity, presumably in the magnetic field, needed to explain the
flares would also produce irregularities in the explansion velocity. On

the contrary, we observe a fairly uniform expansion over several total power peaks.

Although it is not strictly necessary, of course, that 3C 84 and 3C 120 stem from the same physical mechanism, the VLBI observations do not appear to exclude the possibility of their doing so. Although their time scales of variation and motion are different, they both do exhibit distinct structure components which change in flux.

The apparent complexity of 3C 84 shows mostly on intercontinental baselines. On the short baselines, it could pass as a highly unequal double. In other words, if 3C 84 were turned sideways, reduced in flux by a factor of five, moved to a declination of +5 degrees, and observed with the HNC triplet, it might look quite a bit like some of our 3C 120 observations. The insensitivity of Onsala would have disguised any fine structure that might have existed in 3C 120. If the two sources are in fact physically similar, the high resolution observations of 3C 84 should shed some light on the character of the apparent motions. Although each component is not observed to move, a series of them might be excited in succession to mimic expansion. The differences between the sources might, then, boil down to time scale and to the relative spatial scale of the inhomogeneities in the material or magnetic field in the source and the excitation mechanism. Or, within the context of an ejection model, the difference between the sources might be simply the result of a difference in the actual velocities or angles involved.

Both ejection and phase velocity explanations appear to have survived the onslaught of data in modified form. It is clear that, in both cases, what has been added is a requirement for complexity. The simplest forms of the models are not adequate.

C. LOOKING AHEAD

Eventually, VLBI experiments will no doubt become even grander in scale that they are now, and all but the tiniest holes in the (u,v) plane will be filled. The proposed "VLB Network" is already in the planning stages for such operations (Cohen et al. 1975b). Insofar as better coverage always helps, maps can always be better determined.

It is interesting to speculate, however, what windfalls source structure work may reap if and when the planned technical requirements necessary to measure continental drift are implemented. The first will

-85-

be, of course, sensitivity, since wider recording bandwidths are planned. Work could be extended to weaker quasars and perhaps even some of the more ordinary Seyfert galaxy nuclei. Wider synthesized bandwidths provide, purely and simply, more (u,v)-plane coverage and perhaps some spectral information.

Astrometric data of accuracy useful on the scale of a few milliseconds of arc may also result. Closure phase based maps could be used to make corrections for source structure to the phase data used in the astrometric/geodetic solutions, thereby refering them to a known position in the map. Maps from successive experiments could then be superposed in absolute coordinates. Notice that the usefulness of this scheme implies the necessity of source structure corrections for good baseline solutions.

It is apparent from this study that experiments closely spaced in time, approximately every three months, are necessary to follow unambiguously the source structure changes in 3C 120. On the other hand, data over many individual outbursts, years in other words, are necessary to see any pattern. Spectral information is also a must. The accumulation of the VLBI data necessary to specify the mechanism of compact radio sources will, of necessity, be a long and slow process. The Quasar Patrol has shown, however, the value of a systematic monitoring program.

We shall end with a list of questions which might be attacked with the help of very long baseline interferometry, and which might shed some light on the problem.

Do outbursts come in pairs? If so, is there any systematic difference in the power, duration, internal expansion rate, polarization, or any other observable property, between the approaching and receding components? Do any recurrently appear at the same projected position? Or do outbursts come in groups of many? Are the apparent rates and directions of component separation, and hence the true rate and angle in the ejection model, repeatable in the same source? Can the center of ejection, if there is one, be seen as a radio source? Is there any physical motion at all?

REFERENCES CITED

H. D. Aller, E. T. Olsen, M. F. Aller. A. J., in press. "Linear Polarization and Flux Density Variations in the Radio Galaxy 3C 120"

B. H. Andrew. Ap. J. 186, L3, 1973. "Models of VRO 42.22.01 (BL Lacertae)"

H. C. Arp. Ap. J. 152, 1101, 1968. "A Compact Galaxy (III Zw 2) And A Compact Radio Galaxy (3C 120) With Seyfert-Type Spectra"

J. W. M. Baars, A. P. Hartsuijker. Astron. and Astroph. 17, 172., 1972. "The Decrease of Flux Density of Cassiopeia A and the Absolute Spectra of Cassiopeia A, Cygnus A and Taurus A"

C. Bare, B. G. Clark, K. I. Kellermann, M. H. Cohen, D. L. Jauncey. Science 157, 189, 1967. "Interferometer Experiment with Independent Local Oscillators"

C. Behr, E. L. Schucking, C. V. Vishveshwara, W. Wallace. A. J. 81, 147, 1976. "Kinematics of Relativistic Ejection"

P. R. Bevington. Data Reduction And Error Analysis For the Physical Sciences. (New York: McGraw Hill, Inc., 1969)

R. N. Bracewell. The Fourier Transform and Its Applications. (New York: McGraw Hill, Inc., 1965)

N. W. Broten, T. H. Legg, J. L. Locke, C. W. McLeish, R. S. Richards, R. M. Chisholm, H. P. Gush, J. L. Yen, J. A. Galt. Science 156, 1592, 1967a. "Long Baseline Interferometry: A New Technique"

N. W. Broten, T. H. Legg, J. L. Locke, C. W. McLeish, R. S. Richards, R. M. Chisholm, H. P. Gush, J. L. Yen, J. A. Galt. Nature 215, 38, 1967b. "Observations of Quasars Using Interferometer Baselines Up to 3,074 Km."

N. W. Broten, R. W. Clarke, T. H. Legg, J. L. Locke, C. W. McLeish, R. S. Richards, J. L. Yen, R. M. Chisholm, J. A. Galt. Nature 216, 44, 1967c. "Diameters of Some Quasars at a Wavelength of 66.9 Cm."

E. M. Burbidge. Ap. J. 149, L51, 1967. "Redshifts of Thirteen Radio Galaxies"

E. M. Burbidge, G. R. Burbidge. Ap. J. 142, 1351, 1965. "Optical Evidence Suggesting the Occurence of a Violent Outburst in NGC 1275"

A. Cavaliere, P. Morrison, L. Sartori. Science 173, 525, 1971. "Rapidly

C.2

Changing Radio Images"

B. G. Clark, M. H. Cohen, D. L. Jauncey. Ap. J. 149, L151, 1967.
"Angular Size of 3C 273B"

B. G. Clark, K. I. Kellermann, C. C. Bare, M. H. Cohen, D. L. Jauncey.
Ap. J. 153, L67, 1968a. "Radio Interferometry Using a Base Line of
20 Million Wavelengths"

B. G. Clark, K. I. Kellermann, C. C. Bare. M. H. Cohen, D. L. Jauncey.
Ap. J. 153, 705, 1968b. "High-Resolution Observations of
Small-Diameter Radio Sources at 18-Centimeter Wvelength"

B. G. Clark, K. I. Kellermann, M. H. Cohen, D. B. Shaffer, J. J.
Broderick, D. L. Jauncey, L. I. Matveyenko, I. G. Moiseev. Ap. J.
182, L57, 1973. "Variations In The Radio Structure of BL Lacertae"

R. W. Clarke, N. W. Broten, T. H. Legg, J. L. Locke, J. L. Yen. M. N. R.
A. S. 146, 381, 1969. "Long Baseline Interferometer Observations
at 408 and 448 MHz - II. The Observations"

M. H. Cohen. Annual Review of Astron. and Astroph. 7, 619, 1969. "High
Resolution Observations of Radio Sources"

M. H. Cohen, W. Cannon, G. H. Purcell, D. B. Shaffer, J. J. Broderick, K.
I. Kellermann, D. L. Jauncey. Ap. J. 170, 207, 1971. "The
Small-Scale Structure of Radio Galaxies and Quasi-Stellar Sources
at 3.8 Centimeters"

M. H. Cohen, A. T. Moffet, J. D. Romney, R. T. Schilizzi, D. B. Shaffer,
K. I. Kellermann, G. H. Purcell, G. Grove, G. W. Swenson, J. L.
Yen, I. I. K. Pauliny-Toth, E. Preuss, A. Witzel, D. Graham. Ap.
J. 201, 249, 1975a. "Observations with a VLB Array. I.
Inroduction and Procedures"

M. H. Cohen et al. 1975b. "A VLBI Network Using Existing Telescopes: A
Report and Proposal Submitted by the Network Users Group"

M. H. Cohen, A. T. Moffet, J. D. Romney, R. T. Schilizzi, G. A.
Seielstad, K. I. Kellermann, G. H. Purcell, D. B. Shaffer, I. I. K.
Pauliny-Toth, E. Preuss, A. Witzel, R. Rinehart. Ap. J. 206, L1,
1976. "Rapid Increase in the Size of 3C 345"

W. A. Dent. Ap. J. 144, 843, 1966. "Variation In the Radio Emission
From The Seyfert Galaxy NGC 1275"

W. A. Dent. Science 175, 1105, 1972a. "3C 279: Evidence for a
Non-Superrelativistic Model"

W. A. Dent. Ap. J. 177, 93, 1972b. "A Flux-Density Scale For Microwave
Frequencies"

W. A. Dent, G. Kojolan. A. J. 77, 819, 1972. "7.8-GHz Flux Density
Measurements of Variable Radio Sources"

D. S. DeYoung. Ap. J. 177, 573, 1972. "The Distribution of Radiation
from Relativistically Expanding Radio Sources"

D. S. DeYoung, M. S. Roberts. W. C. Saslaw. Ap. J. 185, 809, 1973.
"Detection of 21-Centimeter Hydrogen Absorption In The
High-Velocity Component of the Radio Galaxy Perseus A'"

D. N. Fort. Ap. J. 207, L155, 1976. "The Brightness Distribution of 3C
84"

D. N. Fort, H. K. C. Yee. Astron. and Astroph. 50, 19, 1976. "A Method
of Obtaining Brightness Distributions from Long Baseline
Interferometry"

J. Gubbay, A. J. Legg, D. S. Robertson, A. T. Moffet, B. Seidel. Nature
222, 730, 1969a. "Trans-Pacific Interferometer Measurements at
2,300 MHz"

J. Gubbay, A. J. Legg, D. S. Robertson, A. T. Moffet, R. D. Ekers, B.
Seidel. Nature 225, 1094, 1969b. "Variations of Small Quasar
Components at 2,300 MHz"

D. J. Heeschen. Ap. J. 133, 322, 1961. "Observations of Radio sources
at Four Frequencies"

H. F. Hinteregger, I. I. Shapiro, D. S. Robertson, C. A. Knight, R. A.
Ergas, A. R. Whitney, A. E. E. Rogers, J. M. Moran, T. A. Clark, B.
F. Burke. Science 178, 396, 1972. "Precision Geodesy via Radio
Interferometry"

H. F. Hintergger. Ph. D. dissertation, Massachusetts Institute of
Technology, 1972. "Geodetic and Astrometric Applications of Very
Long Baseline Interferometry"

R. C. Jennison. M. N. R. A. S. 118, 276, 1958. "A Phase Sensitive
Interferometer Technique for the Measurement of the Fourier
Transform of the Spatial Brightness Distribution of Small Angular
Extent"

K. I. Kellermann, I. I. K. Pauliny-Toth. Annual Review of Astron. and
Astroph. 6, 417, 1968. "Variable Radio Sources"

K. I. Kellermann, B. G. Clark, C. C. Bare, O. Rydbeck, J. Ellder, B.
Hansson, E. Kollberg, B. Hoglund, M. H. Cohen, D. L. Jauncey. Ap.
J. 153, L209, 1968. "High-Resolution Interferometry of Small Radio
Sources Using Intercontinental Base Lines"

K. I. Kellermann, D. L. Jauncey, M. H. Cohen, D. B. Shaffer, B. G. Clark,

J. Broderick, B. Ronnang, O. E. H. Rydbeck, L. Matveyenko, I. Moiseyev, V. V. Vitkevitch, B. F. C. Cooper, R. Batchelor. Ap. J. 169, 1, 1971. "High-Resolution Observations of Compact Radio Sources at 6 and 18 Centimeters"

K. I. Kellermann, B. G. Clark, D. L. Jauncey, J. J. Broderick, D. B. Shaffer, M. H. Cohen, A. E. Niell. Ap. J. 183, L51, 1973. "Observations of Further Outbursts In The Radio Galaxy 3C 120"

K. I. Kellermann, B. G. Clark, D. B. Shaffer, M. H. Cohen, D. L. Jauncey, J. J. Broderick, A. E. Niell. Ap. J. 189, L19, 1974. "Further Observations of Apparent Changes in the Structure of 3C 273 and 3C 279"

E. Y. Khachikian, D. W. Weedman. Ap. J. 192, 581, 1974. "An Atlas of Seyfert Galaxies"

T. D. Kinman. A. J. 73, 885, 1968. "Seyfert Galaxy Conference. 27. Photographic Photometry of the Seyfert Galaxy 3C 120"

C. A. Knight, D. S. Robertson, A. E. E. Rogers, I. I. Shapiro, A. R. Whitney, T. A. Clark, R. M. Goldstein, G. E. Marandino, N. R. Vandenberg. Science 172, 52, 1971. "Quasars: Millisecond-of-Arc Structure Revealed By Very-Long-Baseline Interferometry"

T. H. Legg, N. W. Broten, D. N. Fort, J. L. Yen, F. V. Bale, P. C. Barber, M. J. S. Quigley. Nature 244, 18, 1973. "Long Baseline Interferometry of the Seyfert Galaxy 3C 84"

R. Lynds. Ap. J. 159, L151, 1970. "Improved Photographs of the NGC 1275 Phenomenon"

W. J. Medd, B. H. Andrew, G. A. Harvey, J. L. Locke. Mem. R. A. S. 77, 109, 1972. "Observations of Extragalactic Variable Sources At 2.8- and 4.5-cm Wavelength"

R. Minkowski. A. J. 73, 842, 1968. "Seyfert Galaxy Conference. 1. Introductory Remarks"

A. E. Niell, K. I. Kellermann, B. G. Clark, D. B. Shaffer. Ap. J. 197, L109, 1975. "Milli-arcsecond Structure of 3C 84, 3C 273, and 3C 279 at 2 Centimeter Wavelength"

J. B. Oke. A. J. 73, 849, 1968. "Seyfert Galaxy Conference. 5. Continuum Energy Distributions of Seyfert Galaxies and Related Objects"

L. M. Ozernoy, V. N. Sazonov. Astrophysics and Space Science 3, 395, 1969. "The Spectrum and Polarization of a Source of Synchrotron Emission With Components Flying Apart At Relativistic Velocities"

I. I. K. Pauliny-Toth, K. I. Kellermann. Ap. J. 146, 634, 1966. "Variations In the Radio-Frequency Spectra of 3C 84, 3C 273, 3C 279, and Other Radio Sources"

I. I. K. Pauliny-Toth, E. Preuss, A. Witzel, K. I. Kellermann, D. B. Shaffer, G. H. Purcell, G. W. Grove, D. L. Jones, M. H. Cohen, A. T. Moffet, J. Romney, R. T. Schilizzi, R. Rinehart. Nature 259, 17, 1976. "High Resolution Observations of NGC 1275 With a Four-Element Intercontinental Interferometer"

G. H. Purcell. Ph. D. dissertation, California Institute of Technology, 1973. "The Structure of Compact Radio Sources At 606 MHz"

M. J. Rees. Nature 211, 468, 1966. "Appearance of Relativistically Expanding Radio Sources"

G. H. Rieke, F. J. Low. Ap. J. 176, L95, 1972. "Infrared Photometry of Extragalactic Sources"

D. S. Robertson. Ph. D. dissertation, Massachusetts Institute of Technology, 1975. "Geodetic and Astrometric Observations With VLBI"

D. S. Robertson, C. A. Knight, A. E. E. Rogers, I. I. Shapiro, A. R. Whitney, T. A. Clark, G. E. Marandino, N. R. Vandenberg, R. M. Goldstein. B. A. A. S. 3, 474, 1971. "Measurements of the Gravitational Deflection of Radio Waves"

A. E. E. Rogers. Radio Science 5, 1239, 1970. "Very Long Baseline Interferometry with Large Effective Bandwidth for Phase-Delay Measurements"

A. E. E. Rogers, C. C. Counselman, H. F. Hinteregger, C. A. Knight, D. S. Robertson, I. I. Shapiro, A. R. Whitney, T. A. Clark. Ap. J. 186, 801, 1973. "Extragalactic Radio Sources: Accurate Positions From Very-Long-Baseline Interferometry Observations"

A. E. E. Rogers, H. F. Hinteregger, A. R. Whitney, C. C. Counselman, I. I. Shapiro, J. J. Wittels, W. K. Klemperer, W. W. Warnock, T. A. Clark, L. K. Hutton, G. E. Marandino, B. O. Ronnang, O. E. H. Rydbeck. Ap. J. 193, 293, 1974. "The Structure of Radio Sources 3C 273B and 3C 84 Deduced From The Closure Phases and Visibility Amplitudes Observed with Three-Element Interferometers"

M. Ryle, M. D. Windram. M. N. R. A. S. 138, 1, 1968. "The Radio Emission From the Perseus Cluster"

R. H. Sanders. Nature 248, 392, 1974. "Super-relativistic Phase Velocities of Radio Source Components"

W. L. W. Sargent. P. A. S. P. 79, 369, 1967. "A New Intrinsically
    Bright Seyfert Galaxy"

R. T. Schilizzi, M. H. Cohen, J. D. Romney, D. B. Shaffer, K. I.
    Kellermann, G. W. Swenson, J. L. Yen, R. Rinehart. Ap. J. 201,
    263, 1975. "Observations with a VLB Array. III. The Sources 3C
    120, 3C 273B, 2134+004, and 3C 84"

G. A. Seielstad. Ap. J. 193, 55, 1974. "The Rapidly Variable Radio
    Source 3C 120"

K. G. Seyfert. Ap. J. 97, 28, 1943. "Nuclear Emission In Spiral
    Nebulae"

D. B. Shaffer, M. H. Cohen, D. L. Jauncey, K. I. Kellermann. Ap. J. 173,
    L147, 1972. "Rapid Changes In The Visibility Function of the Radio
    Galaxy 3C 120"

D. B. Shaffer, R. T. Schilizzi.. A. J. 80, 75.3, 1975. "18-Cm Visibility
    Functions of High-Frequency Compact Sources"

I. I. Shapiro, H. F. Hinteregger, C. A. Knight, J. J. Punsky, D. S.
    Robertson, A. E. E. Rogers, A. R. Whitney, T. A. Clark, G. E.
    Marandino, R. M. Goldstein, D. J. Spitzmesser Ap. J. 183, L47,
    1973. "3C 120: Intense Outburst(s) of Radio Radiation Detected
    With The Goldstone-Haystack Interferometer"

G. A. Shields, J. B. Oke, W. L. W. Sargent. Ap. J. 176, 75, 1972. "The
    Optical Spectrum of the Seyfert Galaxy 3C 120"

G. A. Shields. Ap. J. 191, 309, 1974. "X-Ray Ionization And The Helium
    Abundance In 3C 120"

N. R. Vandenberg. Ph. D. dissertation, University of Maryland, 1974.
    "Meter Wavelength Observations of Pulsars Using Very Long Baseline
    Interferometry"

H. van der Laan. Nature 211, 1131, 1966. "A Model For Variable
    Extragalactic Radio Sources"

M. F. Walker. Ap. J. 151, 71, 1968. "Studies of Extragalactic Nebulae.
    V. Motions In the Seyfert Galaxy NGC 1068"

M. F. Walker, C. D. Pike, J. D. McGee. P. A. S. P. 86, 870, 1974.
    "Direct Electronographic Observations of the Nebulosity Around 3C
    120"

A. R. Whitney, I. I. Shapiro, A. E. E. Rogers, D. S. Robertson, C. A.
    Knight, T. A. Clark, R. M. Goldstein, G. E. Marandino, N. R.
    Vandenberg. Science 173, 223, 1971. "Quasars Revisited: Rapid
    Time Variations Observed via Very-Long-Baseline Interferometry"

A. R. Whitney. Ph. D. dissertation, Massachusetts Institute of
Technology, 1974. "Precision Geodesy and Astrometry via Very Long
Baseline Interferometry"

J. J. Wittels. Ph. D. dissertation, Massachusetts Institute of
Technology, 1975. "Positions and Kinematics of Quasars and Related
Radio Objects Inferred from VLBI Observations"

J. J. Wittels, C. A. Knight, I. I. Shapiro, H. F. Hinteregger, A. E. E.
Rogers, A. R. Whitney, T. A. Clark, L. K. Hutton, G. E. Marandino,
A. E. Niell, B. O. Ronnang, O. E. H. Rydbeck, W. K. Klemperer, W.
W. Warnock. Ap. J. 196, 13, 1975. "Fine Structure of 25
Extragalactic Radio Sources"

J. J. Wittels, W. D. Cotton, C. C. Couselman, I. I. Shapiro, H. F.
Hinteregger, C. A. Knight, A. E. E. Rogers, A. R. Whitney, T. A.
Clark, L. K. Hutton, B. O. Ronnang, O. E. H. Rydbeck, A. E. Niell.
Ap. J. 206, L75, 1976. "Apparent Super-relativistic Expansion of
the Extragalactic Radio Source 3C 345"

R. S. Wolff, H. Helava, T. Kifune, M. C. Weisskopf. Ap. J. 193, L53,
1974. "X-Ray Morphology of the Perseus Cluster"